The University of Maine
DigitalCommons@UMaine

Electronic Theses and Dissertations | Fogler Library

Summer 8-19-2016

Size as a Trait for Understanding the Role of Zooplankton in the Biological Carbon Pump

Karen Stamieszkin
University of Maine, kstamieszkin@gmail.com

Follow this and additional works at: http://digitalcommons.library.umaine.edu/etd

 Part of the Marine Biology Commons, and the Oceanography Commons

Recommended Citation
Stamieszkin, Karen, "Size as a Trait for Understanding the Role of Zooplankton in the Biological Carbon Pump" (2016). *Electronic Theses and Dissertations*. 2508.
http://digitalcommons.library.umaine.edu/etd/2508

This Open-Access Dissertation is brought to you for free and open access by DigitalCommons@UMaine. It has been accepted for inclusion in Electronic Theses and Dissertations by an authorized administrator of DigitalCommons@UMaine.

The University of Maine
DigitalCommons@UMaine

Electronic Theses and Dissertations | Fogler Library

Summer 8-19-2016

Size as a Trait for Understanding the Role of Zooplankton in the Biological Carbon Pump

Karen Stamieszkin
University of Maine, kstamieszkin@gmail.com

Follow this and additional works at: http://digitalcommons.library.umaine.edu/etd

 Part of the Marine Biology Commons, and the Oceanography Commons

Recommended Citation
Stamieszkin, Karen, "Size as a Trait for Understanding the Role of Zooplankton in the Biological Carbon Pump" (2016). *Electronic Theses and Dissertations.* Paper 2508.

This Open-Access Dissertation is brought to you for free and open access by DigitalCommons@UMaine. It has been accepted for inclusion in Electronic Theses and Dissertations by an authorized administrator of DigitalCommons@UMaine.

SIZE AS A TRAIT FOR UNDERSTANDING THE ROLE OF ZOOPLANKTON IN THE BIOLOGICAL CARBON PUMP

By

Karen Stamieszkin

B.A. Yale University, 2006

M.E.Sc. Yale School of Forestry and Environmental Studies, 2007

A DISSERTATION

Submitted in Partial Fulfillment of the

Requirements for the Degree of

Doctor of Philosophy

(in Oceanography)

The Graduate School

The University of Maine

August 2016

Advisory Committee:

Andrew J. Pershing, Chief Scientific Officer, Gulf of Maine Research Institute, Advisor

Lee Karp Boss, Associate Professor of Oceanography, University of Maine

Jeffrey A. Runge, Professor of Oceanography, University of Maine

Fei Chai, Professor of Oceanography, University of Maine

Deborah K. Steinberg, Professor of Marine Science, Virginia Institute of Marine Science

DISSERTATION ACCEPTANCE STATEMENT

On behalf of the Graduate Committee for Karen Stamieszkin I affirm that this manuscript is the final and accepted dissertation. Signatures of all committee members are on file with the Graduate School at the University of Maine, 42 Stodder Hall, Orono, Maine.

Andrew J. Pershing, Ph.D. Date

Copyright 2016 Karen Stamieszkin

LIBRARY RIGHTS STATEMENT

In presenting this dissertation in partial fulfillment of the requirements for an advanced degree at The University of Maine, I agree that the Library shall make it freely available for inspection. I further agree that permission for "fair use" copying of this dissertation for scholarly purposes may be granted by the Librarian. It is understood that any copying or publication of this dissertation for financial gain shall not be allowed without my written permission.

Signature:

Date:

SIZE AS A TRAIT FOR UNDERSTANDING THE ROLE OF ZOOPLANKTON IN THE BIOLOGICAL CARBON PUMP

By Karen Stamieszkin

Dissertation Advisor: Andrew J. Pershing Ph.D.

An Abstract of the Dissertation Presented
in Partial Fulfillment of the Requirements for the
Degree of Doctor of Philosophy
(in Oceanography)
August 2016

Living organisms impact carbon transport between the atmosphere and the ocean through the biological carbon pump. Some plankton communities augment carbon export from the ocean's surface, and are thought to have a major role in global climate. These export communities are often characterized by larger organisms that sink to depths where the carbon they contain is sequestered from the atmosphere. Zooplankton can enhance export by aggregating prey into larger sinking fecal pellets; however fecal pellet flux is a highly variable component of the biological carbon pump. Relating plankton trophic dynamics to changes in particulate carbon flux is an important step in understanding the ocean's carbon cycle.

This research aims to connect plankton ecology with variability in zooplankton fecal pellet carbon flux, using body size as an organizing trait. A copepod fecal pellet carbon flux model is presented and applied to 25 years of copepod data from the Gulf of Maine. This model uses size-based metabolic rates to estimate fecal pellet production, and sinking and decay functions to estimate flux. The results show that copepod

community size structure determines fecal pellet carbon flux efficiency, but that flux itself is determined by copepod abundance and size. A second iteration of this model, which includes a temperature-dependent pellet decay function and diel vertical migration behavior, is applied to 55 years of copepod data from the North Atlantic Ocean. Analysis shows that fecal pellet carbon flux is decreasing as a result of declining copepod biomass, coincident with ocean warming. However, these changes vary from region to region, highlighting the importance of local dynamics. A study of local-scale trophic dynamics in the Gulf of Maine tests whether feeding and zooplankton fecal pellet production increases particle size, and therefore flux potential, in plankton communities. These experiments show tight coupling between microplankton and mesozooplankton, and demonstrate the importance of fecal pellet production as a mechanism for aggregating smaller particles into larger, sinking fecal pellets. Collectively this work shows that organism body size can be used as an organizing trait to connect individual-scale biology with variability in the biological carbon pump.

DEDICATION

This dissertation is dedicated to all of the research technicians who collectively spend thousands of hours analyzing Continuous Plankton Recorder samples, the people fund that work, and those who make the data available to the scientific community.

ACKNOWLEDGEMENTS

They say it takes a village to raise a child. It takes an entire state and beyond to raise a Ph.D. student. I would like first and foremost to thank my advisor, Andy Pershing, who encouraged and supported this work for the last five years. I also acknowledge my committee members for their guidance, opportunities to go to sea, equipment and lab space. I thank those at the Darling Marine Center who offered equipment, guidance and field support: Jeff Runge, Mary Jane Perry, Ivona Cetinić, Kathleen Thornton, Larry Mayer and Robby Downs. Thanks to Nicole Poulton and David Fields from Bigelow Laboratory for Ocean Science (BLOS) for assisting me in my experiments and for allowing me to use their equipment and lab space. I also acknowledge Nick Record at BLOS for helpful comments, encouragement and some good laughs. The ecosystem modeling lab at the Gulf of Maine Research Institute has offered support, good discussions and comic relief. I acknowledge the National Science Foundation Graduate Research Fellowship Program for supporting three years of my research, as well as the UMaine Michael J. Eckardt Dissertation Writing Fellowship, which supported the final year of my Ph.D. program. Thanks to the UMaine School of Marine Sciences administrative staff and faculty for an excellent course of study and a good academic experience. The love and support of my family and friends was essential to my Ph.D. program experience and completion, and for this I am grateful.

TABLE OF CONTENTS

LIST OF TABLES

LIST OF FIGURES

LIST OF EQUATIONS

LIST OF ABBREVIATIONS

GOM: Gulf of Maine

CPR: Continuous Plankton Recorder

FPC: Fecal pellet carbon

PL: Prosome length

FPV: Fecal pellet volume

FPP: Fecal pellet production

SR: Sinking rate

NAO: North Atlantic Oscillation

AMO: Atlantic Multidecadal Oscillation

CHAPTER 1

DISSERTATION INTRODUCTION

The biological carbon pump is a set of processes through which living organisms impact the transport of carbon between the atmosphere and the ocean (Ducklow et al. 2001). Some plankton communities augment carbon export from the ocean's surface, and are thought to have a major role in global climate on geologic time-scales (Sigman & Boyle 2000). These "export communities" are generally characterized by large, ballasted phytoplankton cells whose production rates are high enough that they escape predation and "bloom" (Buesseler 1998). Export can also occur due to sinking zooplankton fecal pellets, which are essentially aggregates of smaller prey organisms (Honjo et al. 2008); however zooplankton fecal pellet flux is a highly variable component of the biological carbon pump (Turner 2015). Relating zooplankton communities and plankton trophic dynamics to changes in particulate carbon flux is an important step in fully understanding the ocean's carbon cycle (Sanders et al. 2014).

Feedback loops within Earth's climate system are part of what make predicting and understanding climate change such a challenge. One possible feedback involves the biological carbon pump, ocean temperature, and plankton community size structure. Larger biogenic particles in the ocean generally sink more quickly than small particles (Guidi et al. 2008), making them more likely to reach a sequestration depth before being remineralized and recycled in the upper ocean. For this reason, particle size structure can explain changes in carbon export efficiency (Boyd & Newton 1999). Particle size is also affected by water temperature because warmer surface water can lead to water column

stratification and subsequent nutrient limitation. These physical and chemical conditions support small-celled primary producers (Morán et al. 2010), and smaller-bodied organisms in the marine food web (Daufresne et al. 2009). Since smaller particles generally decrease particle export, they can also result in less carbon sequestration at depth, and therefore dampen this mechanism for drawing carbon away from the atmosphere. Thus, the biological carbon pump may be part of a positive feedback with Earth's warming climate and oceans.

In the following chapters, I aim to connect plankton ecology to variability in the biological carbon pump. A size-based copepod fecal pellet carbon flux model, applied to 25 years of the Gulf of Maine Continuous Plankton Recorder (CPR) dataset, is presented in Chapter Two. I explore the model's sensitivity to different parameters and examine the contribution of different copepod taxa to fecal pellet carbon flux. The validity of the model is tested using the limited datasets available. Based upon lessons learned from the first model iteration, I expand upon and improve it, and present the results of applying it to 55 years of the North Atlantic CPR time series in Chapter Three. Chapter Four describes experiments which I designed to test the impact that mesozooplankton (> 200 μm) grazing has on the microplankton and detrital (< 200 μm) size spectrum. These experiments were conducted over eight months in 2014. Collectively these chapters explore the use of body size as an organizing trait which connects individual-scale biology with variability in the biological carbon pump.

CHAPTER 2

SIZE AS THE MASTER TRAIT IN MODELED COPEPOD FECAL PELLET CARBON FLUX

Introduction

Relationships among marine primary production, oceanic carbon flux, global geochemical cycles, and climate are well established. In 1990, Martin published his famous "Iron Hypothesis", based on the premise that increased primary productivity could result in increased carbon flux to the seafloor, shifting Earth's climate toward a cooler regime (Martin 1990). However, this is an incomplete depiction of the processes at work in the world's oceans. Not all phytoplankton cells are equal with regard to flux, with particle size being the primary determinant of phytoplankton carbon flux to depth (Boyd & Newton 1999). Further, a complete understanding of variability in carbon flux must include top down grazing pressure in addition to primary productivity (Behrenfeld & Boss 2014). The set of processes that collectively result in organic matter sinking from the euphotic mixed layer to depth (i.e. the biological carbon pump) is not only an avenue of carbon sequestration in the deep ocean, but also connects the upper water column productivity to benthic productivity. Global patterns of biogeochemical cycling in the ocean reflect marine food web size structure (Legendre & Rassoulzadegan 1996), and these structures persist on a foundation of changing oceanographic and climatic conditions (Lutz et al. 2007).

Mechanisms underlying the relationship between ecosystem structure and biogeochemical cycling can be described on very broad (i.e. ecosystem) and very narrow

(i.e. organism) scales; but scaling up from the latter to the former is a challenge. Mesozooplankton fecal pellet production and sinking is one highly variable component of the oceanic biological carbon pump (Turner 2002). This variability can be better understood by relating individual-scale biology to ecosystem-scale fecal pellet carbon (FPC) flux, or the amount of FPC reaching a target depth per unit time. Using metabolic theory and field observations, we built a size-based copepod FPC model that links Gulf of Maine copepod communities to seasonal and inter-annual patterns in estimated FPC concentration and flux.

We use copepod size as an organizing "master trait" (Litchman & Klausmeier 2008; Litchman et al. 2013) because it connects ecosystem structure with fecal pellet production and sinking rates, and therefore flux. The relative proportion of small to large mesozooplankton varies with latitude, temperature and nutrient regime (San Martin et al. 2006), and the sizes of individual copepods cumulatively result in varying community size spectra. Higher temperatures also result in smaller body size, within species (Record et al. 2012). Body size also determines fecal pellet size (reviewed in Mauchline 1998), and therefore sinking velocity, since settling speed is dependent upon particle size (Guidi et al. 2008). By examining the computed cumulative fecal pellet production of copepod communities over different time scales, we provide a mechanistic explanation for seasonal and interannual FPC flux variability. We test the hypothesis that the copepod community size composition and copepod abundance drive patterns in FPC reaching depth; we expect that higher proportions of larger copepods will result in higher relative FPC export.

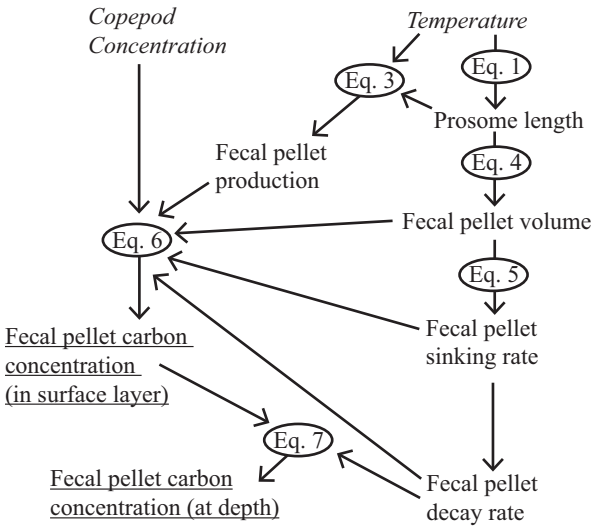

Figure 2.1. Schematic diagram of the fecal pellet carbon model showing inputs (italicized), model variables (plain text) and outputs (underlined); the nodes represent the equations in the paper.

Methods

Our goal is to understand how changes in copepod community size structure and abundance can result in carbon export variability. We built a model that links copepod communities in a surface layer with fecal pellet flux to depth, in the Gulf of Maine. The model begins with copepod body size and builds to total fecal pellet carbon (FPC) produced in the surface layer, incorporating temperature-metabolism relationships. A size-based transport and decay function was used to estimate flux to a particular depth (Fig. 2.1). We applied this model to field observations from the Gulf of Maine Continuous Plankton Recorder (CPR) dataset (Fig. 2.2).

Continuous Plankton Recorder copepod data – Continuous plankton recorders are sampling instruments, towed behind ships of opportunity, which collect and preserve

plankton. The mesh size (270 μm) was chosen to give an accurate representation of the mesozooplankton and large phytoplankton, without clogging (Richardson et al. 2006). However, sampling with a 270 μm mesh under-samples smaller organisms, excluding fecal pellets produced by copepod species smaller than 270 μm from the model results. Comparison of absolute copepod abundance in the Gulf of Maine from the CPR time series and a Bongo net time series (1978-2006) show that the Bongo net is more efficient at capturing the most abundant copepods, possibly due to its lower tow speed. However, trends in interannual and seasonal abundance and composition are statistically similar in the two datasets for total zooplankton, and for the most abundant copepod species (Kane 2009). We applied our model to previously enumerated and taxonomically identified CPR samples (n = 1961). The samples were collected from January 1988 through May 2013, on a 452 km transect primarily between Boston, Massachusetts, United States of America

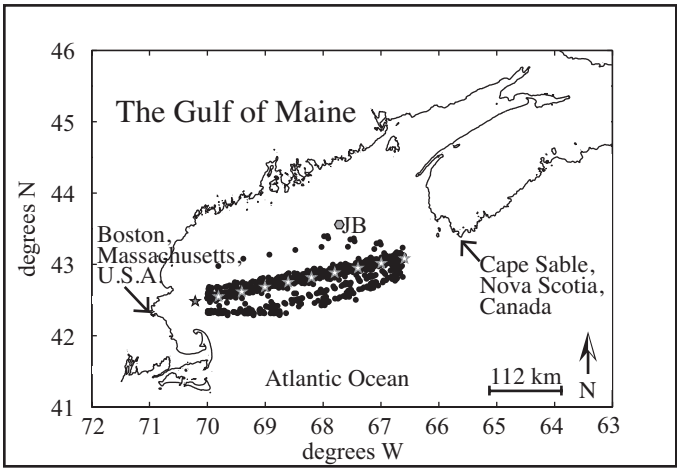

Figure 2.2. The Gulf of Maine with locations of CPR zooplankton samples (black dots, January, 1988 to May, 2013), model temperature stations (stars), sediment trap location (JB = Jordan Basin, hexagon), and key geographic landmarks.

(U.S.A.) and Cape Sable, Nova Scotia, Canada (Jossi et al. 2003) (Fig. 2.2). We excluded nearshore samples because zooplankton community composition tends to be different in coastal versus offshore communities (Record et al. 2010). Each sample represents the organisms in approximately 100 m^3 of seawater, from approximately 7 m depth (Richardson et al. 2006). Only copepod data were included, as copepods make up the majority of the CPR zooplankton dataset (Kane 2009), and are the most numerous mesozooplankton group in the ocean (Mauchline 1998). This subset of the Gulf of Maine CPR time series was chosen for analysis because copepod taxonomic identification and enumeration were consistent throughout. In our model application, we used concentrations of 22 copepod taxa, which make up 94% of the organisms identified over the 25-year period. Of the 6% excluded from analysis, 5.99% were of the CPR identification group, "copepoda". We excluded these organisms due to their non-specific identification. Of the 22 taxa included, 12 were identified to species, 9 to genus, and one to a grouping of two similarly sized genera (*Pseudocalanus/Paracalanus* spp.). The CPR dataset reports the abundances of each copepod taxon by combining copepodid stages. For example, *Calanus finmarchicus* abundance for each sample includes both stage C5 copepodids and adults (CVI), but is reported as one total abundance. Since our model is dependent upon copepod size, which varies with life history stage, we divided each CPR abundance count into the number of stages included in that count. The most abundant taxa in the original CPR dataset are divided by older (CIV or CV to CVI) and younger (CI-CIII or CIV) developmental stages, reflecting some stage structure dynamics. Continuing the example, if a sample reported 500 *C. finmarchicus* m^{-3}, then we divided

that by two to get 250 CV *C. finmarchicus* m^{-3}, and 250 CVI *C. finmarchicus* m^{-3}. Through this process, the original 22 stage/taxon combinations reported in the CPR dataset became 63 unique stage/taxon copepod groups (Table 2.1). More detailed stage information would yield more accurate FPC estimates.

Temperature data – Monthly temperature estimates for the Gulf of Maine were extracted from the Northeast Coast Ocean Forecast System (NECOFS) model (http://fvcom.smast.umassd.edu/necofs/). NECOFS is a forecasting system that incorporates multiple sub-models, including the Finite-Volume Coastal Ocean Model, configured for the Gulf of Maine, Georges Bank and New England Shelf (FVCOM-GOM). Hindcasts and comparative studies have shown that these models are accurate for temperature (Cowles et al. 2008). We therefore elected to use these data to provide a uniform source of depth-integrated temperatures for our entire CPR copepod time series.

We identified 10 locations that were centered along the CPR sampling track (Fig. 2) and extracted monthly temperature at each of those sites, from the NECOFS model. For each CPR copepod sample, we found the closest temperature location, and used a linear interpolation of time between the two months bounding the CPR sample date. We used an average of temperatures from the upper 30 m of the water column.

Table 2.1. Summary of copepod species and stages included in this chapter; the "Percent of total" indicates the percent of all copepods in the CPR dataset represented by a given taxon; "Slope" (m_i) and "Intercept" (b_i) indicate the parameters used to calculate prosome length (PL) in the model, PL = m_i(T) + b_i, where T is temperature in °C; "Method" indicates how the PL-T relationship was determined: Literature = a published relationship was used; Calculated = relationship calculated fitting a line to min and max temperatures and lengths; Estimated = best estimate based upon all available knowledge; Modeled = relationship back-calculated based upon known relationship of a later stage and published growth rates. For full citations, see the Appendix A.

Species	Copepodid stage, sex	Percent of total	Slope	Intercept	Method	Literature used
Calanus finmarchicus	V	10.2	-33.1	2665	Literature	Campbell et al. 2001
Calanus finmarchicus	VIF		-39.1	3073	Literature	Campbell et al. 2001
Temora longicornis	IV	2	-17.7	779.8	Literature	Hirst et al. 1999
Temora longicornis	VM		-45.9	1333.1	Literature	Hirst et al. 1999
Temora longicornis	VIF		-38.65	1265.8	Literature	Deevey 1960; Hirst et al. 1999
Metridia lucens	V	0.5	-23.9	1594	Calculated	McLaren et al. 1989; Batchelder and Williams 1995; Hays et al. 1998
Metridia lucens	VIF		-32	2200	Calculated	Batchelder and Williams 1995; Hays et al. 1998
Centropages hamatus	IV	0.2	-11.6	723	Literature	Hirst et al. 1999
Centropages hamatus	V		-15.65	876.5	Literature	Hirst et al. 1999
Centropages hamatus	VIF		-22.4	1162.5	Literature	Hirst et al. 1999
Paraeuchaeta norvegica	III	< 0.1	-28	1500	Estimated	-
Paraeuchaeta norvegica	IV		-31.9	2903.9	Calculated	Tönnesson et al. 2006
Paraeuchaeta norvegica	V		-26.8	4366.2	Calculated	Tönnesson et al. 2006
Paraeuchaeta norvegica	VIF		-31.6	5683.9	Calculated	Tönnesson et al. 2006

Table 2.1 continued

Species	Copepodid stage, sex	Percent of total	Slope	Intercept	Method	Literature used
Paracalanus/ Pseudocalanus	I	10.4	-17	515.9	Modeled	Deevey 1960; Ji et al. 2009
Paracalanus/ Pseudocalanus	II		-18.9	597.4	Modeled	Deevey 1960; Ji et al. 2009
Paracalanus/ Pseudocalanus	III		-20	691.4	Modeled	Deevey 1960; Ji et al. 2009
Paracalanus/ Pseudocalanus	IV		-23	799.7	Modeled	Deevey 1960; Ji et al. 2009
Paracalanus/ Pseudocalanus	V		-25	924.3	Modeled	Deevey 1960; Ji et al. 2009
Pseudocalanus	VIF		-28.3	1212	Literature	Deevey 1960
*Pseudocalanus**	VIF	8.2	-28.3	1212	Literature	Deevey 1960
Paracalanus	VIF	2.7	-5.95	784	Literature	Uye 1991; Sun et al. 2012
Acartia danae	II	< 0.1	-21.1	622.6	Modeled	McLaren 1978; http://192.171.193.133/detail.php?sp=Acartia%20danae
Acartia danae	III		-25.3	749.5	Modeled	McLaren 1978; http://192.171.193.133/detail.php?sp=Acartia%20danae
Acartia danae	IV		-31.7	946.1	Modeled	McLaren 1978; http://192.171.193.133/detail.php?sp=Acartia%20danae
Acartia danae	V		-44.6	1346.5	Modeled	McLaren 1978; http://192.171.193.133/detail.php?sp=Acartia%20danae
Acartia danae	VIF		-85	2615	Calculated	McLaren 1978; http://192.171.193.133/detail.php?sp=Acartia%20danae
Clausocalanus	VIF	0.1	-25	924.3	Modeled	Deevey 1960; Ji et al. 2009

Table 2.1 continued

Species	Copepodid stage, sex	Percent of total	Slope	Intercept	Method	Literature used
Centropages typicus	IV	12.9	-9.2	1084.3	Modeled	Deevey 1960; McLaren 1989; Liang et al. 1996
Centropages typicus	V		-10.7	1190.8	Modeled	Deevey 1960; McLaren 1989; Liang et al. 1996
Centropages typicus	VIF	11.8	-11.8	1266	Literature	Deevey 1960
Nannocalanus minor	V	< 0.1	-10	175	Estimated	-
Nannocalanus minor	VIF		-11	188	Literature	Ashjian and Wishner 1993
Centropages bradyi	VIF	< 0.1	-11.8	1266	Literature	Deevey 1960
Candacia	III	< 0.1	-16	949.9	Modeled	Richardson et al. 2001; Ji et al. 2009
Candacia	IV		-19.8	1095.1	Modeled	Richardson et al. 2001; Ji et al. 2009
Pleuromamma	II	< 0.1	-4.6	661.6	Calculated	Park, unpubl.
Pleuromamma	III		-7.2	916.2	Calculated	Park, unpubl.
Pleuromamma	IV		-16	1198	Calculated	Park, unpubl.
Pleuromamma	V		-11	1614	Calculated	Park, unpubl.
Pleuromamma	VIF		-24	2253	Calculated	Park, unpubl.

* *Pseudocalanus* spp. adult females were included as their own category, as well as in the *Paracalanus*/*Pseudocalanus* complex

Building the model – Our model has two key outputs: 1) FPC concentration in the surface layer, and 2) FPC concentration at a particular depth (underlined text in Fig. 1). From concentration at depth we also estimated FPC flux. Observed copepod community composition and concentration, and monthly temperature served as the model's foundation (italicized text in Fig. 1). With these data and known relationships between temperature, size, and metabolic rates, we derived a series of related variables necessary for estimating FPC concentration and flux (summarized in Table 2.2).

Copepod lengths – The CPR data set does not contain copepod lengths, which were critical to our model. Copepod prosome length is strongly related to the temperatures at which growth occurs (reviewed in Mauchline 1998). To reflect the impact of changing temperature on body size in our model, we needed a temperature-prosome length (PL_i, μm) relationship for each copepod stage/taxon (i) represented in the CPR dataset:

$$PL_i = m_i T + b_i \tag{2.1}$$

where T is the temperature in °C, and m_i and b_i are parameters either from the literature or estimated. Published temperature-PL relationships were available for one third of the copepod stage/taxon groups, or 39.2% of all copepods in the dataset. We estimated the remaining temperature-PL relationships using one of two methods depending upon the published information available. The first method is a "back-calculation" from older to earlier stages, and therefore requires a known temperature-PL relationship for an older copepodid stage, as well as parameters for a temperature-dependent development

equation and a mass-specific growth equation. Copepod stage duration (D_i, days) is a function of temperature (Belehrádek 1935):

$$D_i = a(\mathrm{T}+\alpha)^{\beta} \quad (2.2)$$

where T is temperature in degrees Celsius, a and α are fitted parameters for each taxon (i). β is -2.05 for Calanoid copepods (Corkett et al. 1986; Campbell et al. 2001; Record et al. 2012) and -2.6 for Cyclopoid copepods (Uye & Sano 1998) due to differences in their growth patterns. Instantaneous growth (g) was estimated using a temperature-dependent exponential model (Huntley & Lopez 1992). If both D and g are known, mass at a given stage can be calculated (Huntley & Lopez 1992; Record et al. 2012). We used a mass-specific inverse-growth equation to estimate the mass of earlier life stages (M_{s-1}, μm^3):

$$M_{s-1} = M_s e^{-gDs-1} \quad (2.3)$$

where g is the mass-specific growth rate, D_{s-1} is the duration of the earlier stage, and M_s is the mass of the older copepodid stage. The units are μm^3 because we used prosome length to the third power to estimate mass and vise versa; the two are consistently proportional to one another in copepods (Hirst 2012). This process was completed with the maximum, mean and minimum temperatures in our dataset, and from these three lengths, a linear model was applied and temperature-PL relationship determined (eq. 2.1). Back-calculation was used to get temperature-PL relationships for approximately one third of the copepod stage/taxon groups, or 59.7% of the copepods in the dataset.

A second method was used when there was not enough published information to back-calculate a relationship. We fit a linear equation to minimum and maximum temperatures in our temperature dataset to maximum and minimum copepod prosome

lengths from field data in published papers. We used this method for 1.1% of the copepods. Finally, copepod species and stages for which no information was available were estimated based upon the trajectory of later stages of that species, or length parameters of congeners; these stage/taxon groups made up < 0.0001% of the copepods in the dataset.

Calculating fecal pellet carbon flux – Metabolic functions, such as fecal pellet production, are scaled both to an organism's size, and to the temperature (Brown et al. 2004). We calculated a fecal pellet production rate (FPP_i, fecal pellets copepod^{-1} h^{-1}), the rate at which each copepod would produce fecal pellets. We used copepod size and local NECOFS temperature in an equation based upon allometric and metabolic temperature dependence relationships (Brown et al. 2004):

$$FPP_i = Ce^{-E/kT} PL_i^{\gamma} \quad (2.4)$$

where C is a scaling constant. E is activation energy (eV), k is the Boltzmann constant (8.62×10^{-5} eV K^{-1}), T is the temperature in K, PL_i is the copepod prosome length (mm), and γ is the mass scaling constant. Allometric scaling of metabolic rates usually refers to the mass of an organism, rather than length; therefore we estimated mass from length to the third power (Hirst 2012). Fecal pellet production rates also depend on prey availability (Besiktepe and Dam 2002). Therefore, parameters E and γ were estimated by fitting a model to observed fecal pellet production under a variety of food conditions, from limiting to non-limiting (See Appendix A). Thus, estimated *FPP* assumes mean feeding conditions.

The volume of a copepod fecal pellet is directly related to the size of the pellet's producer (reviewed in Mauchline 1998). We estimated the volume of a single fecal pellet produced by each copepod (FPV_i, μm^3):

$$\log_{10} FPV_i = \theta \log_{10}(PL_i) + \eta \quad (2.5)$$

where PL_i is prosome length in mm, and θ and η are parameters that we derived from fecal pellet dimensions and the prosome length of the copepod producing the fecal pellet. This was accomplished with a literature review (See Appendix A). We found a strong log-linear relationship between fecal pellet volume and pellet length ($n = 23$, $R^2 = 0.89$); therefore, when pellet volume was not available but pellet length was, this relationship was used to estimate volume.

The proportion of FPC produced near the sea surface that reaches a particular depth depends upon the retention of fecal pellets in the water column (Feinberg & Dam 1998; Wexels Riser et al. 2002; Möller et al. 2011). Fecal pellets generally conform to Stokes Law, which indicates that sinking rate scales with pellet radius squared (Mauchline 1998). Smaller fecal pellets, which therefore sink at disproportionately slow rates, are exposed to disaggregating processes for a longer period of time than larger, rapidly sinking pellets. We can use the sizes and numbers of the fecal pellets produced by a given copepod community, with an estimated retention rate as they sink through the water column, to estimate how much FPC reaches depth. From FPV_i, we estimated the sinking rate (SR_i, m h^{-1}) of each fecal pellet:

$$\log_{10} SR_i = \varphi \log_{10}(FPV_i) + \tau \quad (2.6)$$

where τ and φ were calculated from compiled observations during experiments with different zooplankton feeding on different prey (n = 806, R^2 = 0.60) (L.R. Feinberg and H.G. Dam, unpubl., see Appendix A). FPV_i (μm^3) was calculated as described above (eq. 2.5).

Fecal pellet carbon concentration in the surface layer (FPC_{sfc}, mgC m^{-3}) is a function of the number of pellets produced (FPP_i), the volume of each pellet (FPV_i), the copepod concentration (n_i), and is adjusted for pellets sinking out of the surface layer where we assume FPC concentration to be constant. FPC_{sfc} is one of the key model outputs, and is an estimate of total fecal pellet carbon mass produced by any given copepod community sampled by the CPR. A simple differential equation was used to represent the production of FPC in the surface layer, as well as fecal pellets sinking out (See Appendix B); the following solution represents fecal pellet concentration in the surface layer:

$$FPC_{sfc} = \sum_i \left[\frac{FPP_i \, \kappa \, FPV_i}{r + SR_{i/h}}\right] n_i \qquad (2.7)$$

where FPP_i (fecal pellets copepod^{-1} h^{-1}) and FPV_i (μm^3) are estimated as described above (eq. 2.4 and 2.5, respectively), and n_i is observed copepod concentration of each stage/ taxon category in the CPR dataset (copepods m^{-3}); κ is a constant representing the nearly linear conversion from fecal pellet volume to FPC (Mauchline 1998). We used a conservative fecal pellet volume conversion of 25 ± 5 ngC per FPV_i x 10^6 μm^3, derived from fecal pellets produced in the ocean by copepods feeding on an assemblage of natural prey (Urban-Rich et al. 1998). SR_i is the fecal pellet sinking rate as a function of fecal pellet volume (eq. 2.6); h is the height of the surface layer for which the CPR sample is

representative of copepod concentration. The CPR samples come from approximately 7 m; therefore we estimated that on average, the sample is representative of the top 14 m of the water column, with respect to copepod concentration. The fecal pellet remineralization rate (r) is the rate at which fecal pellets may be broken down and retained in the upper water column. In the ocean this rate changes in space and time (Wexels Riser et al. 2002; Möller et al. 2011), and the extent to which the decomposer community tracks production of detritus in the water column is unknown. We estimated r for sinking fecal pellets by solving an exponential decay function representative of fecal pellet decay in the water column. We assumed that the mean ratio of FPC concentration at depth to FPC concentration in the surface layer (FPC_{sfc}), averaged over the entire time series, was constant. This scenario suggests that the detritivore community varies with the amount of material available, resulting in a constant decay rate (See Appendix B).

We then applied this decay function to the FPC concentration in the surface layer to estimate the amount of FPC reaching the depth of interest ($FPC_{d,}$ mgC m^{-3}):

$$FPC_{sfc} = \sum_{i} \left[\frac{FPP_i \, \kappa \, FPV_i}{r + SR_{i/h}} \, n_i \right] e^{(-r/SR_i)z} \tag{2.8}$$

where FPP_i, FPV_i and SR_i are calculated as described above, n_i is copepod concentration from the CPR dataset, is the fecal pellet volume to carbon conversion constant, r is the remineralization rate, h is the height of the surface layer, and z is the depth of interest. Finally, we estimated FPC flux (mgC m^{-2} d^{-1}) by multiplying FPC_d by pellet sinking rate (SR_i), to give flux units mgC m^{-2} d^{-1}.

Error propagation and sensitivity analysis – There is considerable uncertainty in the parameters that control the dynamics of the model. We estimated the impact of this uncertainty on the output variables. We also examined the sensitivity of the output to changes in the parameters.

We used a resampling method to propagate error through the calculations. Means and standard errors of the parameters were calculated during meta-analysis of published experimental data (Table 2.3). Normal distributions with those calculated means and error terms were assumed for all parameters. We calculated the model outputs (fecal pellet carbon concentration and flux) using parameter values that were randomly resampled from the normal distributions, with replacement ($n = 1760 \pm 20$). The variable values that we report in this paper (Table 2.2) are the averages and standard deviations of these re-calculations. We did not assume a normal distribution of model outputs (FPC concentrations and flux) because the model variables interact non-linearly during the calculation of FPC. We calculated the mean model outputs using the mean of each parameter (henceforth the "mean model"). This is the model that is most likely to occur, based on available data. The 95% confidence intervals, minima and maxima for the model outputs were calculated from all model runs ($n = 1760 \pm 20$), and represent the estimated lower and upper bounds for the true distribution of the model outputs.

Table 2.2. Summary of input variables

Variable	units	minimum	maximum	mean	median	std. dev.
PL_i: prosome length	μm	25.3	5.6×10^3	1.1×10^3	8.8×10^2	44.3
FPP_i: fecal pellet production	fecal pellets copepod^{-1} h^{-1}	0.4	2.3	0.8	0.7	0.04
FPV_i: fecal pellet volume	μm^3	20.2	2.3×10^7	9.3×10^5	1.9×10^5	1.6×10^5
SR_i: fecal pellet sinking rate	m h^{-1}	0.1	8.8	2.2	1.9	0.7

We calculated the model outputs using three different remineralization rates (r in eq. 2.7 and 8): 50%, 75% and 95%. This showed the effect of fecal pellet retention rate as the pellets fall through the water column. We also tested the sensitivity of our model to the variability of each input variable by calculating fecal pellet carbon flux seven times; each time we held the parameters associated with zero, one or two variables constant (i.e. none, FPV, FPP, SR, FPV+FPP, FPV+SR, and FPP+SR). This test allowed us to see whether one input variable disproportionately contributed to the model output variability.

Annual climatology – We calculated a one-year climatology of FPC concentration over an average annual cycle. A biweekly moving average of FPC concentration in the surface layer (FPC_{sfc}) and at the mean depth of the Gulf of Maine (139 m, FPC_d) was determined for each year, from 1988 to 2012; the year 2013 was excluded because data were only available through May that year. The corresponding biweekly means from each year were averaged together to provide the mean annual climatology of FPC concentration. We chose to use a moving average to show the seasonal trends over the course of a year, and to smooth the high spatial heterogeneity

typical of zooplankton distributions over the Gulf of Maine. We also calculated the absolute and relative contributions of copepods from five size ranges, to the FPC reaching the seafloor; this showed how copepod size affects FPC_d over an annual cycle in the Gulf of Maine.

We calculated a FPC export efficiency term (henceforth "FPC flux efficiency"), representing the fraction of FPC produced at the surface that reaches the target depth, to explore the relative importance of copepod concentration and body size. It was calculated as the ratio of FPC_d to FPC_{sfc}. We assumed that 75% of the pellets produced at the surface were remineralized in the water column before reaching the 139 m depth horizon. Fecal pellet retention in the Barents Sea (i.e. the proportion produced reaching a target depth) has been reported as 40% at an ice edge to 96% in the Atlantic sector (Wexels Riser et al. 2002). We used this range as a guideline because fecal pellet retention has not been measured in the Gulf of Maine. Thus, a 75% retention rate represents moderate retention. Mean copepod lengths and mean community concentrations were also calculated to compare to the model outputs.

Comparison of model results to field data – Direct validation of this model would require long-term sediment trap samples from under the Gulf of Maine CPR transect, analyzed for their copepod fecal pellet content; however, such data do not presently exist. We compared our FPC flux estimates to data from Gulf of Maine sediment trap samples. The traps were deployed at 150 m in Jordan Basin, Gulf of Maine (43° 29.9 N; 067° 50.3 W) from 19 September 1995 to 24 April 1997, and 05 April 2005 to 14 April 2006 (Fig. 2.2), and were part of the National Atmospheric and Oceanic

Administration's (NOAA) Regional Marine Research Program (RMRP) and the Ecology and Oceanography of Harmful Algal Blooms (ECOHAB) Program (methods described in Pilskaln et al. 2014). We compared the relative difference between modeled annual FPC flux, to the mean calculated POC flux measured by the 150 m time-series traps in 1995-1997 (n = 39 samples) and 2005-2006 (n = 26 samples). The discrepancy between the location of the sediment traps and the CPR transect limits our ability to make a direct comparison. However, we expect that any correspondence between the two would occur at long time scales; thus we focused on comparing the interannual signals. With this comparison we tested whether changes in the modeled FPC values reflect relative interannual changes in POC flux documented by sediment traps.

Results

Model parameterization – We constructed our model with several sub-models based upon allometric scaling and metabolic theory. Each sub-model was a step toward calculating the amount of fecal pellet carbon (FPC) that a copepod produces, starting with copepod size, and ending with FPC concentration at depth and flux (Fig. 2.1). We parameterized the sub-models by fitting curves to published data (See Appendix A), and resampled parameter distributions to estimate a distribution of modeled FPC outputs (n = 1760 ± 20).

Each copepod species/stage used in this analysis has a unique temperature-prosome length relationship based upon the experimental literature or our modeling work described above (Table 2.1). Fecal pellet production rates were modeled from

relationships in the literature (See Appendix A) between fecal pellet production, prosome length and temperature (n = 235, r = 0.37, p < 0.01) (Fig. 2.3). Estimated fecal pellet production rates are lower than published values, but not unreasonable, making the model estimates of FPC conservative (Table 2.3; See Appendix A). The literature review of fecal pellet volume and their producers' prosome lengths yields a log-linear relationship (n = 188, R^2 = 0.43, p < 0.01) (Fig. 2.4, Table 2.3) as seen in other studies (Uye & Kaname 1994; Mauchline 1998). Fecal pellet sinking rate is also a log-linear function of fecal pellet volume (Table 2.3, L.R. & H. G. Dam unpubl.).

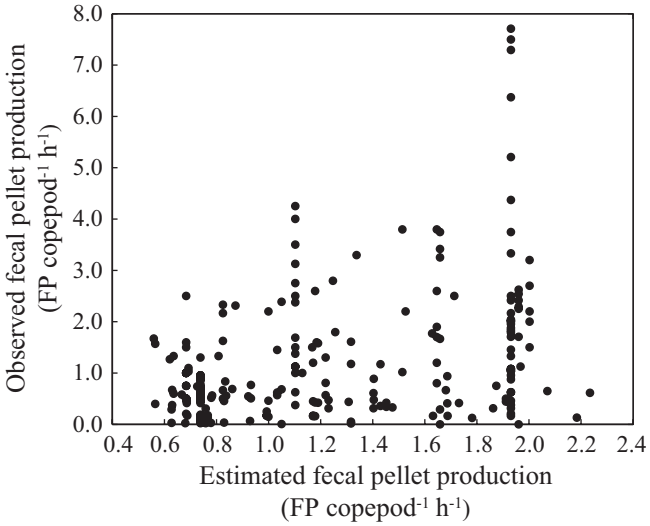

Figure 2.3. Estimated fecal pellet production (*FPP*) versus observed *FPP* (n = 233, r = 0.37, p < 0.01); the *FPP* model assumes mass-dependent scaling of metabolic rates, and an Arrehnius-type temperature function.

Table 2.3. Summary of model parameters and the statistics associated with their fit to respective datasets (See Appendix A for citations): fecal pellet production (*FPP*), fecal pellet volume (*FPV*), and fecal pellet sinking rate (*SR*).

Variable	*n*	R^2	*p*	Parameter	Mean	Standard error
FPP	233	0.14	< 0.01	E	0.28	0.005
				γ	-0.24	0.005
FPV	188	0.43	< 0.01	η	5.4	0.07
				θ	2.58	0.22
SR	806	0.60	< 0.01	τ	-0.03	0.06
				φ	0.32	0.01

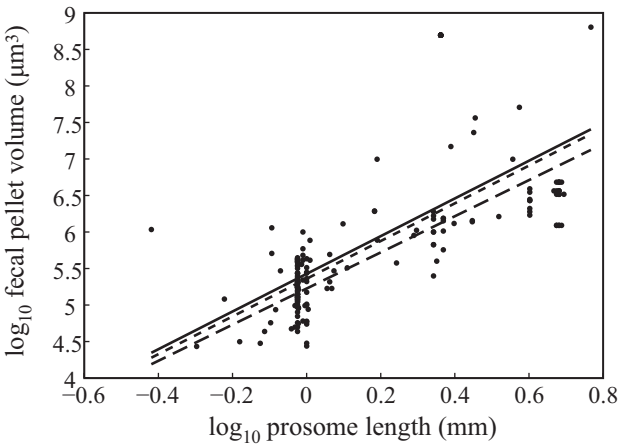

Figure 2.4. Prosome length (*PL*) versus fecal pellet volume (*FPV*), on a log-log scale; dots represent data points used in this paper's analysis of the *PL*-*FPV* relationship, with the solid line indicating the line of best fit (R^2 = 0.43, $p < 0.01$). The dashed lines represent the same relationship determined in previous similar studies: small-dashed from Uye and Kaname 1994, large-dashed from Mauchline 1998.

Annual cycle of fecal pellet carbon concentration and flux – The modeled mean annual cycle of FPC concentration in the surface layer (FPC_{sfc}) shows two distinct peaks: one in the first half of June and a secondary peak in the first half of October (Fig. 2.5A). The FPC concentration at 139 m (FPC_d) shows the same primary peak, but a lesser secondary peak (Fig 2.5B). The model outputs are not normally distributed, but skewed toward lower FPC values. The parameters can be seen as scaling terms, which determine whether the model output is relatively high or low, but for any given model output, FPC will be scaled the same way. In other words, the position of the output within the model's distribution is pre-determined, and the FPC estimates for that model run will be scaled the same way. In this case, it is possible to have FPC concentrations more than three times that predicted by the mean model (Fig. 2.5).

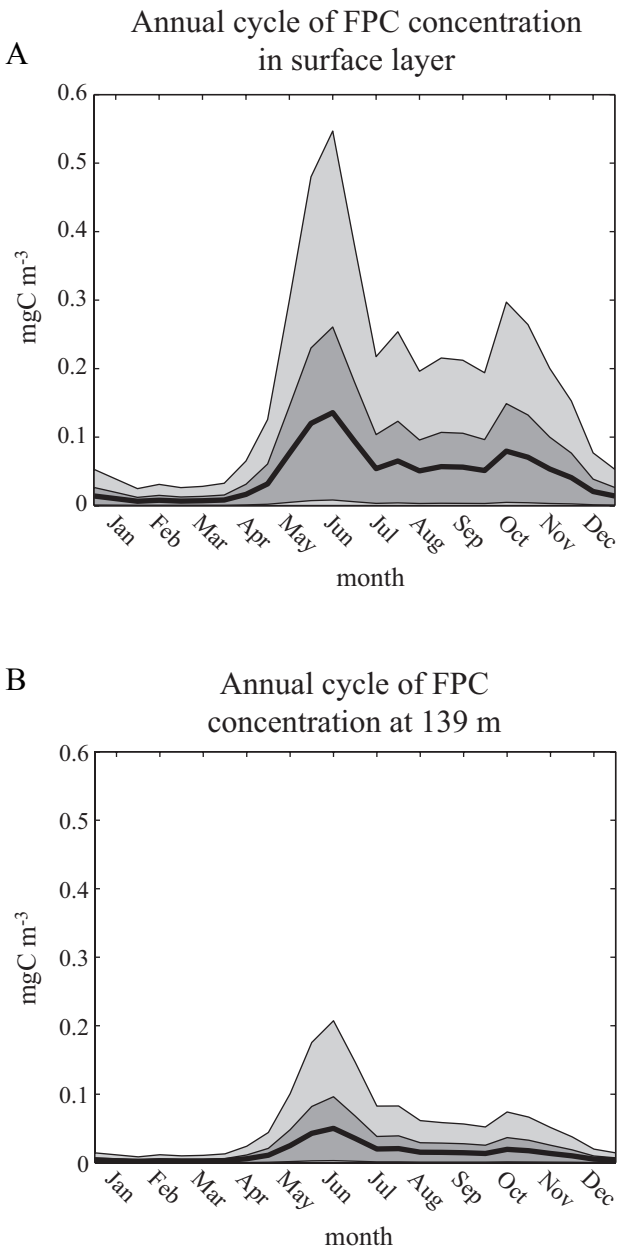

Figure 2.5. Model results: A) annual climatology of fecal pellet carbon concentration in the surface layer (FPC_{sfc}) and B) fecal pellet carbon concentration at 139 m (FPC_d), estimated by the model; the black lines represent the mean model, or the model most likely to occur. Dark gray represents the 95% confidence interval, and light gray represents the minimum and maximum model outputs. Values are represented as a biweekly moving average to emphasize trends, and a 75% retention rate was used.

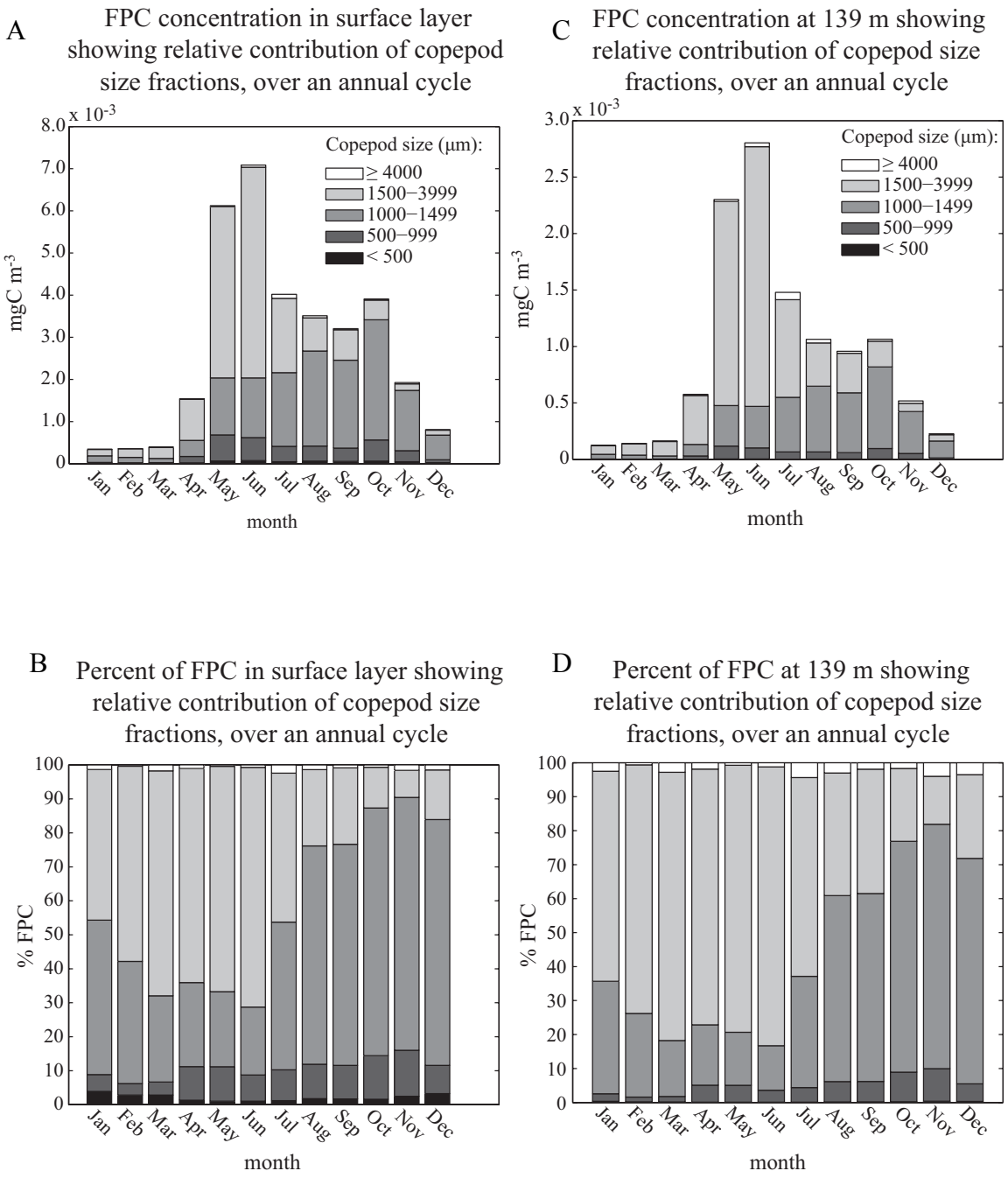

Figure 2.6. Mean fecal pellet carbon concentrations and percent compositions, broken into the contribution of five copepod size-classes represented by shades of gray (< 500 µm black; 500-999 µm dark gray; 1000-1499 µm medium gray; 1500-3999 µm light gray; and ≥ 4000 µm white) for each month; A) annual climatology of fecal pellet carbon concentration in the surface layer (FPC_{sfc}), B) percent composition of FPC_{sfc}, C) annual climatology of fecal pellet carbon concentration at 139 m (FPC_d), D) percent composition of FPC_d. A 75% retention rate was used for all.

We hypothesized that higher numbers of larger copepods would result in higher FPC export. When we divide FPC_{sfc} and FPC_d into the contributions of five copepod size bins, the importance of smaller versus larger copepods is apparent, as is the annual cycle of copepod size in the Gulf of Maine (Fig. 2.6). For an average copepod community during each month, the smaller copepod size classes (< 1500 μm) contribute more FPC to FPC_{sfc} (Fig. 2.6A and 2.6B) than to FPC_d (Fig. 2.7C and 2.7D); and the percent of FPC contributed by the larger copepods is always higher at depth than in the surface layer, for each month. The smallest copepods (< 500 μm) make 1.0% to 3.9% of FPC_{sfc} (Fig. 2.6A and 2.6B), but none of this FPC reaches depth (Fig. 2.6C and 2.6D). The copepods from the largest size bin (≥ 4000 μm) contribute a maximum of 2.4% FPC_{sfc} in July, but up to 4.3% of FPC_d in the same month. The dominant size bin switches between June and August; earlier in the year, the 1500 to 3999 μm group contributes the majority of FPC both to the surface layer and depth. In the latter half of the year, FPC from the 1000-1499 μm group dominates (Fig. 2.6).

We expect a relationship between model inputs (e.g. concentration and length) and the outputs (e.g. FPC), but because the model is non-linear these comparisons can elucidate which factors are driving changes in estimated FPC concentration and flux throughout the annual cycle. When we directly compare copepod concentration to FPC concentrations, we see that the annual cycles of FPC_{sfc} and FPC_d are both tightly coupled to copepod concentration in the surface layer (FPC_{sfc} : $R^2 = 0.96$, $p < 0.01$; FPC_d: $R^2 = 0.83$, $p < 0.01$). However, at the start of July, there is a change in how copepod concentration affects the magnitude of FPC export (Fig. 2.7A); the relationship between

the two over the year is non-linear. We found that a change in copepod size composition explains this shift. The mean copepod length begins to drop in July, as does FPC flux efficiency (ratio of FPC_d to FPC_{sfc}); FPC flux efficiency is more closely associated with mean copepod prosome length ($R^2 = 0.72$, $p < 0.01$), than copepod concentration ($R^2 = 0.02$, $p = 0.49$) throughout the year (Fig. 2.7B). This annual pattern is also reflected in the mid-summer shift from larger to smaller copepod size class contributing most to FPC (Fig. 2.6).

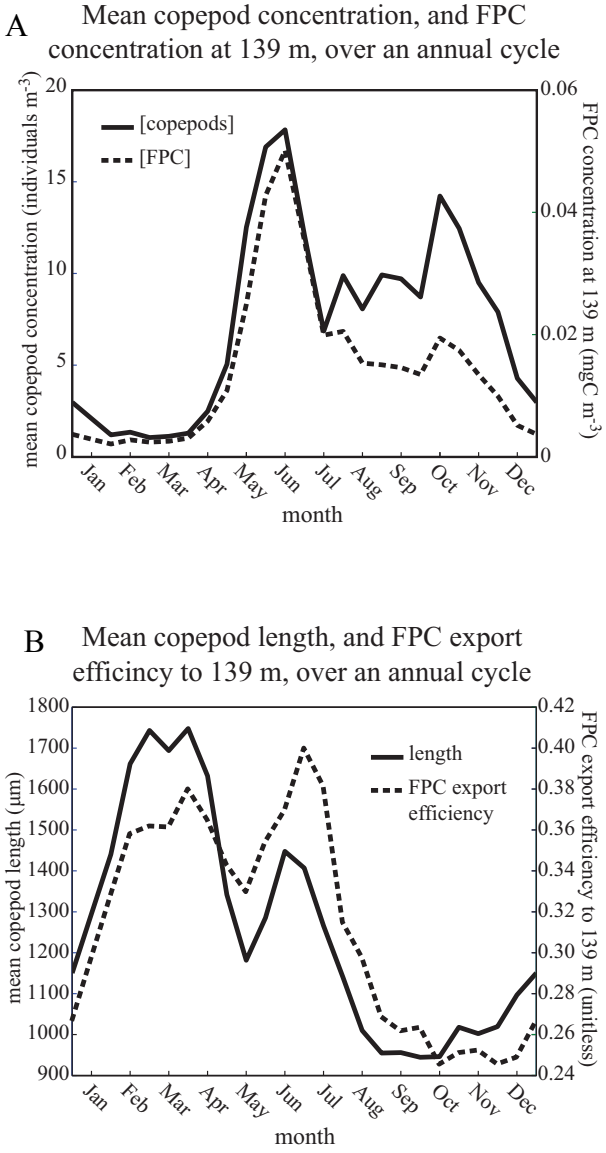

Figure 2.7. A) Annual climatology of copepod concentration represented by the solid line, and annual climatology of fecal pellet carbon concentration at 139 m (FPC_d) represented by the dashed line; B) Annual climatology of copepod community mean length represented by the solid line, and annual climatology of fecal pellet carbon (FPC) flux efficiency (ratio of FPC concentration at 139 m to concentration in the surface layer) represented by the dashed line. All climatologies are represented as biweekly moving averages; retention of fecal pellets in the water column is assumed to be 75%; data from 1988 to 2012 were used.

Model sensitivity – The model outputs show a high level of sensitivity to remineralization or retention rate (r) of fecal pellets as they sink through the water column (Fig. 2.8). We also tested the model sensitivity to each variable and combination of variables by holding the parameters associated with each variable constant, and plotting the width of the 95% confidence interval for FPC flux (Fig. 2.9). Holding the sinking rate parameters constant had the greatest impact on the model outputs, followed by fecal pellet production rate.

Interannual variability in fecal pellet carbon concentration and flux – FPC_{sfc}, FPC_d and FPC flux all show significant interannual variability, but no significant trends over the study period (Fig. 2.10). FPC flux (Fig. 2.10C) mirrors the patterns in FPC_{sfc} and FPC_d (Fig. 2.10A and 2.10B, respectively) with a few exceptions, most notably in 1988 and 1989 when FPC_{sfc} and FPC_d are relatively low, but flux is relatively high. During these two years, the mean copepod prosome length in the Gulf of Maine was up to two times higher than in any other year. All FPC variables are lowest in 1998 as is the variability around the mean model; 2011 and 2012 follow as the next lowest years in FPC flux (Fig. 2.10). The two years of available sediment trap data from Jordan Basin (19 September 1995 to 24 April 1997, and 05 April 2005 to 14 April 2006) corroborate the relative difference between the modeled FPC variables from those two years. The mean 150 m POC flux was 6.8 and 4.2 mg m^{-2} d^{-1} during the earlier and later periods, respectively; all FPC variables reflect this relative difference (Fig. 2.10).

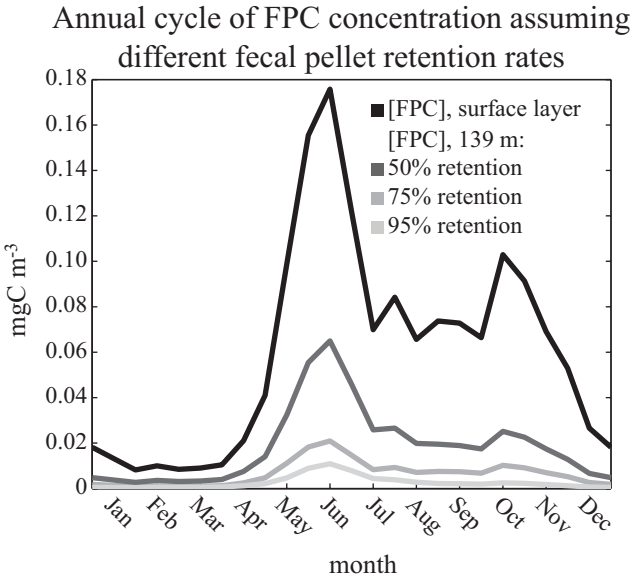

Figure 2.8. Fecal pellet carbon concentration in the surface layer (FPC_{sfc}) represented by the black line; fecal pellet carbon concentration at 139 m (FPC_d) assuming 50% (dark grey), 75% (medium gray) and 95% (light gray) retention of fecal pellets in the water column. Data from 1988 to 2012 were used.

Figure 2.9. 95% confidence interval widths for the mean fecal pellet carbon (FPC) flux, as the model is run holding the parameters for none, one, or two variables constant. A 75% retention rate was used.

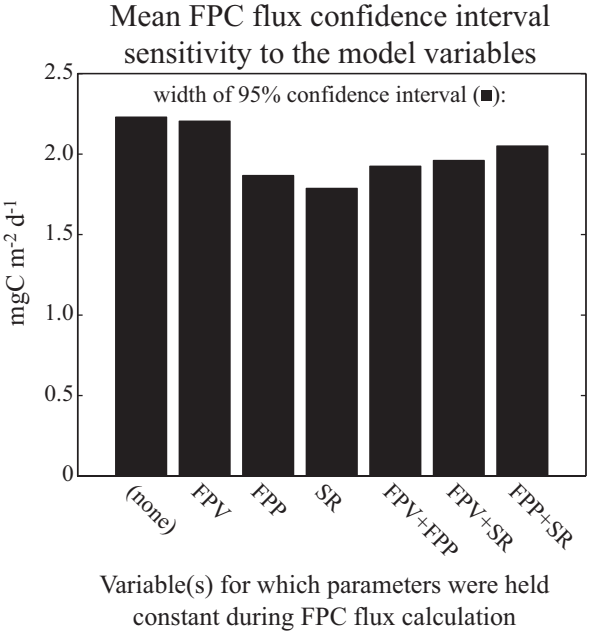

Discussion

Many processes mediate the amount of organic carbon that falls to the seafloor, or past the 1000 m "sequestration depth" in the ocean, where it is considered decoupled from the ocean-atmosphere system (Primeau 2005; Passow & Carlson 2012). The sum of processes that augment flux, such as aggregation and ballasting, and those that decrease it, such as decomposition and remineralization, result in a variable biological carbon pump. Sinking zooplankton fecal pellets represent a highly variable portion of the biological carbon pump; the particulate organic carbon found in sediment traps can be composed of 0 to 100% zooplankton fecal pellets (reviewed in Turner 2002). We suggest that FPC flux variability can be explained in the Gulf of Maine using copepod body size as a master trait.

In our model, the annual cycle of fecal pellet flux efficiency, or the fraction of fecal pellet carbon (FPC) produced that reaches a target depth, is tightly coupled with mean copepod body size. While metabolic theory indicates that smaller copepods produce more fecal pellets per time than larger copepods due to relatively high metabolisms (Brown et al. 2004), larger pellets sink disproportionately faster than small pellets (Guidi et al. 2008; L.R. Feinberg & H.G. Dam, unpubl.), and pellet size is directly related to copepod size. Since pellet size affects not only carbon content per pellet (Urban-Rich et al. 1998), but also sinking rate, it reduces the amount of time that a pellet is exposed to coprophagy, coprohexy and bacterial degradation (Turner 2002) in the water column. Therefore, copepod body size has a compounding effect on FPC flux.

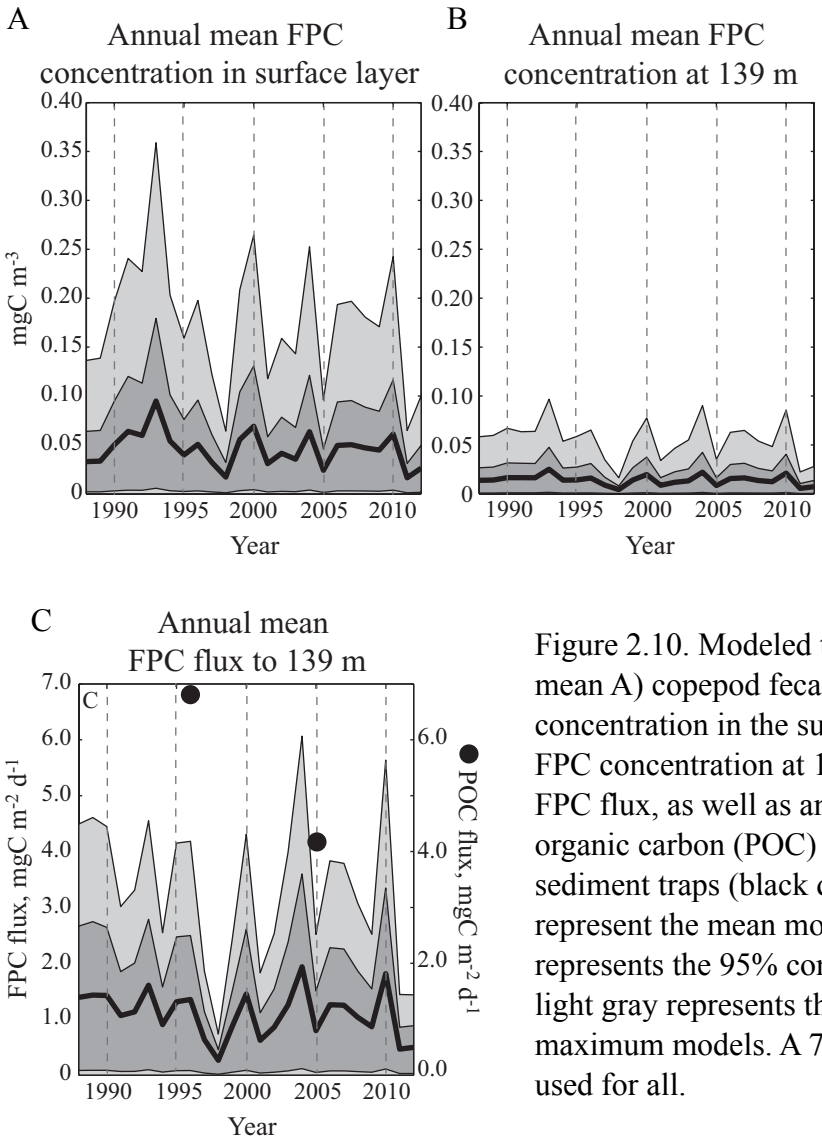

Figure 2.10. Modeled time series of annual mean A) copepod fecal pellet carbon (FPC) concentration in the surface layer (FPC_{sfc}), B) FPC concentration at 139 m (FPC_d), and C) FPC flux, as well as annual average particulate organic carbon (POC) flux measured in sediment traps (black dots); the black lines represent the mean model; dark gray represents the 95% confidence intervals, and light gray represents the minimum and maximum models. A 75% retention rate was used for all.

The extent to which fecal pellets are broken down as they sink through the water column is clearly important, demonstrated by the sensitivity of estimated FPC concentration at depth to percent remineralization (Fig. 2.8). This rate of retention is the least constrained of our model inputs. Bacterial degradation of pellets is a complex function of temperature (Honjo & Roman 1978) and grazer diet (Thor et al. 2003); it can vary spatially in the horizontal and vertical directions (Alonso-Sáez et al. 2007; Baltar et

al. 2007), as well as temporally (Turley et al. 1995). Further, copepods themselves are known to break apart and consume fecal pellets (Iversen & Poulsen 2007). Models of biogenic carbon flux such as this would greatly benefit from a more detailed understanding of the mechanisms behind POC retention as particles sink through the water column.

The interplay between copepod abundance and size throughout the year affects the amount of FPC reaching depth. With size held constant, higher copepod abundance implies that more fecal pellets are produced and may sink. However, copepod size varies seasonally and is decoupled from abundance. The annual cycle of FPC flux efficiency (FPC_d:FPC_{sfc}) compared with that of copepod size highlights the importance of size with regard to the fraction of FPC in the surface layer that reaches depth (Fig. 2.7B). Efficiency is high in the winter because the community is dominated by large species, but actual FPC flux is low because copepod abundance is low. Maximum FPC flux and efficiency occur in the late spring and early summer because mean copepod size and abundance both increase. Gulf of Maine time-series trap data from a number of offshore sites and time periods spanning 1995 – 2010 document late spring/summer total mass flux and POC flux peaks to which fecal pellets contribute along with algal aggregates (Pilskaln et al. 2014; C.H. Pilskaln, unpubl.). In the fall a secondary peak in copepod abundance coincides with the lowest FPC flux efficiency values throughout the year (Fig. 2.7). This is due to relatively small mean body size, resulting in smaller, slower-sinking pellets that are degraded faster than large pellets. We therefore observe a lower

modeled efficiency of pellets reaching the target depth, compared to the spring/summer period.

The model results suggesting that small copepods are less important to fecal pellet flux than large copepods, even when highly abundant, are consistent with findings from the field elsewhere. A northern Norwegian study found that relatively large fecal pellets from adult individuals of the copepod *Calanus finmarchicus* contribute disproportionately to flux compared with the much smaller and more abundant *Oithona similis* (Wexels Riser et al. 2010). During the same field campaign, the summer copepod community was dominated by small copepod species and stages, resulting in high fecal pellet abundance in the water column (Pasternak et al. 2000), but low fecal pellet flux (Wexels Riser et al. 2010). The agreement of these results with the modeled results from the Gulf of Maine supports the mechanistic framework that our model provides. Patterns of copepod fecal pellet flux can be explained using trait-based predictions of individual-scale biology.

Calanus finmarchicus is the only large-bodied, highly abundant copepod in the Gulf of Maine. The primary peak in FPC flux during late spring/early summer is driven by *C. finmarchicus* abundance. The diversity in the Gulf of Maine copepod community can be reduced to body size to explain variability in FPC flux; however, *C. finmarchicus* dynamics are a unique and primary factor in interannual differences in flux, due to the species' relative large size and high abundance. Advection is an important mode of *C. finmarchicus* transport into and around the Gulf of Maine (Lynch et al. 1998; Greene & Pershing 2000). Mode shifts in the North Atlantic Oscillation, a decadal-scale climate

oscillation, can change Northwest Atlantic and Gulf of Maine circulation, impacting *C. finmarchicus* abundance (Greene & Pershing 2000; Conversi et al. 2001). Temperature and chlorophyll concentrations can also affect *C. finmarchicus* abundance by impacting the body size and egg production of females (Melle et al. 2014). *C. finmarchicus* abundance is declining in the North Sea (Beaugrand, 2009), and its range is projected to shift north, excluding the Gulf of Maine (Reygondeau & Beaugrand, 2011). Although long-term sediment trap data are lacking for direct model validation, there is a correlation between the annual growth of a long-lived benthic clam from the Gulf of Maine, and Gulf of Maine *C. finmarchicus* abundance measured by the CPR (Wannamaker et al. 2009). The clam can be seen as a living sediment trap, with growth reflecting prey availability near the seafloor. This relationship is consistent with variations in *C. finmarchicus* leading to changes in the flux of organic material to the benthos. Based upon our model results, a decrease in *C. finmarchicus* in the Gulf of Maine would likely lead to a decrease in carbon export and delivery to the benthos.

The interannual changes in our modeled FPC concentration at depth (mgC m^{-3}), as well as flux (mgC m^{-2} d^{-1}) are broadly consistent with the interannual variability in available sediment trap data (C.H. Pilskaln, unpubl.). This comparison indicates that our model may accurately reflect relative changes in FPC flux. The magnitude of FPC flux estimated by the model fits well within the range of reported FPC fluxes in the literature from different systems, and within the POC estimates from the sediment traps.

FPC fluxes measured at similar depths around the world range from less than 1 mgC m^{-2} d^{-1} (Goldthwait & Steinberg 2008; Gleiber et al. 2012) to 135 mgC m^{-2} d^{-1} (Stukel et al. 2013).

Sinking rate was the variable that had the most impact on the model's mean 95% confidence interval width, followed by fecal pellet production rate (Fig. 2.9). Experimental work aimed at fine-tuning the parameterization of these variables would improve our model. As discussed above, fecal pellet remineralization rate also has a significant impact on our model outputs. An improved fecal pellet decay function that varies with environmental parameters such as temperature, depth, and time of year would improve the model's estimate of flux. The model depends heavily upon the conversion from fecal pellet volume to fecal pellet carbon. This conversion is known to change seasonally and with prey type (Urban-Rich et al. 1998). Improvement of the fecal pellet volume to carbon conversion would improve this model as well.

Our model shows the potential for changes in zooplankton composition and concentration to drastically alter the FPC flux. This variability underscores the complexity of ground-truthing models of FPC flux. The ocean is a patchy environment and zooplankton patches persist over varying spatial and temporal scales (Folt & Burns 1999). Zooplankton fecal pellet flux events are therefore episodic and hard to document. Our novel approach to modeling fecal pellet flux, using Gulf of Maine CPR zooplankton abundances, aims to reflect the patchy nature of zooplankton and discontinuous nature of fecal pellet flux over time and space. Further, by incorporating the effects of size on metabolism into the model, we more finely resolve how a changing zooplankton

community could impact FPC flux to depth. Our model results suggest that by incorporating just community size composition, estimates of zooplankton-mediated carbon flux may be improved.

The importance of copepod body size in determining FPC flux is clear, but the physical and chemical conditions that support larger- or smaller-bodied copepod communities ultimately drive interannual variability in flux. Our results show decadal changes in FPC flux. These changes are consistent with the previously documented ecosystem shift in the 1990's, when smaller copepods became more dominant and *Calanus finmarchicus* declined (Pershing et al. 2005). The decrease in modeled FPC flux and export efficiency during the late 1990's is also reflected in sediment trap data. These data document a decrease in mean annual POC export to sub-euphotic depths in the Gulf between the 1990's and 2000's. Additionally, mean annual FPC flux in 1998, 2011 and 2012 stand out as the lowest in the modeled dataset. 1998 is associated with a "great salinity anomaly" (MERCINA 2012), a major oceanographic perturbation in the Gulf of Maine. The years 2011 and 2012, the final two years in our dataset, are part of a steep warming trend in the Gulf of Maine, which started in 2005. Gulf of Maine temperatures in 2012 reached record highs (Mills et al. 2013). As the North Atlantic Ocean is changing, the mean size of its copepods is decreasing (Beaugrand 2010). Understanding the specific mechanisms by which physical and chemical conditions shape copepod community size structure and ecosystem state will improve understanding of variability in the copepod community, in fecal pellet carbon flux, and ultimately in the biological carbon pump.

CHAPTER 3

DRIVERS OF CHANGE IN MODELED COPEPOD FECAL PELLET CARBON FLUX ACROSS THE NORTHERN NORTH ATLANTIC OCEAN, 1958 TO 2013

Introduction

The ocean is currently a sink for atmospheric carbon dioxide (CO_2), including anthropogenic sources of CO_2, which are contributing to a rapidly changing global climate (Sabine et al. 2004). Marine organisms mediate the transport of carbon between the atmosphere and ocean, altering its phase and oxidation state in a set of processes delineated as the biological carbon pump (Sigman & Boyle 2000, Ducklow et al. 2001). When particulate organic carbon (POC) is exported below a "sequestration depth," it is effectively separated from the atmosphere for up to several millennia (Sigman & Boyle 2000, de la Rocha & Passow 2007). POC exported from the euphotic zone includes aggregates of biogenic material, such as phytodetritus. It also includes fecal pellets produced by zooplankton, both near the sea surface (Turner 2015) and at mesopelagic depths to which they vertically migrate (Al-Mutairi & Landry 2001, Schnetzer & Steinberg 2002). Copepods in diapause themselves represent particulate organic carbon which can be eaten by mesopelagic fauna and entrained in the mesopelagic food web (Jonasdottir et al. 2015). Zooplankton fecal pellet carbon flux is highly variable and can constitute from none to all of the vertical POC flux caught in sediment traps (Turner 2015).

As oceanographic conditions change with global climate, so do plankton communities. Warming ocean temperatures affect plankton communities in several ways, including spatial distribution (Richardson & Schoeman 2004), phenology (Poloczanska et al. 2013) and size structure (Daufresne et al. 2009, Morán et al. 2010). Plankton community size composition can impact the efficiency of the biological carbon pump, since smaller particles are more likely to be remineralized before sinking below a sequestration depth. Warmer conditions lead to smaller-bodied plankton communities (Daufresne et al. 2009), and higher remineralization (Wohlers et al. 2009). Therefore, warming caused by anthropogenic CO_2 emissions is expected to lead to lower POC export.

Copepods are one of the most numerous metazoans in the ocean, making them an important component of marine ecosystems. Copepods and other mesozooplankton contribute to the biological carbon pump by aggregating small prey into larger fecal pellets, increasing particle size and carbon export potential. Larger copepods produce larger fecal pellets, making them disproportionately important to fecal pellet carbon flux (Beaugrand et al. 2010, Stamieszkin et al. 2015). In this study, we test the hypothesis that copepod communities in the northern North Atlantic Ocean are shifting toward smaller-sized community composition, resulting in decreasing fecal pellet carbon flux. We apply an individual-scale fecal pellet production model to 55 years of surface copepod abundance and composition data from the North Atlantic Continuous Plankton Recorder program (Richardson 2006). We compare the relative impact of temperature-dependent

metabolic rates and growth on fecal pellet carbon flux, compared with the impact of changing plankton community composition.

Methods

We examined the effects of copepod community composition on fecal pellet carbon flux from the ocean surface. Building from our previous model that computed fecal pellet carbon flux based upon copepod size, metabolism, and temperature (Stamieszkin et al. 2015), we incorporated diel vertical migration and a temperature-fecal pellet decay function. We applied this size-based model to copepod abundance and species composition data from the North Atlantic Continuous Plankton Recorder program, to estimate changes in fecal pellet carbon flux from January 1958 through December 2013 across the North Atlantic Ocean.

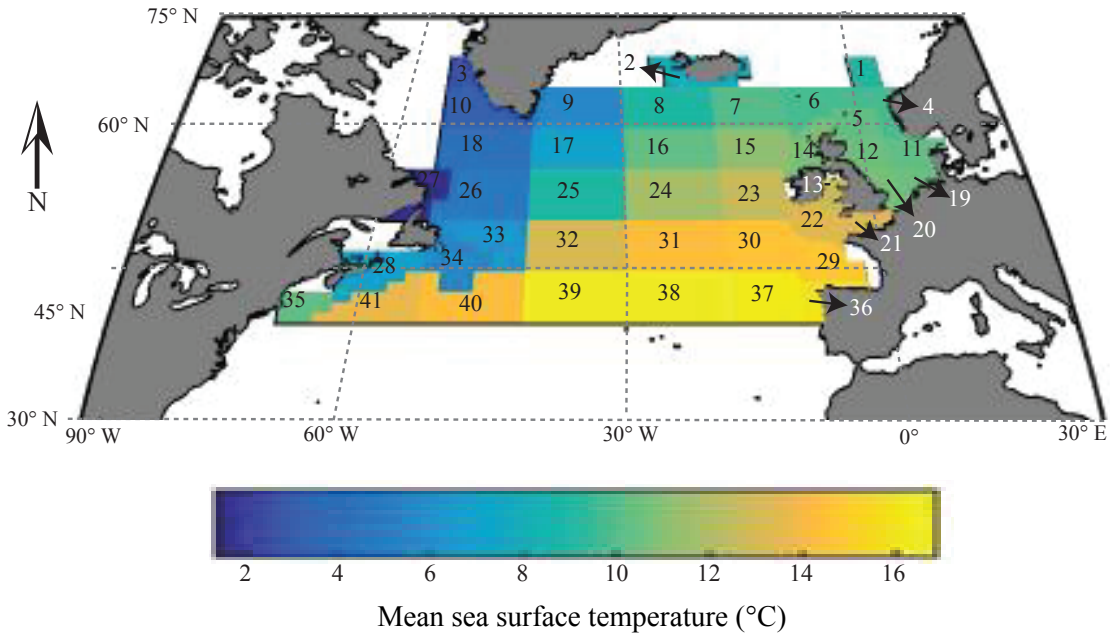

Figure 3.1. Map of the northern North Atlantic Ocean with standard Continuous Plankton Recorder areas numbered; color represents mean sea surface temperature from the model GECCO2 (°C).

Data inputs - Two types of data served as model inputs: copepod concentration and water temperature. Copepod concentration data were provided by the Sir Alister Hardy Foundation for Ocean Science (SAHFOS) Continuous Plankton Recorder (CPR) program (doi: 10.7487/2014.272.1.41). CPRs are instruments attached to ships of opportunity, which sample with 270 µm mesh at approximately 7 m depth as they are towed (Richardson et al. 2006). These data were collected from January 1958 through December 2013 in the northern half of the North Atlantic Ocean and the North Sea; this large area has been divided into 41 standard CPR areas, which generally reflect oceanographic regions and provide a consistent way to break up the large dataset (Richardson 2006, Fig. 3.1). CPRs under-sample smaller organisms due to the mesh size

used, excluding fecal pellets produced by copepod species smaller than 270 μm from the model results. However, when compared to data collected with bongo nets, trends in interannual and seasonal abundance and composition are statistically similar for total zooplankton, and for the most abundant copepod species (Kane 2009). CPRs also only sample a narrow subsurface layer of the water column. Therefore, the results of this model application represent fecal pellet carbon flux from a surface layer only. Despite these limitations, the North Atlantic CPR data have been used extensively to study large-scale changes in plankton community structure over long time periods (Beaugrand et al. 2002, Villarino et al. 2015) due to the dataset's spatial and temporal breadth.

The CPR copepod concentrations were previously enumerated and identified to species or genus level, and in some cases grouped also by copepodid stage. We focused our study on copepods because they are one of the most abundant and ubiquitous metazoans in the ocean, and because the extensive literature on copepod biology and physiology allowed us to parameterize our model. We included the 25 taxonomic/stage groups that comprised 99% of the copepods in the dataset (Table 3.1). The CPR copepod data were not consistently separated by copepodid stage, but because our model was size-based, we divided the concentrations of each taxon among the number of stages that it represented (Stamieszkin et al. 2015). For example, *Calanus finmarchicus* copepodid stages 5 and 6 (adult) are grouped together in the database. For our calculations, we divided the recorded concentration between the two stages. These divisions resulted in 66 unique taxon/stage groupings (Table 3.1).

Table 3.1. Summary of copepod taxa that make up 99% of the dataset and were used in the model; “traverse” indicates a different method of organism enumeration

Taxon	**Copepodite stages**
Acartia spp.	CII to CVI
Calanus spp.	CI to CIV
Calanus finmarchicus	CV to CVI
Calanus helgolandicus	CV to CVI
Calanus hyperboreus	CV to CVI
Centropages hamatus	CIV to CVI
Centropages spp.	CIV to CVI
Centropages typicus	CIV to CVI
Clausocalanus spp.	CVI
Corycaeus spp.	CIV to CVI
Mecynocera clausi	CV to CVI
Metridia spp.	CI to CIV
Metridia spp. (traverse)	CI to CVI
Metridia lucens	CV to CVI
Oithona spp.	CIV to CVI
Oncaea spp.	CIV to CVI
Paracalanus/Pseudocalanus spp.	CI to CV
Pseudocalanus spp.	CVI
Paracalanus spp.	CIII to CVI
Paraeuchaeta norvegica	CIII to CVI
Pleuromamma spp. (traverse)	CV to CVI
Pleuromamma borealis	CVI
Scolecithricella spp.	CVI
Temora longicornis	CIV to CVI

The temperature data were generated by GECCO2, a reanalysis model based on the Massachusetts Institute of Technology general circulation model (MITgcm). The model estimates monthly average temperature on a 1° by 1° horizontal grid, as well as by depth, with higher depth resolution closer to the surface (Köhl & Stammer 2008). We computed monthly temperature profiles averaged over each CPR region. These were used by the copepod model to compute temperature at a given depth, which influences the body size of copepods, their metabolic rates, and the rate at which fecal pellets are remineralized.

Model Design - We designed a size-based model to estimate mean fecal pellet carbon flux through different depth horizons, per day. It was modified from the fecal pellet flux model introduced in Chapter One (Stamieszkin et al. 2015); a detailed description of the methods used to build the model is described therein. The framework of the model was based on estimating the distribution of surface-dwelling (0 to 25 m deep) copepods over a 24-hour period for each day of the year, applying metabolic rates to estimate fecal pellet carbon production in the water column, and then calculating the flux of carbon as the pellets sink and decay (Fig. 3.2).

Copepod size is a central variable in many parts of the model. Fecal pellet production rate for each copepod was estimated using metabolic size and temperature dependence relationships (Brown et al. 2004, Stamieszkin et al. 2015); and fecal pellet volume was estimated with a log-linear prosome length-fecal pellet volume relationship (reviewed in Mauchline 1998, Stamieszkin et al. 2015). Copepod prosome length (a common measure of size) was estimated from temperature because it is linearly related to

the temperature at which the copepods grow, within the temperature range experienced by these species (reviewed in Mauchline 1998). Taxon/stage groups whose temperature-length relationships had not been established previously were estimated either by back-calculating from older stages, estimating based on known length and temperature observations, or using the relationship for a similar species (Stamieszkin et al. 2015).

Figure 3.2. Model schematic

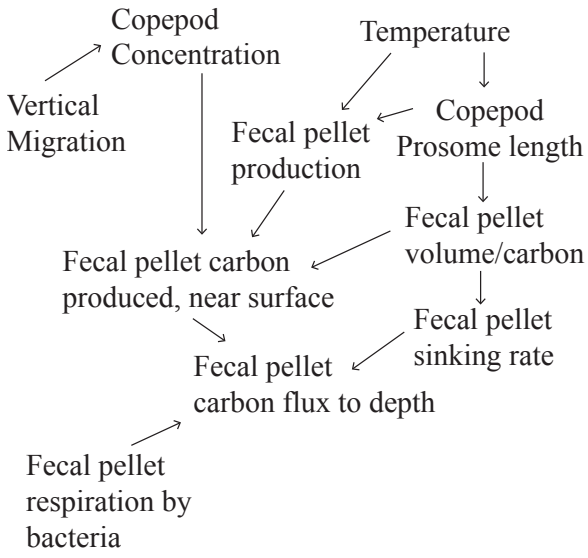

The CPR program collects surface plankton samples along transects in a given standard area approximately once per month. Therefore, in order to estimate total fecal pellet carbon flux, we created climatologies of the CPR data, and did an analysis of diel vertical migration (DVM) behavior. By combining this information, we estimated vertical profiles of each copepod stage and taxon for each day of the year, in a given area and 5-year period. The region sampled by the CPR was divided into 41 standard CPR areas **(**Fig. 3.1**,** Richardson et al. 2006). We calculated 5-year mean annual climatologies of

copepod concentration in each area. The climatologies were periodic splines fit to the available CPR samples within each region and period (see Pershing et al. 2005 for methods). This procedure allows us to estimate the abundance of each taxon on any day of the year. Similar to the copepod concentrations, temperature climatologies were calculated for discrete depths by first averaging monthly temperatures from model grid points within each CPR area and 5-year period, and then fitting a spline function to these data.

Organisms that vertically migrate contribute to the biological carbon pump. As these animals migrate to deeper, darker waters during the day, they egest and respire carbon on their way down and at depth; this results in active transport of particulate and dissolved carbon (Steinberg et al. 2000, Al-Mutairi & Landry 2001). Since the CPR samples are collected near the sea surface, they naturally exclude copepods that migrate to deeper waters both seasonally and daily. In the case of seasonal migration performed by some copepod species during which the copepods remain at depth for months in diapause, metabolism is depressed to near-basal rates (Maps et al. 2014). Therefore, while not included in our analysis, these hibernating copepods are not producing significant amounts of fecal material while at depth. In the case of DVM, samples taken during daylight hours represent the copepods that have remained at the surface, rather than migrating down. We determined whether a taxon performed DVM by comparing abundance during the day and night. Independent of the climatologies described above, we aggregated the CPR copepod concentration data for a given CPR region, five year period, and season. These concentrations were binned by the hour of day (1 to 24) in

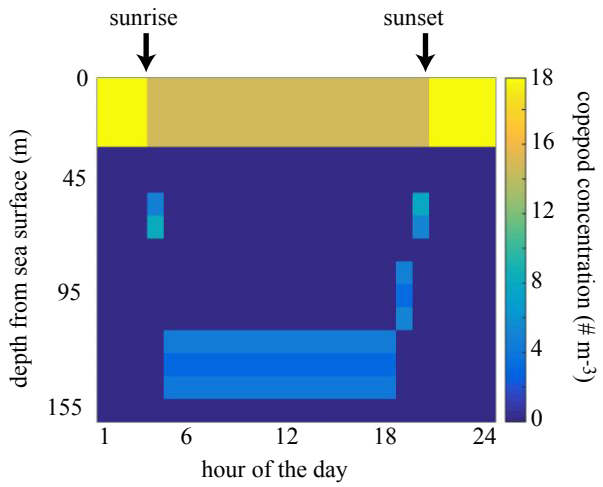

Figure 3.3. Example of copepod concentration over a 24 hour day, showing vertical migrators

which they were sampled, and averaged together to give a mean concentration of each taxon over a representative day. If there were less than 16 out of 24 hours that contained abundance data, then DVM behavior for that taxon was marked as indeterminate in the region and time period. When there were enough hours represented in the data, we fit a sine curve to the daily abundance cycle using a parameter optimization function (fminsearchbnd, J. D'Errico 2006, Matlab v. R2014b). We established two sets of criteria to objectively determine whether a taxon performed DVM: 1) The sine function model had to fit the observed mean daily concentration profile better than a mean concentration model over the day, as decided with an Akaike's Information Criterion; and 2) the mean daytime concentration had to be at least 25% less than the mean nighttime concentration. If these two criteria were met, the taxon was marked as a "migrator" in that season, location and 5-year period; otherwise it was marked as a "non-migrator."

We had to make assumptions about the timing of vertical migration in relation to local sunrise and sunset. We assumed that the copepods began their descent in the hour of sunrise and took two hours to reach their migration depths, which we estimated with prosome length (Ohman & Romagnan 2015). At sunset, we assumed that the copepods arrived at the surface, and started migrating three hours before. We approximated the effect of sinking down versus swimming up by having it take longer to reach the surface (3 h) than depth (2 h). When the average depth of a region was shallower than the estimated migration depth of the copepods, they were allowed to migrate to the bottom. We also assumed that 80% of copepods within each day that were thought to migrate actually did, giving conservative estimates of vertical migration. Using the copepod concentration climatologies estimated from the CPR data, and the estimated vertical migration behavior and depth, we calculated vertical profiles of copepod concentration for each day of the year in a given area and five-year period (Fig. 3.3). By applying the fecal pellet production model to these copepod concentrations, we calculated daily profiles of fecal pellet volume produced at different depths in the water column, for each CPR standard area and 5-year period of the CPR dataset. We assumed that copepods did not feed once they left the surface and that egestion stopped after two hours.

Large fecal pellets sink faster than smaller pellets, and as pellets sink they lose mass through decomposition and remineralization. We explicitly modeled both sinking and remineralization of fecal pellets. The water column from the surface to 1000 m (or the bottom if shallower) was divided into depth bins that matched the temperature model output. The concentration of pellets of given volume was tracked by dividing pellet

volume into 121 evenly spaced bins between 0 and 6 $x10^7$ μm^3. The fecal pellet production rates of copepods in the water column represented a source term for the remineralization and sinking module, and fecal pellets were added to the appropriate depth and volume bin during each time step. At each time step, we then calculated the volume-specific remineralization rate in each depth and volume bin. These rates were then used to update the fecal pellet volume concentration in each bin using a first order upwind scheme. We next applied the sinking rate, moving a fraction of the pellets in each bin into the next deeper bin, again, using a first-order upwind scheme. The flux across the bottom of the 30 m and 1000 m depth bins were totaled over each day.

A general relationship for estimating remineralization rates of fecal pellets has not been established; we therefore aggregated available information to approximate fecal pellet remineralization in the model. Carbon-specific degradation rates for diatom aggregates have been measured at 12 ± 3% at 15 °C, and dropped 3.5 times at 4 °C (Iversen & Ploug 2013), and shallower remineralization has been shown to occur at warmer temperatures in the field (Marsay et al. 2015). Also, a study conducted at one site in the Sargasso Sea indicates a 75% reduction in the remineralization of organic material between 150 and 500 m (McDonnell et al. 2015). We designed a volume-specific remineralization rate (r_{remin}) based on a linear relationship with temperature:

$$r_{remin} = 0.005\ T + 0.011 \tag{3.1}$$

where T is water temperature in degrees Celsius. Due to the typical temperature profile in the ocean, where temperature decreases exponentially with depth. This relationship

provided remineralization rates that were consistent with particulate organic carbon profiles and an exponential decrease in remineralization activity with depth (Fig. 3.4), similar to remineralization rates derived from particulate organic carbon profiles (Martin et al. 1987, Boyd & Trull 2007).

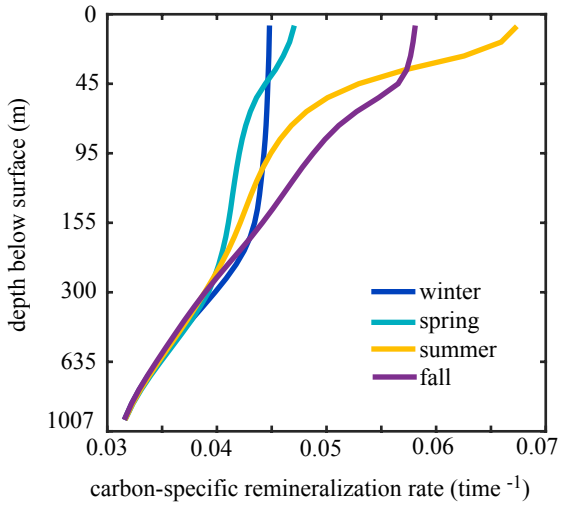

Figure 3.4. Examples of remineralization profiles from Area 18 in winter, spring, summer and fall.

In summary, we calculated annual climatologies (365 d) of fecal pellet carbon flux through 30 and 1000 m, for 5-year periods (1958-2013). This was done for each standard CPR area to account for spatial variability. Flux through 30 m was calculated to estimate fecal pellet carbon export from the copepods sampled by the CPR. As the fecal pellets sank, a temperature-dependent remineralization rate was applied. Flux through 1000 m represented fecal pellet carbon that reached a sequestration depth, and that could be considered sequestered from the atmosphere-ocean interface.

Analysis - We calculated mean annual fecal pellet carbon flux (mgC m^{-2} d^{-1}) by summing estimated flux (mgC m^{-2} d^{-1}) for each day of an annual climatology, in each standard area. We also calculated fecal pellet carbon flux efficiency, defined as the flux through the 1000 m depth horizon divided by the flux through the 30 m horizon. Flux efficiency was estimated to reflect how much of the fecal pellet carbon sinking from the surface (upper 30 m) reached a sequestration depth (1000 m). For each CPR region, we calculated the temporal trend in 30 m and 1000 m flux and flux efficiency by regressing the time series of each variable against 5-year period. A trend was only calculated if there were more than six 5-year periods sampled sufficiently in an area.

Identifying which input variables drive change in fecal pellet carbon flux over time was a goal of this work. The input variables of copepod size, concentration, and temperature influence flux in non-linear ways through copepod biomass (a combination of size and abundance), copepod metabolic processes, and fecal pellet size and remineralization rates. We compared the time series of fecal pellet carbon flux and flux efficiency to these different variables to discern which were most important. We also examined in more depth the drivers of change in two standard CPR areas where flux was increasing (Area 9) and decreasing (Area 36) over the time series. Simple linear regression of different variables and individual copepod taxa versus fecal pellet carbon flux were used to determine some drivers of change.

Model Sensitivity - We conducted three sensitivity experiments to understand which processes had the most impact on modeled fecal pellet carbon flux. We compared a "standard" model run (run_0), in which copepods migrated, and temperature and copepod

composition varied from period to period, to a run in which each of those elements was held constant, one at a time (run_{exp}). The ratio run_0 to run_{exp} showed how much the variable being held constant affected modeled fecal pellet flux.

The first experiment looked at the impact of changes in temperature on the fecal pellet flux patterns observed. Temperature determines the size and fecal pellet production of individual copepods. It also impacts remineralization rates of organic material. For this experiment, the output from the full model was compared to a run during which the annual temperature cycle was held constant throughout the time series. This tested the direct effect of temperature on fecal pellet carbon flux.

Temperature directly impacts fecal pellet flux through its effects on copepod size and remineralization. Temperature also influences the structure of the copepod community (Beaugrand et al. 2009). For the second experiment, we compared the full model with a run in which the copepod communities in each area were held constant over the time series. This allowed us to assess the impact of changes in community composition compared with the direct impact of temperature.

The third experiment was aimed at quantifying the impact that diel vertical migration behavior had on fecal pellet carbon flux. Vertical migration can increase carbon flux because copepods are actively transporting and releasing carbon deeper in the water column (Steinberg et al. 2000, Al-Mutairi & Landry 2001). We compared a run in which the copepods migrated to a run in which they remained that the sea surface and continued to feed through the day.

Results

Averaged over the study period, flux through the surface waters (30 m, Fig. 3.5A, Fig. 3.6A) and past 1000 m (Fig. 3.5B, Fig. 3.6B) is higher closer to the North American and European continents. Maximum flux through 30 m occurs in the southeast quadrant of the North Sea (Area 19, 49.0 mgC m^{-2} y^{-1}) and minimum flux through 30 m occurs at the center of the study region's southern boundary, just north of the North Atlantic oligotrophic subtropical gyre (Area 39, 7.2 mgC m^{-2} y^{-1}). Mean fecal pellet carbon flux through the 1000 m depth horizon is highest in the southwest corner of the domain (Area 35, 25.1 mgC m^{-2} y^{-1}). It is lowest at the southeastern edge of the study region, offshore of the Iberian Peninsula (Area 37, minimum = 2.9 mgC m^{-2} y^{-1}).

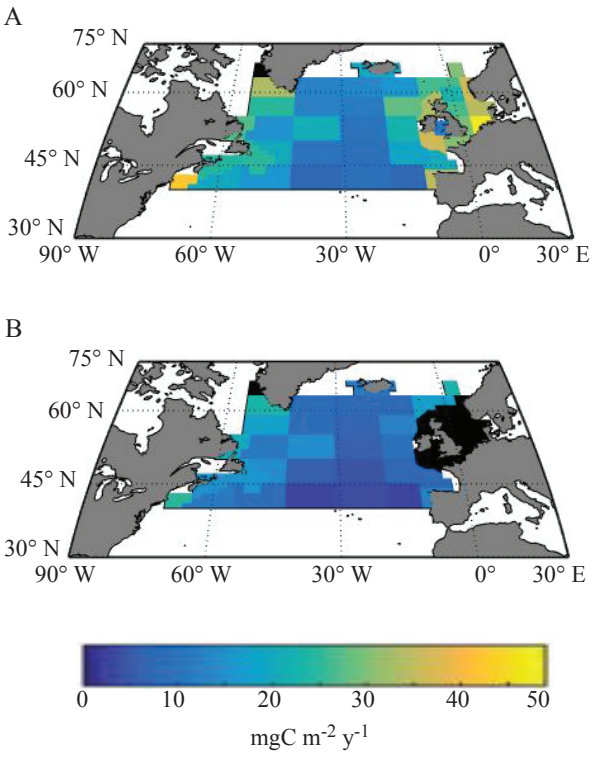

Figure 3.5. Mean copepod fecal pellet carbon flux (mg C m^{-2} y^{-1}) from 1958 to 2013, across the northern North Atlantic Ocean through A) 30 m and B) 1000 m; areas which are blacked out indicate insufficient data or mean depth less than 1000 meters (5B only).

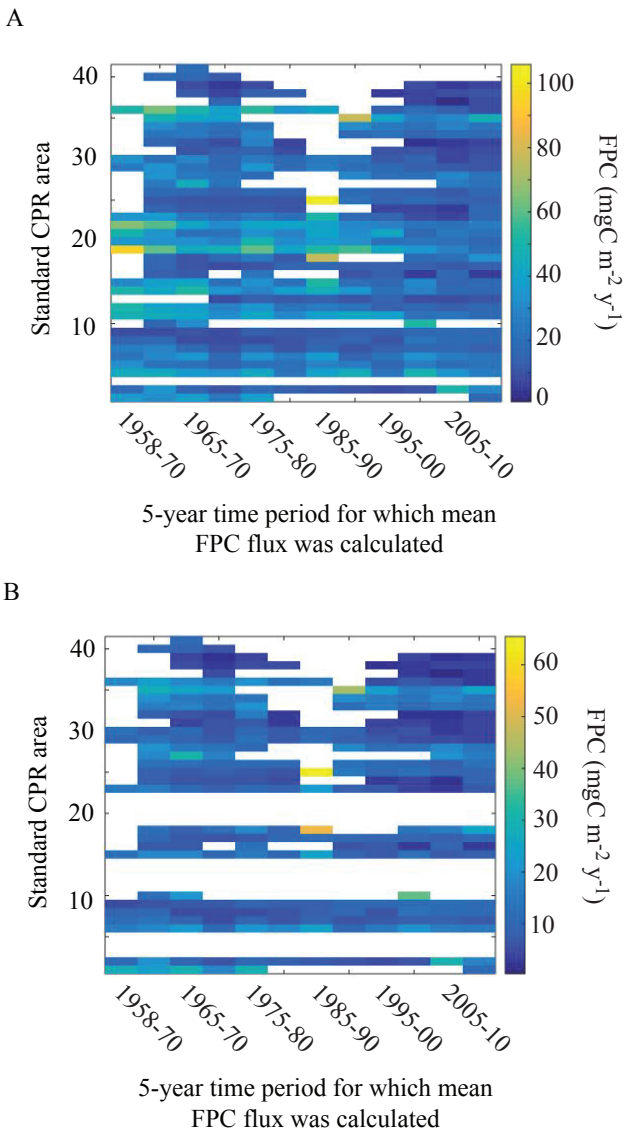

Figure 3.6. Mean copepod fecal pellet carbon (FPC) flux (mgC m^{-2} y^{-1}) through A) 30 m and B) 1000 m, for each standard CPR area; whited out regions either had insufficient data or the mean depth of the area was less than 1000 m (B).

Fecal pellet carbon flux changes through time, but the change is not consistent over the region (Fig. 3.6, Fig. 3.7). In most regions flux through the 30 m horizon is decreasing over the study period and 25% of the areas have significant downward trends ($p < 0.05$). The steepest decline in flux through 30 m is occurring off the coast of the Iberian Peninsula (Area 36, slope = -4.8 mgC m^{-2} y^{-2}, $p << 0.01$, $R^2 = 0.85$). Other areas where this shallow flux is significantly decreasing include the North Sea, and waters along the eastern side of the study region (mean slope = -2.7 mgC m^{-2} y^{-2}, $p < 0.05$, mean

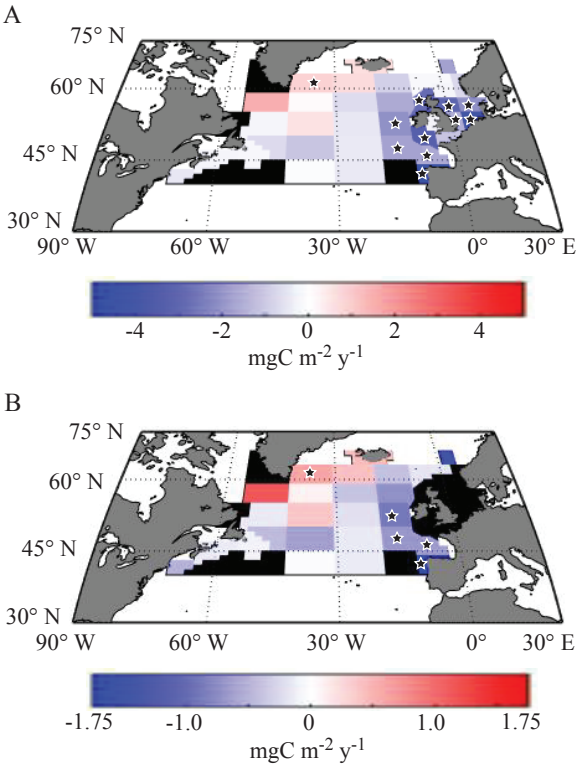

Figure 3.7. Change in mean copepod fecal pellet carbon flux (mg C m^{-2} y^{-1}) from 1958 to 2013, across the northern North Atlantic Ocean through A) 30 m and B) 1000 m; areas which are blacked out indicate insufficient data (< five 5-year periods available) or mean depth is less than 1000 meters (6B only). Stars indicate significant trends ($p < 0.05$).

$R^2 = 0.64$, Fig. 3.7A). The only area with a significant upward trend in fecal pellet carbon flux through 30 m is off the southeastern coast of Greenland (Area 9, slope = 0.86 mgC m^{-2} y^{-2}, $p << 0.01$, $R^2 = 0.88$, Fig. 3.7A). Fecal pellet carbon flux is also increasing notably in the Labrador Sea (Area 18, Fig. 3.7A); however the trend is not significant.

The trends of fecal pellet carbon flux through 1000 m mirror those of flux through 30 m; however, change over the time series is less dramatic at depth than near the surface, and fewer areas show significant trends (Fig. 3.7B). Flux through 1000 m off the coast of the Iberian Peninsula is decreasing most (Area 36, slope = -1.7 mgC m^{-2} y^{-2}, $p << 0.01$, $R^2 = 0.84$), and flux to 1000 m is increasing only in the waters east of Greenland (Area 9, slope = 0.59 mgC m^{-2} y^{-2}, $p << 0.01$, $R^2 = 0.89$).

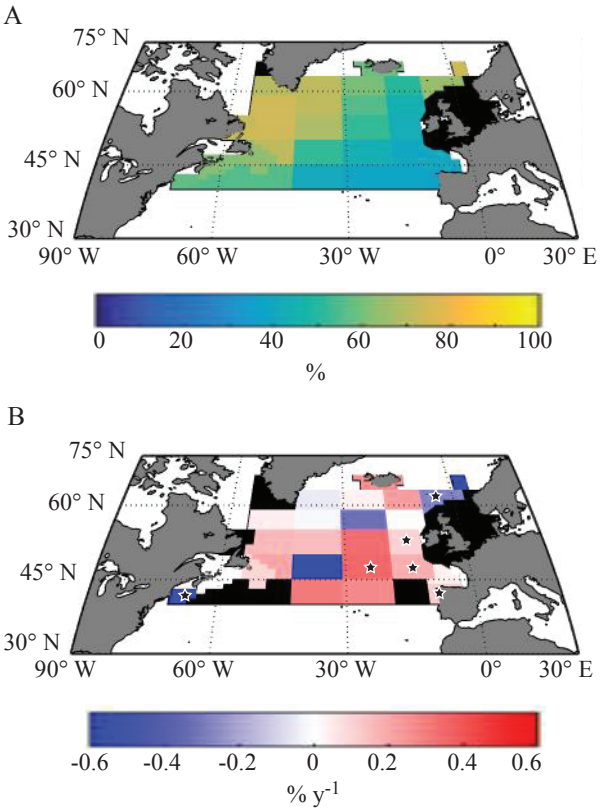

Figure 3.8. A) Mean copepod fecal pellet carbon flux efficiency (ratio of flux through 1000 m to 30 m, %) from 1958 to 2013, across the northern North Atlantic Ocean and B) change in flux efficiency over the time series; areas which are blacked out indicate insufficient data (< five 5-year periods available) or mean depth is less than 1000 meters (6B only). Stars indicate significant trends ($p < 0.05$).

Fecal pellet carbon flux efficiency, or the percent of fecal pellet carbon which sinks from the upper water column (30 m) down to a sequestration depth (1000 m), is on average higher in the northwestern North Atlantic (Fig. 3.8A). Maximum mean flux efficiency over the entire time series is 75%, which occurs in the Norwegian Sea (Area 1); adjacent to this area, also in the Norwegian Sea, flux efficiency is significantly decreasing (Fig. 3.8B). Regions in the Labrador Sea also have high flux efficiency, but are not changing significantly over the time series. Flux efficiency is generally lower in the southeastern portion of the study region; minimum flux efficiency is 37%, and is observed off the Iberian Peninsula (Area 36). Flux efficiency is decreasing significantly in the northeastern and southeastern-most areas (Fig. 3.8B), with a maximum downward trend in and around the Gulf of Maine (Area 35, slope = -0.54 % yr^{-1}, $p < 0.01$, R^2 =

0.85). Flux efficiency is generally increasing significantly in the southeast portion of the study region, with a maximum increasing trend north of the North Atlantic subtropical oligotrophic gyre (Area 31, slope = 0.35 % yr^{-1}, $p = 0.04$, $R^2 = 0.55$). Overall flux efficiency is not changing much over the study period.

The study area contains many oceanographically diverse subregions. To understand the mechanisms driving changes in fecal pellet carbon flux, we focused on two areas experiencing the most change: Area 36 off the west coast of the Iberian Peninsula (negative trend), and Area 9 off the southeastern coast of Greenland (positive trend). Most of the standard CPR areas with significant trends in modeled copepod fecal pellet carbon flux show an average decrease over the 55-year time series (Fig. 3.7). Flux reaching 1000 m is decreasing the most off the Iberian Peninsula (Area 36, Fig. 3.7B); and while flux efficiency between 30 and 1000 m is low (Fig. 3.8A), it is significantly increasing there (Fig. 3.8B).

The biomass of most taxa is decreasing in this region (Area 36), and is correlated with decreasing fecal pellet carbon flux. Most notably these taxa include *Acartia* spp. ($R^2 = 0.78$, $p << 0.01$) and *Pseudocalanus*/*Paracalanus* spp. ($R^2 = 0.82$ to 0.85, $p << 0.01$). The decrease in the most abundant taxa (and thus biomass) is compensated for, to a limited degree, by an increase in some medium and large taxa such as *Centropages* and *Metridia* spp. On average, copepod concentrations in this region are decreasing over time, but mean copepod size is increasing (Fig. 3.9). This means that flux is decreasing but that the copepod community is becoming more efficient at exporting carbon to the deep sea.

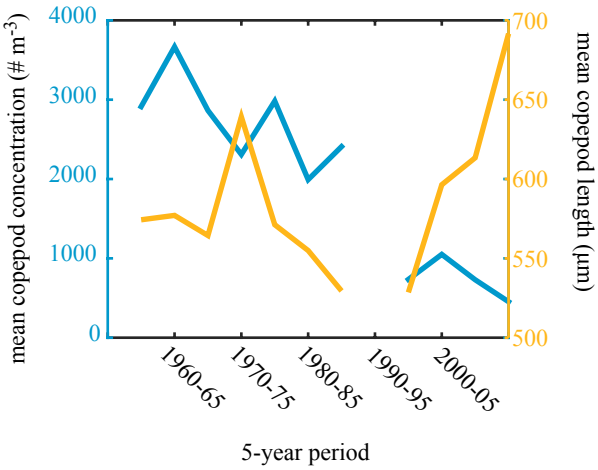

Figure 3.9. The mean copepod concentration (blue) and prosome length (yellow) in Area 36 over time.

Fecal pellet carbon flux is significantly increasing in one standard area: the waters off the eastern coast of Greenland (Area 9, Fig. 3.7). The increase in carbon flux is driven by an increase in copepod biomass ($R^2 = 0.60$ $p < 0.01$), in particular, *Calanus* spp. copepodids ($R^2 = 0.72$ to 0.74, $p << 0.01$), *Calanus finmarchicus* copepodid stages five and adults ($R^2 = 0.33$, $p = 0.05$), and *Pseudocalanus* and *Paracalanus* spp. copepodid stages one to adult ($R^2 = 0.32$ to 0.73 $p = 0.05$ to $<< 0.01$) are significantly correlated to the increase in fecal pellet carbon flux over the time series. Flux efficiency in this region is not significantly changing.

Modeled fecal pellet carbon flux through 30 m is closely tied to surface copepod concentration ($R^2 = 0.94$, $p << 0.01$). Flux through 1000 m is also related to copepod concentration ($R^2 = 0.88$ $p << 0.01$), but not as closely because there are other factors affecting how much of the fecal pellet carbon produced near the sea surface reaches depth (Fig. 3.10). When we consider flux efficiency (the ratio of flux at 1000 m to flux at 30

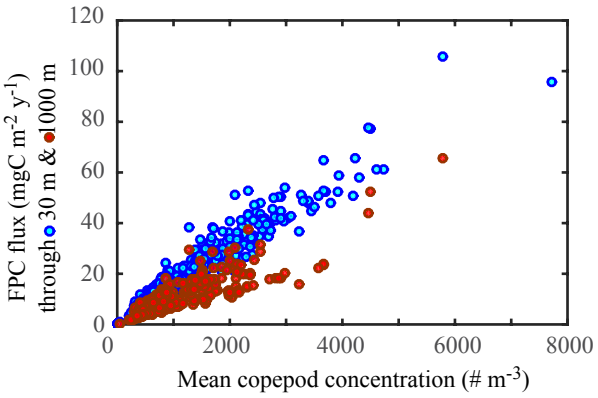

Figure 3.10. Mean copepod concentration versus fecal pellet carbon (FPC) flux to 30 (blue) and 1000 (red) m

m), we find a linear relationship with mean copepod length (Fig. 3.11A) and an asymptotic relationship with mean copepod biomass (Fig. 3.11B) for a given area and 5-year period. When copepod concentration and length are compared, we find that at low concentrations in an area and time period, it is possible to find copepods of any size within the range of this dataset. At the highest concentrations, however, mean copepod size is usually small (Fig. 3.12). We compare mean temperature for a region and 5-year period to mean copepod length (Fig. 3.13A) and mean copepod biomass (Fig. 3.13B) and find that both decrease with increasing temperature.

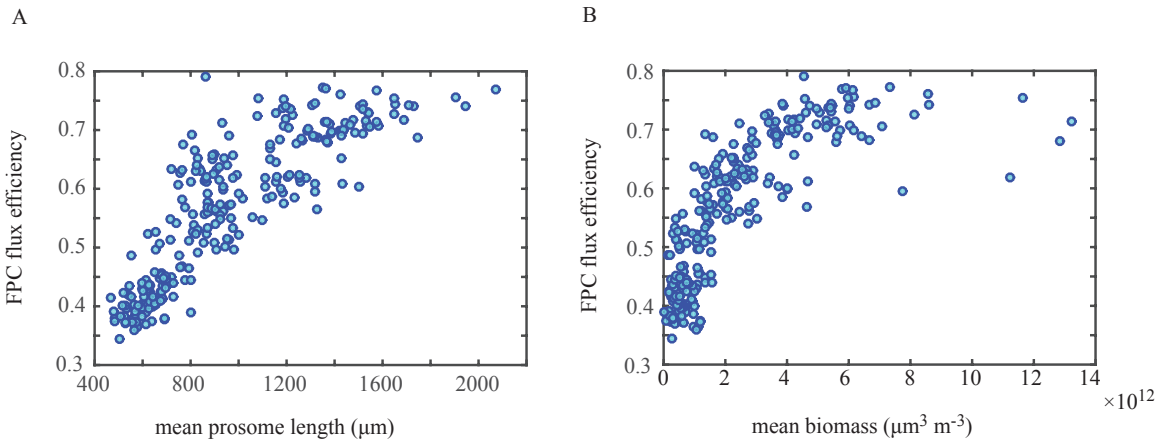

Figure 3.11. A) Prosome length and B) biomass versus fecal pellet carbon (FPC) flux efficiency between 30 and 1000 m

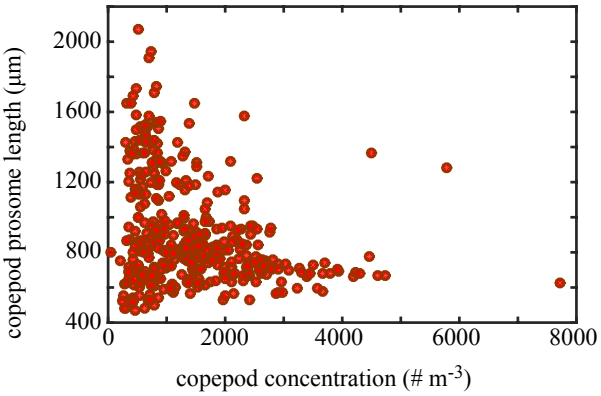

Figure 3.12. Mean copepod concentration versus prosome length

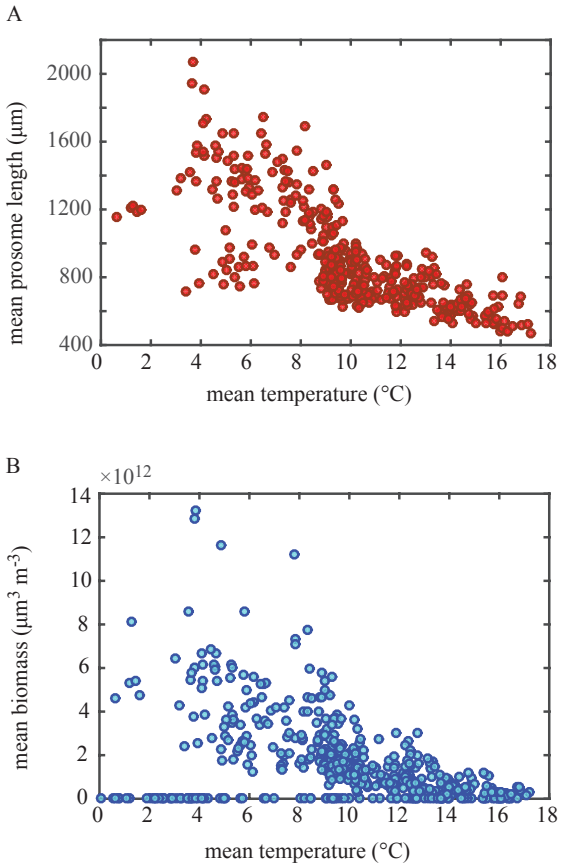

Figure 3.13. Mean sea surface temperature versus A) prosome length and B) biomass

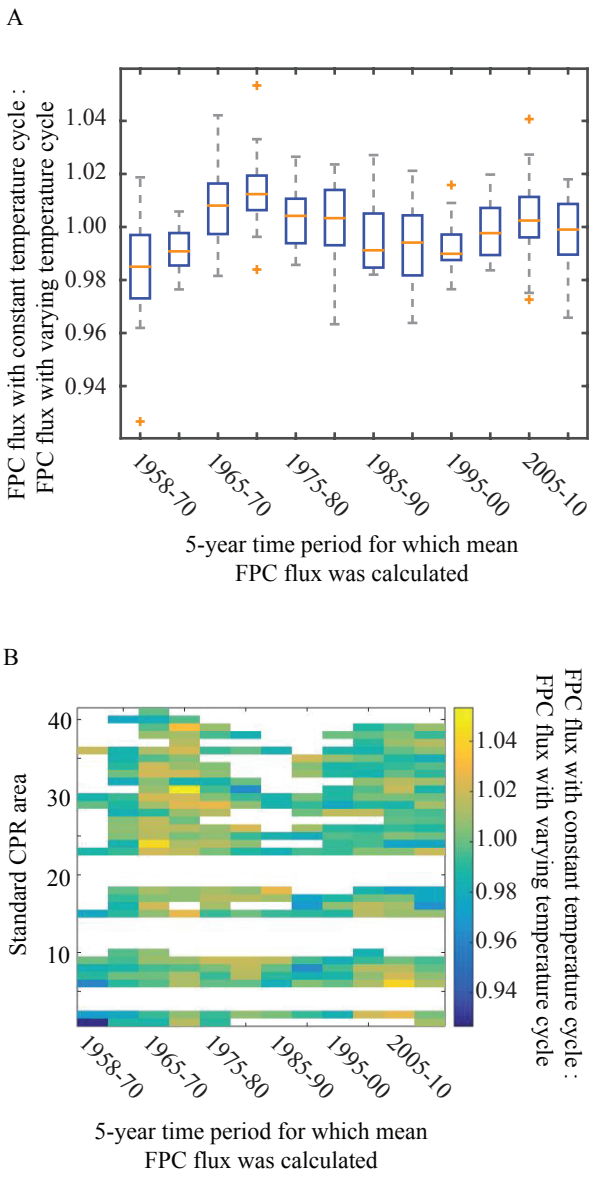

Figure 3.14. The ratio between mean fecal pellet carbon flux with the annual temperature cycle held constant, and with it varying from 5-year period to period: A) a box plot showing the median as a yellow line, 25th and 75th percentiles within the blue boxes, whiskers to the most extreme points not considered outliers, and yellow pluses representing outliers; and B) the ratio over time (x-axis) and space (y-axis); white areas indicate either insufficient data or CPR areas with mean depths of less than 1000 m.

Sensitivity analysis reveals the relative impact of different variables on the model output. The direct impacts of temperature on copepod metabolism and size are relatively small (Fig. 3.14). When the annual temperature cycle is held constant over the time series (run_{exp}), and compared to a model run in which the temperature cycle varies among 5-year periods (run_0), there is no significant difference (Fig. 3.14A). The median ratio of run_{exp} to run_0 is 1.0 ± 0.01 ($n = 14965$). On average over the study region, fecal pellet carbon flux is greater with temperatures held constant ($run_{exp} > run_0$) by the most during

the period 1970-75 (Fig. 3.14A). Holding the annual temperature cycle constant did not affect the different standard CPR areas differently from one another (Fig. 3.14B).

The impact of changing copepod community composition over the time series is also explored by holding the annual cycle of each copepod taxon constant through time. The ratio of fecal pellet carbon flux calculated while holding the taxonomic cycles constant (run_{exp}) to that calculated with varying community composition (run_0) does not vary greatly until the 1995-2000 time period (Fig. 3.15). Median ratio of run_{exp} to run_0

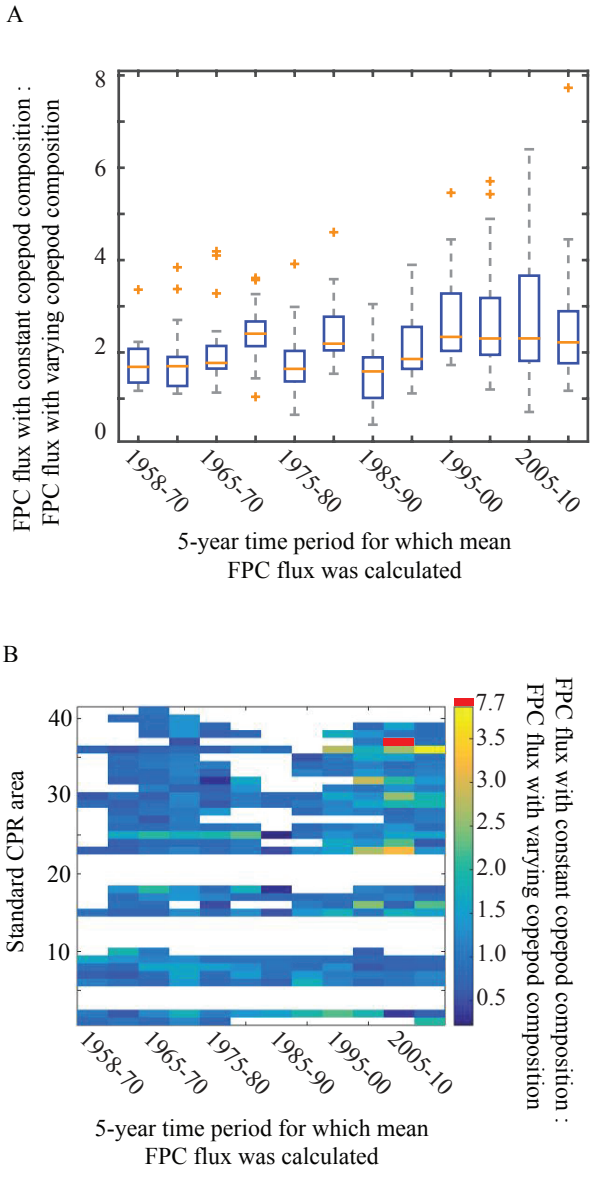

Figure 3.15. The ratio between mean fecal pellet carbon flux with the copepod composition held constant, and with it varying from 5-year period to period: A) a box plot showing the median as a yellow line, 25th and 75th percentiles within the blue boxes, whiskers to the most extreme points not considered outliers, and yellow pluses representing outliers; and B) the ratio over time (x-axis) and space (y-axis); white areas indicate either insufficient data or CPR areas with mean depths of less than 1000 m.

over the time series is 1.02 ± 0.50. After 1995, mean fecal pellet carbon flux is greater when the copepod community does not vary over the time series (run_{exp}, Fig. 3.15A). For this period median ratio of run_{exp} to run_0 is 1.1 ± 0.62. This pattern holds for most of the standard CPR areas, with exception of the more northern areas (Areas 1-9, Fig. 3.15B).

Diel vertical migration behavior impacts copepod fecal pellet carbon flux differently depending upon whether copepods that remain at the sea surface continue to feed throughout the day when migrators are at depth. Allowing non-migrating copepods to feed all day has a significant and consistent impact on modeled fecal pellet carbon flux. When we do not allow the copepods to migrate (run_{exp}), fecal pellet carbon flux is consistently higher than when we do (run_0, Fig. 3.16A). The median ratio of run_{exp} to run_0 is 1.0 ± 0.16 (n = 14965). Averaged over all the areas, fecal pellet carbon flux does not vary significantly among 5-year periods in the time series (Fig. 3.16A). There are spatial differences, however. Fecal pellet carbon flux from a large block (Areas 17, 18, 25, 26) in the northwestern part of the study area is disproportionately higher when the copepods do not vertically migrate (Fig. 3.16B).

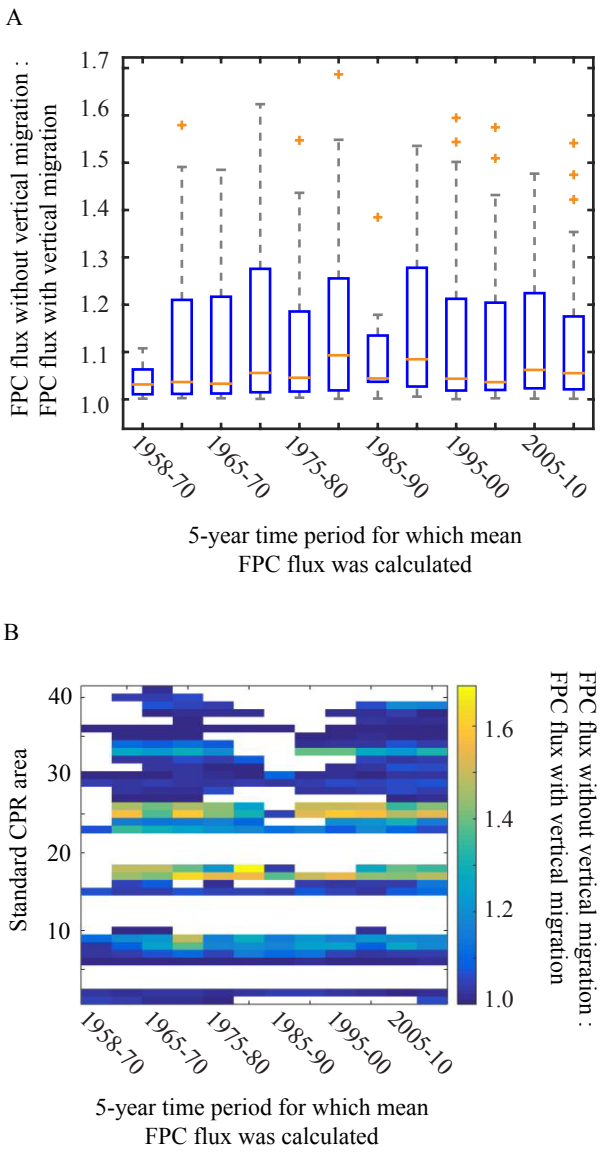

Figure 3.16. The ratio between mean fecal pellet carbon flux with the copepods not migrating, and with them migrating; the copepods that are migrating are not feeding one hour into migration, while those at the surface continue to feed. This ratio is represented as: A) a box plot showing the median as a yellow line, 25th and 75th percentiles within the blue boxes, whiskers to the most extreme points not considered outliers, and yellow pluses representing outliers; and B) the ratio over time (x-axis) and space (y-axis); white areas indicate either insufficient data or CPR areas with mean depths of less than 1000 m.

Discussion

The goal of this model is to examine the effect of changing copepod community structure on copepod fecal pellet carbon flux and flux efficiency, using size-related growth, metabolic processes, sinking rates, and vertical migration behavior. The point sampling scheme of the CPR dataset makes estimating a continuous process, such as fecal pellet flux, challenging. However, datasets with the large spatial and temporal extent of the North Atlantic CPR program are rare. Using climatologies of copepod abundance allows us to transform the CPR data into a continuous abundance function, and to estimate flux for every day of the time series; this also means that the flux estimates from this model are background estimates, and are not likely to reflect ephemeral bloom events. At the Bermuda Atlantic Time Series (BATS) site, fecal pellet carbon flux estimated with sediment traps at 1500 m depth, between December 2006 and November 2007, averaged 0.07 to 0.27 mgC m^{-2} d^{-1} (Shatova et al. 2012), compared with our mean estimated flux in CPR region 40 (closest to BATS) of 0.02 to 0.07 mgC m^{-2} d^{-1} through 1000 m. The flux estimates from Shatova et al. (2012) include periods of increased productivity driven by the passage of eddies through the region. Fecal pellet carbon flux climatologies produced by our model do reflect similar patterns in seasonal flux variability to those presented in Shatova et al. (2012). However, the discrepancy in magnitude of flux indicates that our flux estimates capture long-term variability in background flux, more than short-lived bursts of flux from daily to weekly events. A coastal study off the Iberian Peninsula (within CPR area 36) measured on-shelf and off-shelf fecal pellet carbon flux using floating sediment traps (Wexels Riser et al. 2001).

They found that copepod fecal pellet carbon flux from 50 to 200 m off-shelf was usually < 3 mgC m^{-2} d^{-1}, above 50 m on-shelf it averaged 61.9 m^{-2} d^{-1}, and above 50 m off-shelf it averaged 5.5 m^{-2} d^{-1}. Our model estimates that fecal pellet carbon flux through 30 m in this region are considerably lower, averaging 0.02 to 0.18 m^{-2} d^{-1}, and through 150 m are 0.02 m^{-2} d^{-1} to 0.15 m^{-2} d^{-1} over the time series. One cause for this discrepancy is that CPR region 36 includes mostly offshore waters sampled by the CPR, rather than the highly productive and nearshore waters sampled by Wexels Riser et al. (2001). Overall, compared with measured fecal pellet carbon flux, our model estimates are conservative but comparable in offshore regions for which data are available (i.e. Shatova et al. 2012), and underestimate flux through the surface waters in coastal regions. These discrepancies also highlight the importance of timescale. Our flux estimates are based upon averages over long temporal and large spatial scales. Sediment trap data, on the other hand, are short-term measurements of a relatively small area, especially from floating sediment traps.

In this fecal pellet carbon flux model, we assume that prey availability near the sea surface is uniform because we do not have access to detailed prey field information over the study region and period at this time. However, copepod fecal pellet production and fecal pellet volume increases asymptotically with prey availability (reviewed in Machine 1998, Besiktepe & Dam 2002). Fecal pellet carbon concentration per pellet volume is also impacted by prey. Krill fecal pellets contain relatively less carbon when the krill are feeding at high prey concentrations due to differences in absorption time in the gut (Atkinson et al. 2012). Prey type plays a role in pellet carbon content as well

(Urban-Rich et al. 2001, Atkinson et al. 2012). This model will be improved by including cycles of prey concentration and composition, and copepod responses to these cycles.

In evaluating the impact of different model variables, we find that allowing vertical migration has a surprising effect. We expected vertical migration to increase fecal pellet carbon flux because the copepods are producing fecal pellets deeper in the water column, exposing the pellets to less remineralization before sinking to 1000 m (Hansen & Visser 2016). However, modeled fecal pellet carbon flux increases when the copepods do not migrate to depth during the day (Fig. 3.16). Flux is increased under this scenario because the copepods in our model are assumed to feed when they are at the surface. When they migrate, they stop feeding and stop producing fecal pellets once their guts are emptied (2 h after descent from surface). Thus, in our model, the slight increase in flux due to copepods moving downward is not enough to outweigh the potential flux from continuous feeding at the surface. This result poses the question of whether feeding continues at depth. Previous work generally indicates that copepod guts are less full during the day, when they are deeper in the water column (Atkinson et al. 1996, Dagg et al. 1998). This work, however, relies on the detection of Chlorophyll *a* in copepod guts. If copepods are feeding on non-photosynthetic prey at depth, it could go unnoticed. It has also been suggested that patterns in diel prey selectivity may be related to prey mobility and/or predator avoidance (Wu et al. 2010). There is also indication from laboratory and field experiments that migrating copepods increase their feeding rates and digestion following periods of starvation (Runge 1980, Hassett & Landry 1988). Fecal pellet

production rates in our model do not account for rapid feeding after starvation at depth in the diel cycle, making our estimates of fecal pellet flux potentially too low. The results of this sensitivity analysis highlight the difference between surface production export versus water column production export, as well as raises questions about diel feeding patterns in copepods and how they might affect the active vertical transport of POC.

The northern half of the North Atlantic Ocean, our study region, encompasses a range of oceanographic conditions supporting different copepod species assemblages. Over the CPR time series (1958-2013), physical conditions have changed due to natural climate oscillations and more recently, acute warming (Reygondeau et al. 2015). Our study indicates that changes in copepod community composition have the greatest impact on flux, when compared with changes in temperature. In our analysis, holding the annual cycle of copepod abundances constant increases flux, as well as variability, in the later half of the time series (Fig. 3.15A). This indicates that the copepod community in the North Atlantic is shifting towards one that produces less flux than the mean reference community; this shift occurs after 1985. A dramatic northward shift in the distribution of copepod communities is observed in other studies of the CPR time series after 1985 (Harris et al. 2015). As warmer water communities move north (Beaugrand et al. 2009), our model indicates that copepod biomass, flux (Fig. 3.13B), and flux efficiency (Fig. 3.11B) will decrease. At a time series station (L4) in the English Channel, similar decreases in copepod biomass to those we found in the CPR data have been observed, with change being driven by natural decade and multidecadal climate oscillations (e.g.

the North Atlantic Oscillation, NAO, and the Atlantic Multidecadal Oscillation, AMO), overlain in more recent years by acute and rapid warming (Reygondeau et al. 2015).

The areas where fecal pellet carbon flux is decreasing (Fig. 3.7) are in the warmer part of the study area (Fig. 3.1); and the waters west of the Iberian Peninsula, where flux is decreasing the most, are some of the warmest. There, copepod concentrations are also decreasing (Fig. 3.9). An analysis of the CPR phytoplankton and zooplankton datasets together shows an overall positive correlation between copepod and phytoplankton abundance (Richardson & Schoeman 2004). The same study suggests that warming temperatures bolster phytoplankton populations in cooler regions, while it dampens them in regions that are warmer to begin with. While this southern region shows decreasing flux, the proportion of the fecal pellet carbon produced that is reaching 1000 m is increasing (Fig. 3.8B). This increasing flux efficiency is caused by increasing average size of copepods in the region (Fig. 3.9), driven mainly by *Centropages* and *Metridia* spp. In 1998 Wexel Riser et al. (2001) observed low fecal pellet carbon flux at a station in this region, despite large numbers of small calanoid copepods present. The majority of fecal pellet flux was attributable to relatively large fecal pellets (Wexels Riser et al. 2001). This region is influenced not only by shifts in the NAO, but also seasonal upwelling. While increased NAO winter values negatively impacted offshore copepod abundance, variable winter upwelling conditions affected coastal production from year to year. Upwelling favorable winters supported greater productivity of coastal copepods (Bode et al. 2009) and perhaps the larger species that are driving fecal pellet flux efficiency in this area. The modeled fecal pellet carbon flux estimates presented here are based upon 5-year

climatologies and given the impact of the NAO, a decadal oscillation, these results may be sensitive to the time-scale of the climatologies used.

Flux in most of the study region is decreasing, but in the western North Atlantic, fecal pellet carbon flux shows the opposite trend. The increase in flux off the southeastern coast of Greenland is being driven by increases in the biomass of subarctic community-type species (as defined by Beaugrand et al. 2009): *Calanus* spp. copepodids (stages one to four), *Calanus finmarchicus* copepodid stages five and adults, and *Pseudocalanus* and *Paracalanus* spp. copepodid stages one to adult. While *Calanus* spp. copepodids are the most abundant copepods in this region (Fig. 3.17B), *Calanus finmarchicus* copepodid stages five and adult contribute most to copepod biomass due to their large size (Fig. 17A). Late stage *Calanus finmarchicus* are therefore driving the increase in fecal pellet flux in this region. The increase in calanoid copepod biomass off of Greenland may also be related to an increase in phytoplankton abundance. A temperature increase in this relatively cool part of the study area (Fig. 3.1) could lead to increased stratification, phytoplankton and zooplankton production (Reygondeau et al. 2015), and as our calculations suggest, increased fecal pellet flux. The importance of *Calanus finmarchicus* to fecal pellet carbon flux was also found in the Gulf of Maine (Stamieszkin et al. 2015). This pattern highlights the importance of size in addition to abundance in driving fecal pellet carbon flux.

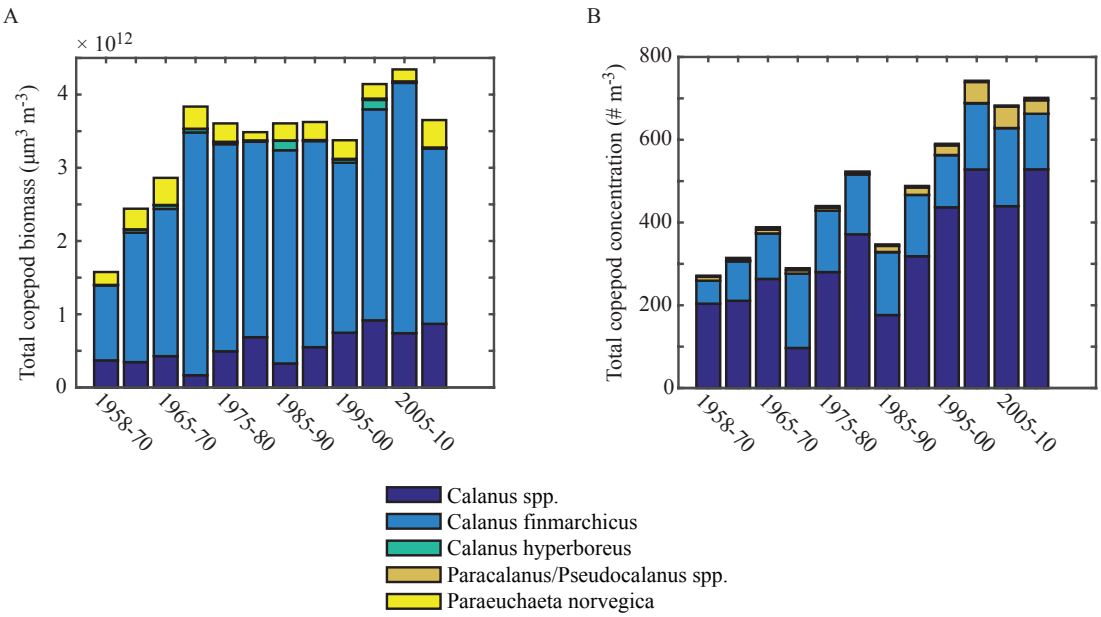

Figure 3.17. Bar graphs of total annual A) biomass and B) concentration of dominant copepod taxa in Area 9 over the time series; these taxa represent 99.5% of all copepods by biomass.

The composition of marine communities is responding to climate change. As ocean temperatures warm, communities shift north; primary production responds to increased stratification, and zooplankton biomass responds to phytoplankton availability. The North Atlantic patterns of warming temperatures and decreasing copepod biomass are clear; we find that warming leads to reduced copepod mean size and biomass (Fig. 3.13), and thus to reduced fecal pellet carbon flux (Fig. 3.11B). However, local physical dynamics and change within copepod communities can cause modeled fecal pellet carbon flux in particular regions to differ. For example, in the region off the Iberian Peninsula flux is decreasing as a result of declining biomass, but the decrease is dampened due to an increase in a few larger copepod species. In waters east of Greenland, warming is coincident with an increase, rather than decrease, in biomass and fecal pellet flux. We

have identified generalized patterns relating fecal pellet carbon flux to copepod communities and temperature, but these relationships must be used with an understanding of local conditions. Future work will focus on incorporating phytoplankton dynamics, as well as trade-offs between the export of unconsumed phytoplankton biomass versus fecal pellets, in the biological carbon pump.

CHAPTER 4

ZOOPLANKTON GRAZING EFFECTS ON PARTICLE SIZE SPECTRA IN NATURAL PLANKTON COMMUNITIES

Introduction

There are two contrasting ways to view plankton communities in the ocean: as size-structured and as species-structured. The interchangeability of different species of similar size is central to a size-based ecosystem view. This concept is supported by the finding that zooplankton grazers have an optimal size range in which they feed regardless of the prey type (Kiørboe 2008, Wirtz 2012, Boyce et al. 2015). However, this interchangeability is counter to traditional food web models, which emphasize connections between individual species or taxonomic groups. The size-based view also contradicts the established ecological concepts of keystone and foundational species, which suggest that a few species play disproportionally large roles in structuring their ecosystems, or in storing and moving energy to other trophic levels (Paine 1966, Jones et al. 1944).

Plankton community size structure is usually characterized by a power-law relationship between body size and biomass within a size class (Sheldon et al. 1972). Differences in this relationship among ecosystems can be attributed to bottom-up controls, such as nutrient availability (Sprules & Munawar 1986, Taniguchi et al. 2014), and top-down controls, such as predation (Zhou 2006, Taniguchi et al. 2014). Predation itself is constrained by size, with individual predators or grazers selecting prey within a narrow size range of approximately 10% of their own body size (Kiørboe 2008). Others

have found a log-linear relationship between predator and prey size, corroborating narrow prey selection (Wirtz 2012, Boyce et al. 2015). Pelagic tunicates are a notable exception to these allometric rules. These gelatinous filter-feeding zooplankton can be multiple centimeters long, but can feed on sub-micron sized plankton (Sutherland et al. 2010). This adaptation and gelatinous body plan are specialized to allow pelagic tunicates to persist in episodically food-replete environments (Acuña 2001).

Early grazing experiments that used natural assemblages of microplankton prey showed that copepods graze preferentially on the most abundant prey particles regardless of their size (Parsons et al. 1967, Poulet 1973), or consume larger particles first, followed by the most abundant (Richman et al. 1977). Due to the strong size-structuring in the ocean, size is considered a "master trait" in marine ecology (Litchman & Klausmeier 2008, Litchman et al. 2013, Barton et al. 2013) and food web models based upon size spectra (abundance as a function of individual length or mass) are well established in the field of oceanography (Banas 2011, Zhou et al. 2010, Taniguchi et al. 2014).

Size is also an important variable in understanding the efficiency of the biological carbon pump. The biological carbon pump is a set of processes that moves biogenic carbon from the surface to the deep ocean (Ducklow et al. 2001). When biogenic carbon sinks deep enough, often out of a surface mixed layer, it is decoupled from the atmosphere-ocean interface (de la Rocha & Passow 2007). When a higher proportion of particles produced at the ocean's surface sink below this depth, the biological carbon pump is sequestering carbon more efficiently. In the field, the production of larger

particles can explain increases in carbon export efficiency (Boyd & Newton 1999), because particle size is directly related to sinking rate (Guidi et al. 2008). Therefore, understanding the processes that give rise to particle size structure is critical to understanding variability in the ocean carbon cycle (de la Rocha & Passow 2007).

Interactions among plankton trophic levels play a central role in shaping particle size structure through grazing, respiration, excretion and egestion (Legendre & Michaud 1998, Ward et al. 2014). These metabolic rates and processes often scale allometrically with body size (Brown et al. 2004). Particles that are not consumed by grazers sink if they are large and dense enough; for example, large, ballasted diatoms often contribute disproportionately to particle flux measured at depth (Buesseler 1998). Small particles that would otherwise not sink can be aggregated by grazers and egested as larger fecal pellets, which also contribute to measured particle flux (Turner 2015, Wiedmann et al. 2014, Laurenceau-Cornec et al. 2015). Larger mesozooplankton produce larger fecal pellets which are more likely to sink below the surface mixed layer (Uye & Kaname 1994, Mauchline 1998, Stamieszkin et al. 2015). Mesozooplankton size structure therefore impacts particle size and flux potential in two ways: 1) in consuming particles within a particular size range but leaving those too small or too large, and 2) by creating larger particles from those consumed.

In this study, we present results from a series of experiments designed to examine the net effect of mesozooplankton grazing and egestion on particle size structure. The experiments use natural assemblages of mesozooplankton grazers, as well as

phytoplankton and microzooplankton prey, collectively termed microplankton. We analyze the experiments using imaging technology, which allows us to consider both size and species simultaneously. We are interested in how the plankton community structure, in terms of size and species composition, changes over the course of the year under different physical conditions. We hypothesize that the impact of mesozooplankton grazing on the microplankton community will reflect the size preferences of the grazers, and that when we increase the mesozooplankton grazing pressure, gaps in the microplankton size structure reflecting the narrow size-selection window will appear. An alternative hypothesis is that we will observe a species or taxon-specific prey preference, which results in the removal of a taxonomic group. Finally, we hypothesize that fecal pellet production by the mesozooplankton will shift the particle spectrum toward larger particles, increasing the potential for downward particle flux.

Materials and Methods

We conducted five experiments in 2014, at different times of year to capture the seasonal variability in plankton community structure and physical conditions. We used natural assemblages of both mesozooplankton grazers and microplankton prey.

Field collections - Plankton were collected at one station (DMC2) approximately 5 nm from the mouth of the Damariscotta River, in the Gulf of Maine (43º 45.027' N, 069º 20.236' W) (Fig. 4.1). Sampling and experiments were conducted over seven months, from the beginning of April to the end of October 2014 (Table 4.1). We collected the microplankton community (< 200 μm) by sampling 24 L of whole seawater from the

chlorophyll maximum, using 3 L Niskin bottles. We gently passed the water through tubes fitted with 210 μm mesh directly from the Niskin bottles into a large cooler to remove mesozooplankton. The mesozooplankton (≥ 200 μm) community was sampled with a 200 μm mesh, 0.5 m ring net and a non-filtering cod end. We conducted one vertical tow to approximately 100 m depth, which was 5 to 10 m above the seafloor, thereby sampling the entire mesozooplankton community. Once onboard, the live mesozooplankton were immediately diluted and transferred into containers of whole seawater, and placed into a cooler with ice.

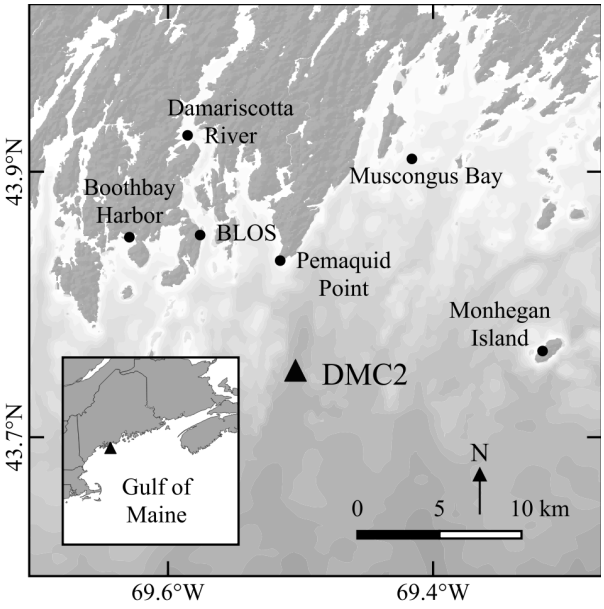

Figure 4.1. Map of the study region; station DMC2 is marked by a triangle; Bigelow Laboratory for Ocean Sciences (BLOS) and other landmarks are indicated by dots.

Lab incubations - Laboratory work was conducted at Bigelow Laboratory for Ocean Science (BLOS) in East Boothbay, Maine, U.S.A. (Fig. 4.1). We started the laboratory experiments within 2 to 3 h of the field collections, ensuring that the plankton were alive and active. Each experiment included treatment and control containers, in triplicate. Each of the six incubation containers consisted of two nested 1 L tripour beakers. The inner beaker had a 210 μm mesh bottom, so that fecal pellets produced by mesozooplankton would fall through the mesh and be protected from coprophagy (Urban-Rich 2001). The incubation containers were filled with 600 ml of 210 μm-filtered seawater, containing the microplankton community. We then added 100 ml live mesozooplankton suspension to the treatment containers, and 100 ml of 210 μm-filtered mesozooplankton suspension water (without grazers) to the control containers, so that there was 700 ml water in all containers. The containers were incubated at ambient near-surface temperature for 4 h. Preliminary experiments showed that there was no significant difference when the containers were incubated in the dark versus the light, likely due to the short incubation time; we therefore incubated all containers in the dark.

Table 4.1. Summary of experimental conditions. Incubation temperature is as close to ambient temperature as possible. Microplankton area based diameters (ABDs) are from FlowCam analysis. Mesozooplankton prosome lengths (PLs) are measurements made after the experiments, using ImageJ software and preserved samples. Numbers reported are the mean ± one standard deviation.

Date of experiment	**Incubation temperature (ºC)**	**Microplankton ABD (µm)**	**Mesozooplankton PL (µm)**
03 April 2014	2.0	26.5 ± 15.0 n = 759	230.0 ± 156.4 n = 557
06 May 2014	5.5	48.2 ± 28.4 n = 1114	652.5 ± 747.7 n = 93
07 July 2014	14.0	23.8 ± 14.7 n = 5967	1317.0 ± 961.9 n = 142
25 August 2014	15.0	32.5 ± 17.3 n = 4203	874.4 ± 370.8 n = 94
21 October 2014	12.0	32.0 ± 18.6 n = 2516	691.4 ± 223.5 n = 124

After the 4 h incubation, the inner mesh-bottom beaker was removed and the strained contents (zooplankton ≥ 210 μm) were preserved in 5-6% buffered formalin for analysis. The beakers containing the remaining 700 ml seawater, microplankton that had not been grazed, and fecal pellets, were placed into an ice bath to halt grazing and degradation, until they were subsampled (150 ml) for FlowCam® analysis (see "Lab analysis" below). The rest of the sample (550 ml) was refrigerated at 3-5 °C to minimize degradation processes, until it was processed via microscopy.

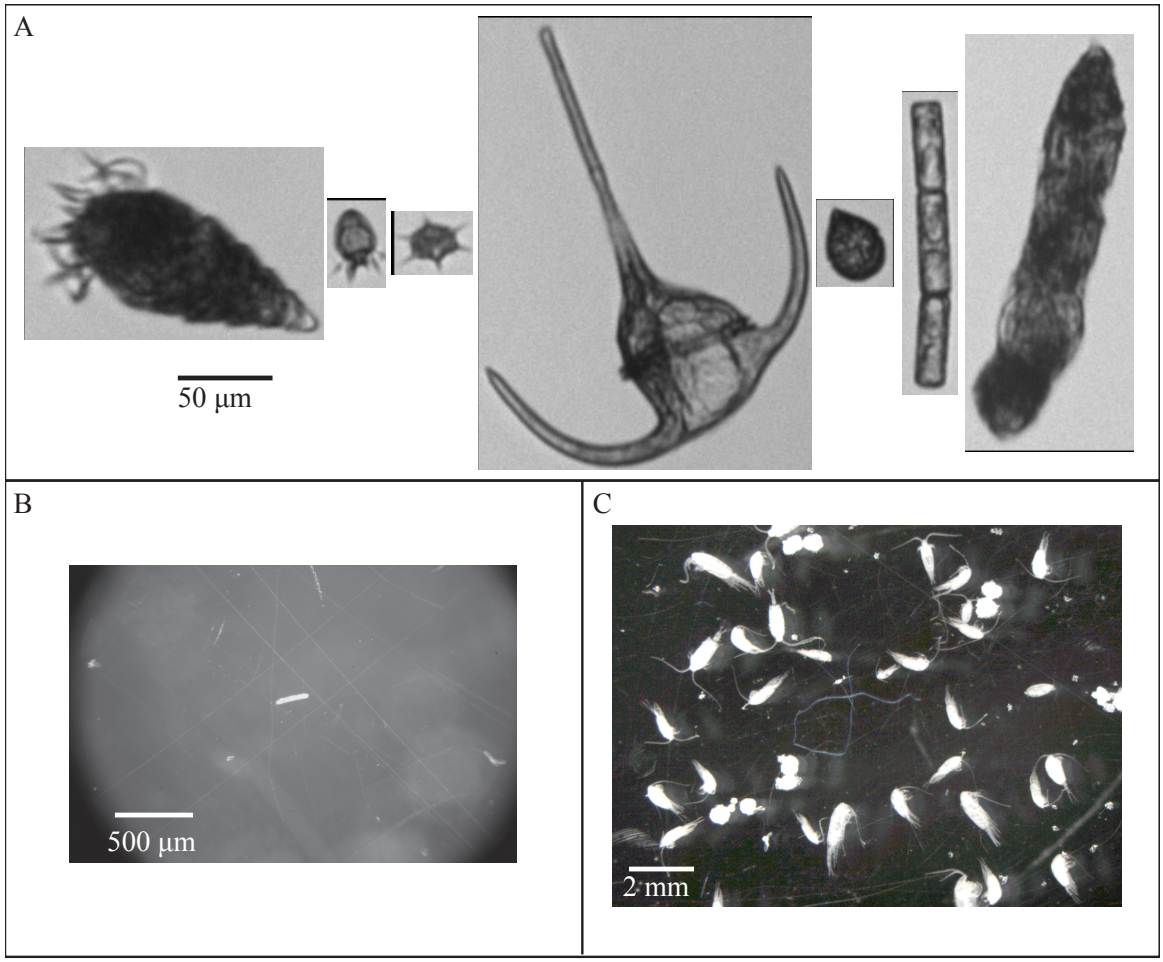

Figure 4.2. Example images from the experiment analysis: A) FlowCam images from left to right, *Laboea* sp., small ciliate, silicoflagellate, large *Ceratium* sp., small dinoflagellate, small chain diatom, mesozooplankton fecal pellet; B) fecal pellets to be analyzed with ImageJ; C) copepod grazers analyzed with ImageJ software.

Lab analysis - We analyzed 150 ml of the incubated seawater with a Fluid Imaging Technologies, FlowCam® (VS IV) in "trigger mode," which collects images of the naturally fluorescing particles in the sample due to chlorophyll autofluorescence (Fig. 4.2A). This mode of data acquisition has been used previously in grazing experiments (Ide et al. 2008). The FlowCam software, VisualSpreadsheet®, also collects a suite of measurements for each particle image, including area based diameter (ABD). We used a lower limit of 10 µm ABD because smaller particles were unidentifiable and close to the instrument's lower range of particle detection using a 4 x objective (1 um per pixel). The upper limit of microplankton size was 200 µm due to how we defined and separated meso- and microplankton. Fecal pellets collected in the incubation containers from the remaining 550 mL were processed within 8-16 h of the incubation after being stored at 3-5 °C. We subsampled and photographed a minimum of 50 representative fecal pellets from a known fraction of the sample collected, using a Canon Rebel T3i digital camera attached to an Olympus SZ60 microscope (Fig. 4.2B). Similar to the fecal pellets, the preserved mesozooplankton from all experiments were subsampled and photographed using a Leica DFC290 with FireCam® software (Fig. 4.2C). We used open source ImageJ software to estimate ABD for fecal pellets and prosome length (PL) for mesozooplankton (Abràmoff et al. 2004).

Particle classification and data analysis - We estimated the size and concentration of particles before (initial samples) and after (control and treatment samples) the incubations, using the FlowCam. However, the FlowCam only captures images of a fraction of the particles that pass through it; we therefore applied a correction

factor to estimate particle concentration (no. mL^{-1}). When calculating the effect of mesozooplankton grazing on the microplankton community, we had to also take into account microzooplankton grazing (Nejstgaard et al. 1997). The difference in microplankton community concentration and size structure between the initial samples (pre-incubation) and the control samples (post-incubation, no mesozooplankton) was due to microzooplankton grazing (heterotrophs < 200 μm). Therefore, when calculating the impacts of mesozooplankton grazing (> 200 μm), treatment samples (post-incubation, mesozooplankton present) were compared to control samples, rather than to initial samples. Incubations times were short (4 h) to limit possible trophic cascade effects inside the incubation containers (Klaas et al. 2008).

We binned the collected images into taxonomic and size categories to explore the experiment results, using a histogram function (Matlab v. R2014b). VisualSpreadsheet software was used for automated identification of particles from the FlowCam samples. We binned the particles into general taxonomic categories: microzooplankton, chain diatoms, centric or pennate diatoms, dinoflagellates, colonial phytoplankton, silicoflagellates and unidentified. Microplankton were labeled "unidentified" if they were too small (mostly < 20 μm) or out of focus to identify by taxon. The unidentified microplankton were included in the size analyses. All classifications were confirmed by eye.

Binning data by size inherently adds some subjectivity to an analysis. We therefore chose bin widths based upon the sizes of the organisms in our samples. We also

tested several bin widths to make sure those that we selected did not conceal any important information about the community size structure. When calculating mean particle and mesozooplankton sizes (Table 4.1), we aggregated measurements from each triplicate within an experiment, to show variability within the communities for each of the five experiments. When calculating mean particle and grazer concentrations, and mean grazing impact, we calculated the means and standard deviations among triplicates for each experiment, to demonstrate the reproducibility of our experimental design.

We compared size distributions of the particles consumed by the mesozooplankton grazers with the size distributions of the grazers themselves. This was done by calculating the number of microplankton consumed which fell within a range of size bins, as described above. We then parameterized a log-linear relationship between the abundances of grazers and prey using a least-squares linear regression (Matlab v. R2014b). We also compared the abundances using published relationships (Kiørboe 2008, Wirtz 2012, Boyce et al. 2015). Finally, we estimated a relationship between a grazer size metric and the volume of particles produced during the incubations, again using a linear regression function (Matlab v. R2014b).

Results

Our goal in conducting multiple experiments over a year was to sample the entire annual seasonal cycle, but an extraordinarily severe winter prevented us from completing work after November 2014. The ambient sea surface temperature during the study period (April to November) ranged from 2ºC to 15ºC.

The taxonomic composition of the autofluorescing microplankton community (< 200 μm) varied over the duration of the study (Fig. 4.3). Microzooplankton constituted 42% of the microplankton by abundance in April and 70% in May. Most of the microzooplankton present in April were small (≤ 60 μm), whereas approximately half of the microzooplankton present in May were large ciliates of the genus *Laboea*. Small chain diatoms (≤ 40 μm) dominated in July, small dinoflagellates were the most abundant microplankter in August (≤ 50 μm), and silicoflagellates were most abundant in October (Fig. 4.3). Unidentified microplankton made up 35% of the total, on average.

Figure 4.3. Microplankton community composition

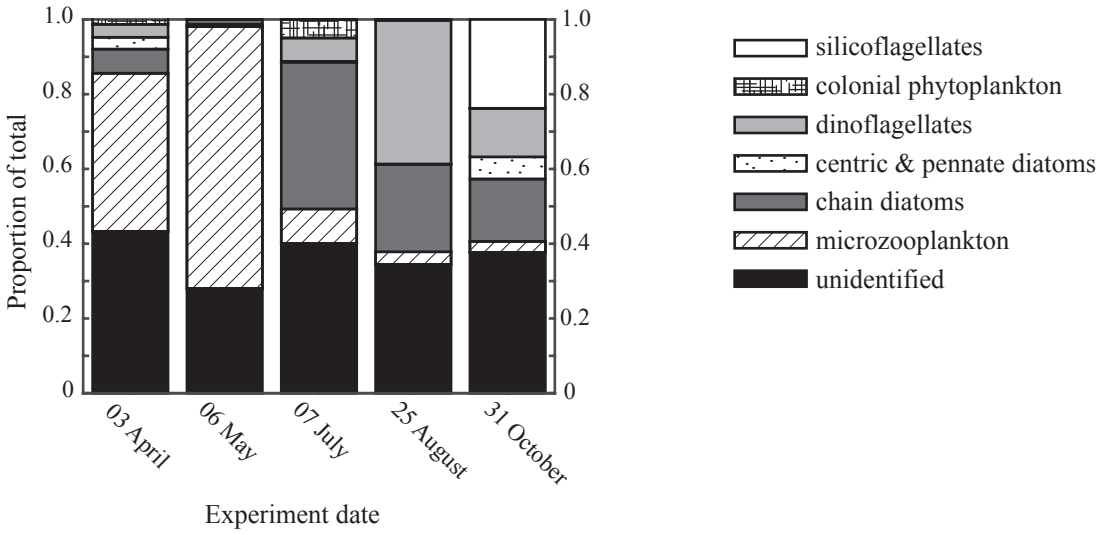

Figure 4.4. Microplankton size distribution from five experiments: A) 03 April 2014, B) 06 May 2014, C) 07 July 2014, D) 25 August 2014 and E) 31 October 2014. The distributions are represented as proportion of total individuals in each size bin. Bin width is 20 µm and size is estimated as area based diameter (µm).

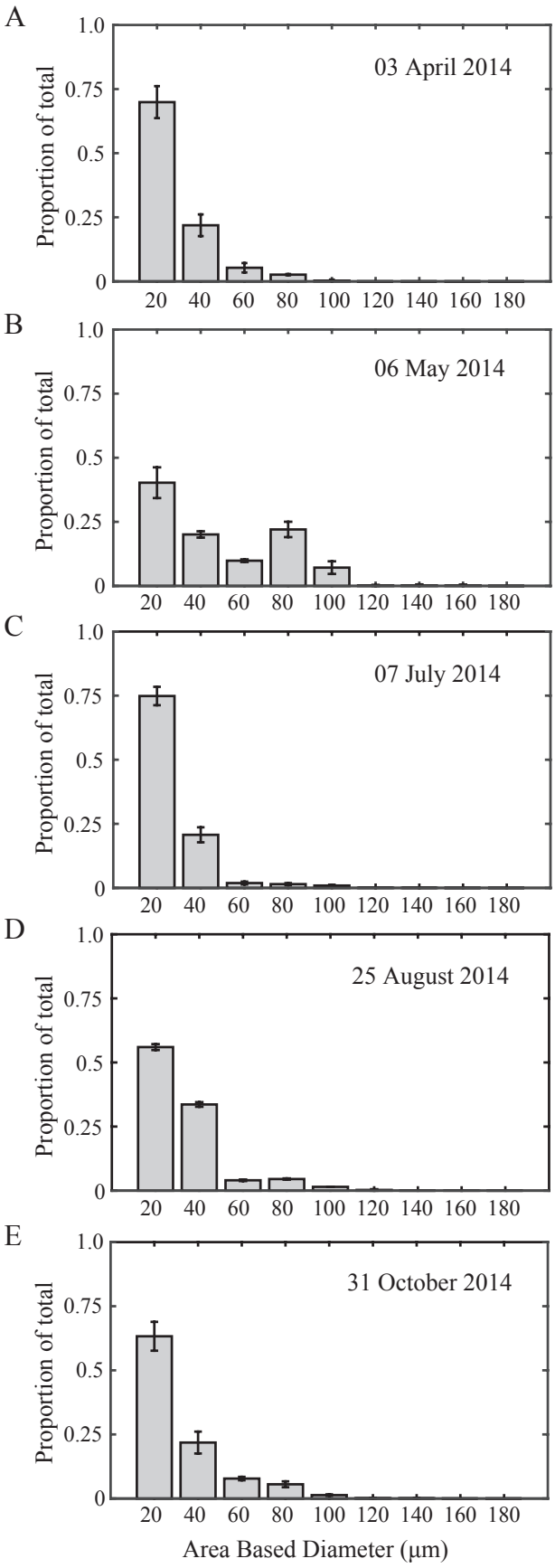

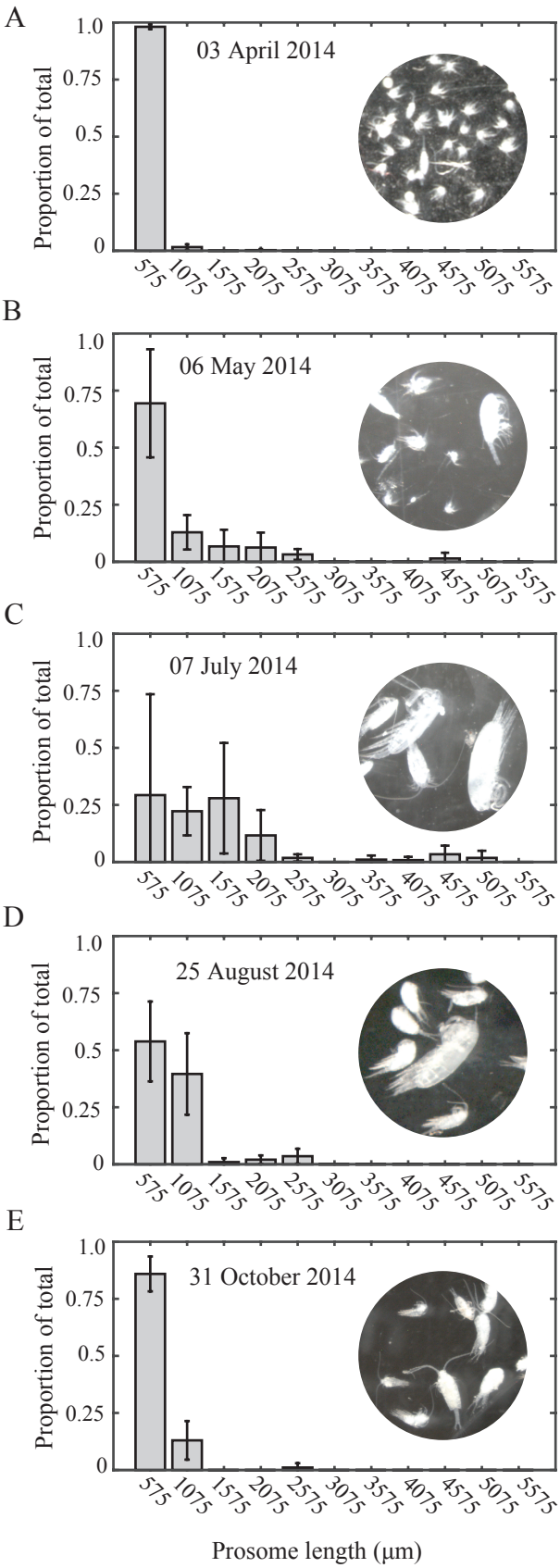

Figure 4.5. Mesozooplankton size distribution from five experiments: A) 03 April 2014, B) 06 May 2014, C) 07 July 2014, D) 25 August 2014 and E) 31 October 2014. The distributions are represented as proportion of total individuals in each size bin. Bin width is 500 µm and size is estimated as prosome length (µm). Inlaid images show general shifts in composition.

Microplankton size structure shifted throughout the experiments (Fig. 4.4). Mean microplankton size ranged from 23.8 ± 14.7 μm in July to 48.2 ± 28.4 μm in May (Table 4.1). The smallest microplankter included in the analysis was 10.0 μm ABD, due to instrument limitation based on the microscope objective used (4 x), and the largest microplankter measured was 164.5 μm ABD. The natural communities of microplankton had log-linear distributions in all experiments except for the one conducted in May (Fig. 4.4B).

Mesozooplankton community composition and size structure varied throughout the experiments as well. Copepods dominated the mesozooplankton community during all experiments except in April, when barnacle nauplii (*Balanus* spp.) were most abundant (Fig. 4.5A). Barnacle nauplii were still abundant in May, but mixed with calanoid copepods, including *Calanus finmarchicus* copepodids and adults, and genus *Pseudocalanus* (Fig. 4.5B). In July the mesozooplankton grazers were composed mostly of calanoid copepods, including late stage *Calanus finmarchicus,* and genera *Acartia*, *Pseudocalanus*, *Temora*, and *Centropages*. Cladocera were also present in the July mesozooplankton grazer community (Fig. 4.5C). During the August experiment the mesozooplankton included the genera *Centropages, Temora, Pseudocalanus* and *Calanus finmarchicus* (Fig. 4.5D). One of the three treatment containers also contained a Chaetognath; however, no consistent pattern in particle abundance indicated that the Chaetognath significantly altered the grazing impact of the mesozooplankton community. The Chaetognath was not included in the grazer body size analyses. The mesozooplankton grazer community in the final experiment, conducted at the end of

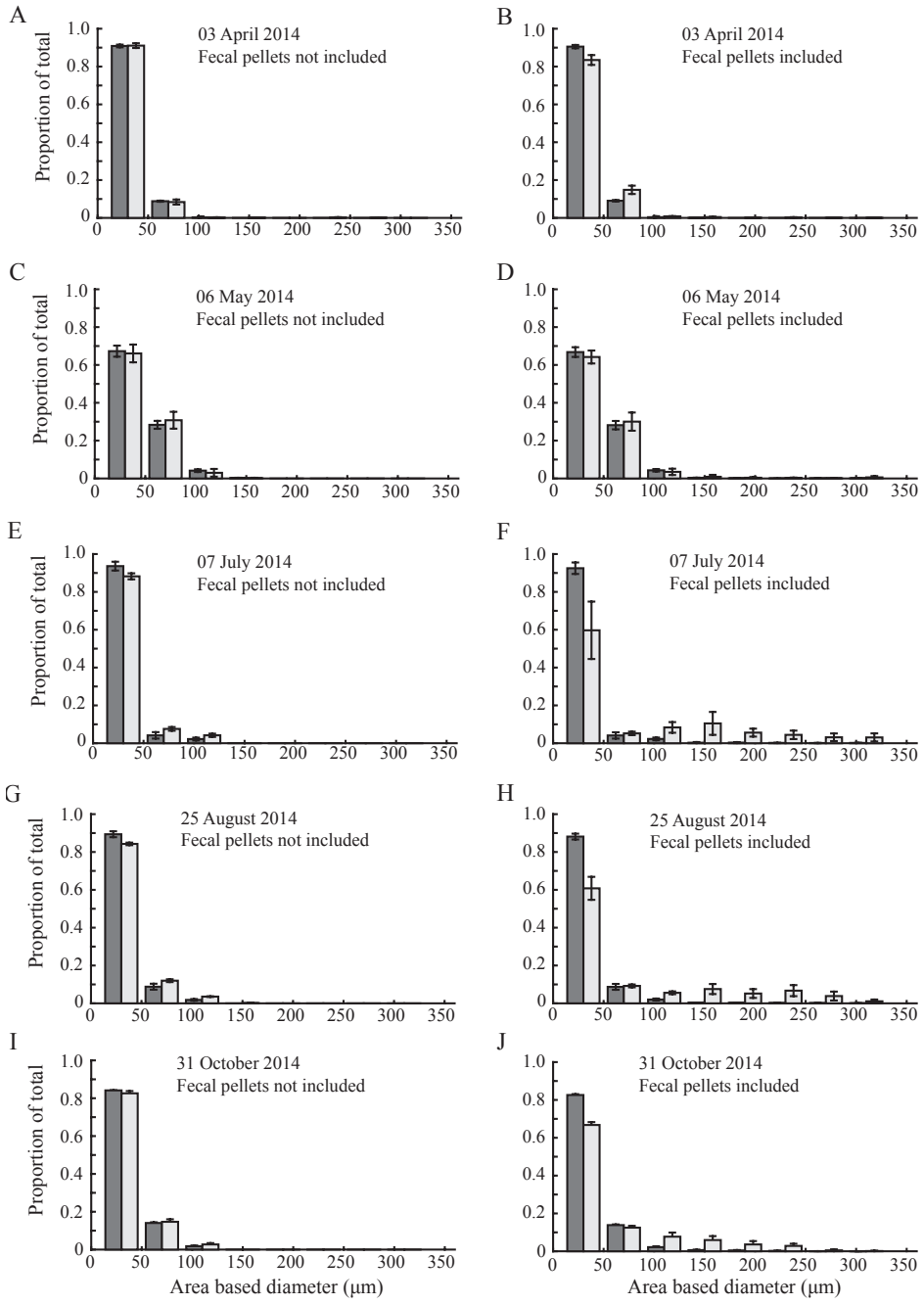

Figure 4.6. Microplankton size distributions from five experiments in 2014; each row represents data from one experiment. Dark gray bars represent results from the containers that contained no mesozooplankton grazers ("control"); light gray bars represent results from the containers containing mesozooplankton grazers ("treatment"). The lefthand column shows effects of grazing on the particle size distribution; the righthand column shows the effects of grazing and fecal pellet production on particle size distribution. The distributions are represented as proportion of total particles in each size bin. Bin width is 40 μm and size is estimated as area based diameter (μm).

October, was composed mostly of the genus *Temora,* and also contained some *Pseudocalanus and Centropages*. Late stage *Calanus finmarchicus* were also present, but sparse (Fig. 4.5E).

Mean mesozooplankton prosome length (PL) ranged from 230.0 ± 156.4 μm in April, to 1317.0 ± 961.9 μm in July (Table 4.1). These results were driven by the overwhelming dominance of small barnacle nauplii in April, and late stage *Calanus finmarchicus* in July (Fig. 4.5A and 4.5C, respectively). The smallest mesozooplankter measured 75.7 μm in PL and was found in the May experiment. The largest mesozooplankter measured $5.3x10^3$ μm and was in the July experiment.

The goal of these experiments was to study the grazing impact of mesozooplankton on particle size structure. We therefore calculated the percent of microplankton grazed to show that grazing did indeed occur, rather than to quantify specific grazing rates. We found that mesozooplankton grazing resulted in an average net loss of at least 10.4 ± 1.2% of microplankton in May, and at most 55.7 ± 12.6% in July (Table 4.2). However, grazing by the mesozooplankton did not result in a distinct change in microplankton size structure, as hypothesized. The size distribution of microplankton in the control containers, which contained no mesozooplankton grazers, was rarely different from the distribution of microplankton in the treatment containers, in which grazers were grazing (Fig. 4.6A, 4.6C, 4.6E, 4.6G, 4.6I). The only changes in size distribution related to grazing were observed in July and August, when particle relative abundance decreased in the 10 to 50 μm size bin, and subsequently increased in the 50 to 90 μm size bin (Fig. 4.6A, 4.6C); however, these effects were minimal. Given the known

relationships between individual mesozooplankton grazer size and prey size range (Kiørboe 2008, Wirtz 2012, Boyce et al. 2015), we looked for a community-level relationship between grazer community size structure and the size structure of microplankton prey consumed. No such relationship was apparent in this study.

Table 4.2. Microplankton and mesozooplankton grazer concentrations from each experiment. Numbers reported are the mean ± standard deviation of replicate measurements (n = 3), except the initial microplankton concentration from 03 April 2014 (n = 2). Note: grazer concentration has been increased from that in the field and does not necessarily reflect natural concentrations.

Experiment date	**Initial microplankton concentration (# ml^{-1})**	**Control microplankton concentration (# ml^{-1})**	**Treatment microplankton concentration (# ml^{-1})**	**Grazer concentration (# ml^{-1})**	**Percent grazing by mesozoo-plankton (%)**
03 April 2014	7.5 ± 2.1	7.4 ± 0.9	5.8 ± 0.9	1.5 ± 0.2	21.7 ± 3.2
06 May 2014	7.3 ± 0.3	5.7 ± 0.6	5.1 ± 1.0	0.1 ± 0.0	10.4 ± 1.2
07 July 2014	39.5 ± 6.6	26.2 ± 8.4	11.0 ± 3.0	0.9 ± 0.1	56.0 ± 12.5
25 August 2014	27.4 ±2.6	19.5 ± 1.1	11.0 ± 1.3	0.3 ± 0.0	43.5 ± 3.5
21 October 2014	16.4 ±2.3	12.4 ± 0.4	9.0 ± 0.3	0.3 ± 0.1	29.9 ± 0.9

Grazing by mesozooplankton alone did not significantly change the microplankton size structure. However, a shift in particle size distribution was observed in nearly all experiments when the production of fecal pellets that resulted from grazing was included in the analysis. The average size of particles increased from 26.4 to 35.9 μm in April (Fig. 4.6B), 23.8 to 87.7 μm in July (Fig. 4.6F), 32.4 to 82.6 μm in August (Fig. 4.6H), and 31.9 to 61.6 μm in October (Fig. 4.6I). In May average particle size did not significantly change (47.8 to 48.7 μm; Fig. 4.6D). While we did not find a singular relationship between grazer community size structure and the size structure of microplankton consumed, we did find a log-linear relationship between median grazer prosome length (PL) and mean volume of particles produced during the incubation period (Vol_{mean}, $R^2 = 0.65$, $p << 0.01$, Fig. 4.7):

$$\log_{10}(Vol_{mean}) = 1.4 \log_{10}(Vol_{mean}) + 6.7 \quad (4.1)$$

We compared this community-level relationship with individual-based relationships in the literature and found that they were similar (Uye & Kaname 1994, Mauchline 1998, Stamieszkin et al. 2015), indicating that the known body length to fecal pellet volume relationship can be scaled up from individual organisms to a community.

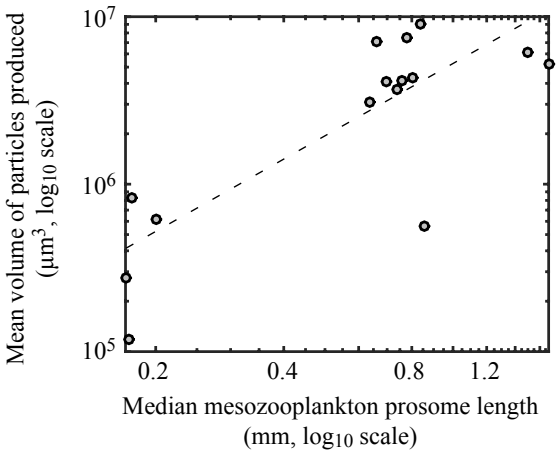

Figure 4.7. Median mesozooplankton prosome length (PL, mm) versus mean volume of particles produced during the incubations (Vol_{mean}, μm^3); most of these particles were mesozooplankton fecal pellets. Both axes are on a $\log_{10}$ scale. The dotted line is a line of best fit (R^2 =0.65, $p << 0.01$): $\log_{10}(Vol_{mean}) = 1.4 \log_{10}(PL) + 6.7$

Discussion

Most plankton grazing experiments focus either on size or species. Experimental approaches have tended to emphasize the species-specific view and consider the effects of grazing by only one or a few grazer species. For example, it has been shown that calanoid copepods often prefer ciliate prey (Atkinson 1995, Atkinson 1996, Nejstgaard et al. 1997, Bollens & Penry 2003, Castellani et al. 2008, Fileman et al. 2010). However, prey preference can also change with season (Teegarden et al. 2001, Bollens & Penry 2003, Castellani et al. 2008), diel cycles (Wu et al. 2010) and prey toxicity (Teegarden 1999, Ger et al. 2016). Rather than focus on species, we use size as an organizing trait, which allows us to connect trophic dynamics directly to particle size spectra and particulate organic flux potential.

Based upon plankton predator-prey size relationships (Kiørboe 2008, Wirtz 2012, Boyce et al. 2015), we hypothesized that grazing by mesozooplankton on microplankton would create gaps in the particle size spectrum, and that these gaps would be predictable

based upon the size structure of the grazers. However, in our grazing experiments we found little evidence for preference, either for size or species. The shapes of the prey size spectra after grazing were similar to those with no grazing (Fig. 4.6A, 4.6C, 4.6E, 4.6G, 4.6I), indicating that mesozooplankton in our experiments were eating prey in proportion to their abundance (Fig. 4.8). Non-selective feeding has been documented in older literature and our results align well with these patterns (Parsons et al. 1967, Poulet 1973, Richman et al. 1977). However, these studies were constrained by the technology available, and were unable to detect more fragile, mixotrophic prey (Verity & Paffenhöfer 1996). The use of FlowCam for analyzing grazing experiments enables a more standardized analysis of particle size, and by processing live samples rather than preserved, the likelihood of losing particles through preservation and handling is decreased.

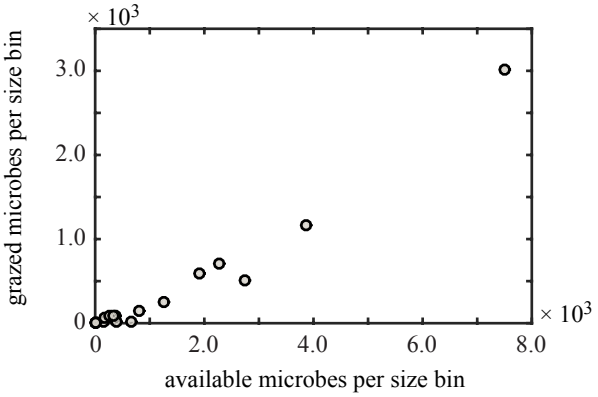

Figure 4.8. The number of microplankton, in one of 15 size bins (bin width of 20 μm), from the initial samples (the microplankton available for consumption), versus the number of microplankton grazed by mesozooplankton from each size bin. The results of all experiments were combined.

These experiments are unique because they use whole natural assemblages of grazers and prey. Previous work using natural prey communities has focused on a limited number of grazer types (Parsons et al. 1967, Poulet 1973, Richman et al. 1977, Atkinson 1995, Nejstgaard et al. 1997, Teagarden et al 2001, Bollens & Penry 2003, Castellani et

al. 2008, Fileman et al. 2010, Wu et al. 2010), and published size relationships between grazers and prey are based on individual organisms, rather than whole communities (Kiørboe 2008, Wirtz 2012, Boyce et al. 2015). When the cumulative effects of individual grazers are considered, the emergent community-scale patterns are quite different. Rather than grazing down narrow size ranges of prey, as would be predicted by individual predator-prey size relationships, the mesozooplankton community has a uniform grazing effect. This effect results in microplankton being consumed in proportion to their abundance.

The uniform grazing effect could be explained in two ways. First, the predators may be feeding indiscriminately across the full range of prey sizes and types. This seems unlikely given the large range of predator sizes (Table 4.1). Instead, we propose that the grazer and microplankton communities are tightly coupled and have developed over time to fit one another in the field; therefore when we intensify grazing in our treatment containers, the particle abundance changes, but not the size distribution. Any prey that was preferred by one of the available predators was already grazed down to the point where they blend in with other similar sized prey. This has the effect of broadening the size classes over which each predator feeds. Furthermore, the abundance of each predator reflects the past abundance of its possible prey.

Another way to consider this is a reshaping of the Red Queen hypothesis, borrowed from evolutionary biology (VanValen 1973). The Red Queen hypothesis posits an evolutionary arms race between predator and prey in which the two are constantly

evolving in tandem to maximize consumption by the predator, and escape by the prey, allowing both to accumulate biomass at converse times. In a plankton community, microplankton proliferate within the restrictions of nutrients and physical factors, and mesozooplankton life cycles are adapted to time periods of high prey availability (Longhurst 1995, Tommasi et al. 2013, Friedland et al. 2015). Hence, there is usually a tight coupling between plankton trophic levels, and it would be expected that available prey items will be grazed. This scenario gives rise to the even distribution of grazing over a prey size spectrum.

Exceptions to this pattern of even grazing occur when a species diverts resources to protect itself from predation or outcompete other grazers. Pelagic tunicates do this by investing in a gelatinous body plan, which enables them to be relatively large and feed on relatively small prey (Acuña 2001, Sutherland et al. 2010). We observed a notable example of this in our experiments. A large species of the dinoflagellate genus *Ceratium* (example image in Fig. 4.2A) was abundant during the July experiment, and present in the August and October experiments. Its relative large size (~ 50 to 100 μm) and spines likely protect it from significant grazing (Verity & Paffenhöfer 1996). Using size as an organizing trait allows outliers like *Ceratium* to stand out as not being grazed; its abundance remains nearly the same between control and treatment containers (Fig. 4.9). By investing in spines and size, *Ceratium* is able to reduce its predation mortality, although likely using resources that could be used for reproduction. Another explanation could be that we did not collect grazers large enough to consume these large *Ceratium* cells. Based on the individual predator to prey size ratio of 10:1 (Kiørboe 2008, Boyce et

al. 2015), the mesozooplankton grazers in our experiments could have consumed these cells, but did not. This suggests that while grazing in proportion to abundance may be the default, there are opportunities for individual species to break out of the size spectrum through a major investment in adaptations which reduce mortality.

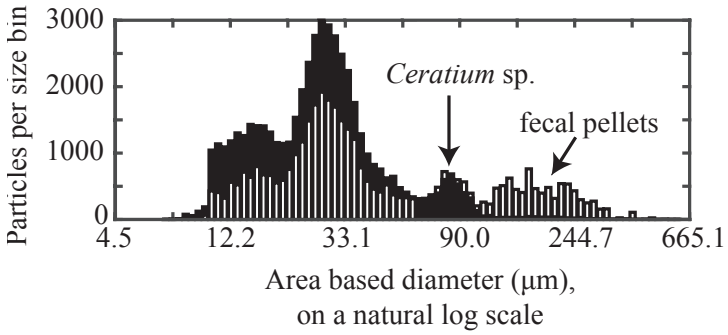

Figure 4.9. Particle size distribution for all experiment data combined; bars are approximate 6.5 μm wide. Black bars represent the particles in control containers after incubation (no mesozooplankton grazing) and white bars represent the particles in treatment containers after incubation (mesozooplankton present and grazing). Particle abundance per size bin is the FlowCam count per 700 ml sample container.

In this study we consider not only particles that are grazed, but also particles that are produced. The production of fecal pellets clearly adds particles to the larger size bins within the particle size spectrum considered (Fig. 4.9). By collectively grazing most particles in the 10 to 50 μm size range, and aggregating those into larger fecal pellets in the 100 to 500 μm size range, mesozooplankton grazers in our experiments increase mean particle size. Larger fecal pellets sink faster and are therefore more likely to contribute to particle flux out of the surface ocean (Stamieszkin et al. 2015). In these experiments, mesozooplankton grazing and egestion therefore increased the potential for fecal pellet

carbon flux. When mesozooplankton feed, they also create smaller particles by breaking apart prey items (Poulet 1973). It is likely that smaller particles were produced by feeding in these experiments. However, the particles were either unidentifiable, or smaller than 10 μm and not included in this analysis. Future experiments could use additional technology, such as flow cytometry, to capture a wider size range of particles.

In the analysis of these experiments, we consider particle size as a proxy for carbon content. While this is generally a reasonable assumption (Alldredge 1998, Mullin et al. 1966, Menden-Deuer & Lessard 2000), the carbon content, and stoichiometry of microplankton change depending upon taxonomy and evolutionary history (Menden-Deuer & Lessard 2000, Quigg et al. 2003), nutrient availability (Geider & la Roche 2002), as well as other factors reviewed by Klausmeier et al. (2008). The stoichiometry of zooplankton fecal pellets also varies depending upon the composition of prey begin consumed (Urban-Rich et al. 2001, Atkinson et al. 2012) and amount of prey available (Atkinson et al. 2012). In future iterations of these experiments, nutrient analysis of microplankton and fecal pellet stoichiometry would provide information useful to quantifying the relationship of mesozooplankton grazing to nutrient cycling, and export.

Predator-prey size relationships in the literature primarily focus on individual-level selection, and these relationships do not directly scale up to the community level. Further, models of optimal mesozooplankton prey size have limited applicability to natural plankton communities, since a grazer may never cross paths with prey of the optimal size, but must still feed. In order to understand the trophic dynamics that affect

particle size spectra, and therefore the efficiency of the biological carbon pump, it is essential to be able to scale up from the the individual organism to the community level. Future experimental and modeling work should take into consideration trophic dynamics at the community level, and consider grazing and particle production along a continuum. The abstraction of taxonomic information using the size as a descriptive trait allows us to take that community view, and work towards a mechanistic understanding of how trophic interactions affect particle flux potential.

CHAPTER 5

DISSERTATION CONCLUSION

The goal of my dissertation research was to explore some of the impacts that mesozooplankton have on the ocean's biological carbon pump. I incorporated modeling and experimentation methods; both used organism size as a central trait. The modeling work focused on copepods because they are ubiquitous and abundant in the world's oceans, a lot is known about their metabolic processes, and because the Continuous Plankton Recorder has sampled them effectively over large areas and multiple decades. These datasets offer a unique opportunity to study change in the ocean over large spatial and temporal scales. The models that I described in Chapters Two and Three used metabolic relationships with body size and temperature to estimate fecal pellet carbon flux in the Gulf of Maine (Chapter Two) and northern North Atlantic Ocean (Chapter Three) over the last several decades. Chapter Four described experiments conducted off of the Damariscotta River Estuary, in the Gulf of Maine. These experiments used natural mesozooplankton and microplankton communities to quantify the impact of grazing on microplankton and detrital size spectra.

The work presented in Chapter Two was aimed at developing a model to test the importance of copepod body size on fecal pellet carbon flux. I hypothesized that larger copepods would contribute disproportionately to fecal pellet flux because of the compounding effects of pellet size: they sink faster and therefore less material is remineralized before the pellets reach a particular depth horizon or the seafloor. I found that large copepods were more important to variability in fecal pellet flux, but that

abundance was also important. While I used a trait-based approach to model fecal pellet carbon flux, focused on size as an organizing trait, the copepod species *Calanus finmarchicus* was the primary diver of fecal pellet carbon flux because they are both large and abundant in the Gulf of Maine. Sensitivity analysis of the Gulf of Maine model revealed that remineralization rate of the fecal pellets had the greatest impact on variability of flux estimates made by the model.

The second iteration of the copepod fecal pellet carbon flux model was presented in Chapter Three. In this model, I incorporated a more realistic temperature-dependent remineralization function, as well as copepod diel vertical migration behavior. The model was applied to 55 years of Continuous Plankton Recorder copepod abundance and taxonomic data. The major findings of this chapter were that copepod biomass, which is a combination of size and abundance, drives fecal pellet carbon flux. In addition warming throughout the North Atlantic over the last several decades has generally led to a decline in biomass and consequently, a decline in fecal pellet carbon flux. While these patterns applied broadly to the study region, I also found that local dynamics led to different responses to warming. In some areas fecal pellet carbon flux decreased as a result of declining biomass, but an increase in the abundance of a few larger taxa lessened this effect and increased export efficiency at the same time. Another unexpected finding presented in Chapter Three was that warming in the coolest regions of the northern North Atlantic is actually increasing copepod biomass and fecal pellet flux. Chapter Three also raises some questions about the impact of diel vertical migration behavior on the biological carbon pump. While vertical migration did result in active transport and release

of carbon deeper in the water column, flux increased more when the copepods remained at the surface and fed throughout the day. This raised new questions about diel feeding patterns, and the export of surface versus water column production.

Chapter Four described a series of grazing experiments aimed at quantifying the impact of mesozooplankton grazing on particle size structure. Based upon published predator to prey size ratios, I hypothesized that grazing would create holes in the microplankton size spectrum. I also tested the hypothesis that the aggregation of prey into fecal pellets would shift the particle size spectrum toward larger particles. These experiments were novel because they used complete natural assemblages of mesozooplankton grazers and their microplankton prey. A FlowCam (Fluid Imaging Technologies) imaging system allowed me to observe taxonomic, as well as size-based, prey selectivity. The findings of this work were different from what I had expected. Rather than narrow ranges of prey being removed from the particle size spectrum, I found that prey was grazed in proportion to its abundance, across the size spectrum, with the exception of one large, spiny dinoflagellate. Proportional grazing indicated a tight coupling between trophic levels that is not always observed in simplified laboratory experiments, but likely represents more realistic trophic interactions in the marine system. The production of larger fecal pellets did shift the particle size spectrum toward larger sizes, as hypothesized.

Organism size was an overarching theme in my dissertation research. The fecal pellet carbon flux models demonstrate how size could be used to connect individual-scale processes with community-scale impacts on carbon cycling. The generalized

relationships between temperature and copepod biomass, as well as biomass and fecal pellet carbon flux in Chapter Three could be used in global-scale carbon flux modeling efforts. The experiments presented in Chapter Four revealed a tight coupling between trophic levels that resulted in a smoothed prey size spectrum, and increased particle size due to fecal pellet egestion. A question that emerged from this work was whether mesozooplankton augment or inhibit carbon flux.

The aggregation and egestion of small prey as larger fecal pellets can increase carbon flux if prey organisms are too small to effectively sink themselves. However, when copepods consume phytoplankton and other prey, they not only aggregate it into larger fecal pellets, but also store and respire a fraction of the carbon. Fecal pellet flux is therefore a less efficient avenue for carbon export, compared with sinking phytoplankton. In the future, I will continue the modeling efforts presented in Chapters Two and Three, and incorporate microplankton community dynamics to explore this trade-off. I hope to elaborate on the grazing experiments in Chapter Four to parameterize models which reflect coupling between mesozooplankton and microplankton communities. Through an iterative feedback process between experiments and models, a better understanding of the conditions and communities that give rise to different carbon flux scenarios will be generated, as well as information about the impacts of changing oceanographic conditions on the biological carbon pump.

REFERENCES

Abràmoff MD, Magalhães PJ, Ram SJ (2004) Image processing with ImageJ. Biophotonics 11: 36-42.

Acuña JL (2001) Pelagic tunicates: Why gelatinous? Amer Natur 158: 100-107.

Alldredge A (1998) The carbon, nitrogen and mass content of marine snow as a function of aggregate size. Deep-Sea Res I 45: 529-541.

Al-Mutairi H, Landry MR (2001) Active export of carbon and nitrogen at Station ALOHA by diel migrant zooplankton. Deep-Sea Res II 48: 2083-2103.

Alonso-Sáez L, Gasol JM, Arístegui J, Vilas JC, Vaqué D, Duarte CM, Agustí S (2007) Large-scale variability in surface bacterial carbon demand and growth efficiency in the subtropical northeast Atlantic Ocean. Limnol Oceanogr 52: 533-546.

Atkinson A (1995) Carnivory and feeding selectivity in five copepod species at the onset of a spring bloom in the Bellinghausen Sea, Antarctica. ICES J Mar Sci 52: 385-396.

Atkinson A (1996) Subantarctic copepods in an oceanic, low chlorophyll environment: ciliate predation, food selectivity and impact on prey populations. Mar Ecol Prog Ser 130: 85-96.

Atkinson A, Ward P, Murphy EJ (1996) Diel periodicity of Subantarctic copepods: relations between vertical migration, gut fullness and gut evacuation rate. J Plankton Res 18: 1387-1405.

Atkinson A, Schmidt K, Fielding S, Kawaguchi S, Geissler PA (2012) Variable food absorption by Antarctic krill: Relationships between diet, egestion rate and the composition and sinking rates of their fecal pellets. Deep-Sea Res II 59: 147-158.

Baltar F, Aristegui J, Gasol JM, Hernandez-Leon S, Herndl GL (2007) Strong coast-ocean and surface-depth gradients in prokaryotic assemblage structure and activity in a coastal transition zone. Aquat Microb Ecol 50: 63-74.

Banas NS (2011) Adding complex trophic interactions to a size-spectral plankton model: Emergent diversity patterns and limits on predictability. Ecol Model 222: 2663-2675.

Barton AD, Pershing AJ, Pitchman E, Record NR, Edwards KF, Finkel ZV, Kiørboe T, Ward BA (2013) The biogeography of marine plankton traits. Ecol Lett 16: 522-534.

Beaugrand G, Reid PC, Ibañez F, Lindley JA, Edwards M (2002) Reorganization of North Atlantic marine copepod biodiversity and climate. Science 296: 1692-1694.

Beaugrand G, Luczak C, Edwards M (2009) Rapid biogeographical plankton shifts in the North Atlantic Ocean. Glob Change Biol 15: 1790-1803.

Beaugrand G, Edwards M, Legendre L (2010) Marine biodiversity, ecosystem functioning, and carbon cycles. P Natl Acad Sci USA 107: 10120-10124.

Behrenfeld MJ, Boss ES (2014) Resurrecting the ecological underpinnings of ocean plankton blooms. Ann Rev Mar Sci 6: 167-208.

Belehrádek J. 1935. Temperature and living matter. Protoplasma Monogr. 8: 1-277.

Besiktepe S, Dam HG (2002) Coupling of ingestion and defecation as a function of diet in the Calanoid copepod Acartia tonsa. Mar Ecol Prog Ser 229: 151-164.

Bode A, Alvarez-Ossorio MT, Cabanas JM, Miranda A, Varela M (2009) Recent trends in plankton and upwelling intensity off Galicia (NW Spain). Prog Oceanogr 83: 342-350

Bollens GCR, Penry DL (2003) Feeding dynamics of Acartia spp. copepods in a large, temperate estuary (San Francisco Bay, CA). Mar Ecol Prog Ser 257: 139-158.

Boyce DG, Frank KT, Leggett WC (2015) From mice to elephants: overturning the 'one size fits all' paradigm in marine plankton food chains. Ecol Lett 18: 504-515.

Boyd PW, Newton PP (1999) Does planktonic community structure determine downward particulate organic carbon flux in different oceanic provinces? Deep-Sea Res I 46: 63-91.

Boyd PM, Trull TW (2007) Understanding the export of biogenic particles in oceanic waters: Is there consensus? Prog Oceanogr 72: 276-312.

Brown JH, Gillooly JF, Allen AP, Savage VM, West GB (2004) Toward a metabolic theory of ecology. Ecology 85: 1771-1789.

Buesseler KO (1998) The decoupling of production and particulate export in the surface ocean. Global Biogeochem Cy 12: 297-310.

Campbell RG, Wagner MM, Teegarden GJ, Boudreau CA, Durbin EG (2001) Growth and development rates of the copepod Calanus finmarchicus reared in the laboratory. Mar Ecol Prog Ser 221: 161-183.

Castellani C, Irigoien X, Mayor DJ, Harris RP, Wilson D (2008) Feeding of Calanus finmarchicus and Oithona similis on the microplankton assemblage in the Irminger Sea, North Atlantic. J Plankt Res 30: 1095-1116.

Conversi A, Piontkovski S, Hameed S (2001) Seasonal and interannual dynamics of Calanus finmarchicus in the Gulf of Maine (Northeastern US shelf) with reference to the North Atlantic Oscillation. Deep-Sea Res II 48: 519-530.

Corkett CJ, McLaren IA, Sevigny JM (1986) The rearing of the marine Calanoid copepods Calanus finmarchicus (Gunnerus), C. glacialis Jaschnov and C. hyperboreus Krøyer with comment on the equiproportional rule. Syllogeus 58: 539-546.

Cowles GW, Lentz SJ, Chen C, Xu Q, Beardsley RC (2008) Comparison of observed and model-computed low frequency circulation and hydrography on the New England Shelf. J Geophys Res Oce 113: C09015.

Dagg MJ, Frost BW, Newton J (1998) Diel vertical migration and feeding in adult female Calanus pacificus, Metridia lucens and Pseudocalanus newmani during a spring bloom in Dabob Bay, a fjord in Washington USA. J Mar Syst 15: 503-509.

Daufresne M, Lengfellner K, Sommer U (2009) Global warming benefits the small in aquatic ecosystems. Proc Natl Acad Sci 106: 12788-12793.

Ducklow HW, Steinberg DK, Buesseler KO (2001) Upper ocean carbon export and the biological pump. Oceanography 14: 50-58.

Feinberg LR, Dam HG (1998) Effects of diets on dimensions, density and sinking rates of fecal pellets of the copepod Acartia tonsa. Mar Ecol Prog Ser 175: 87-96.

Fileman E, Petropavlovsky A, Harris R (2010) Grazing b the copepods Calanus helgolandicus and Acartia clausi on the protozooplankton community at station L4 in the Western English Channel. J Plankt Res 32: 709-724.

Folt CL, Burns CW (1999) Biological drivers of zooplankton patchiness. Trends Ecol Evol 14: 300-305.

Friendland KD, Leaf RT, Kane J, Tommasi D, Asch RG, Rebuck N, Ji R, Large SI, Stock C, Saba VS (2015) Spring bloom dynamics and zooplankton biomass response on the US Northeast Continental Shelf 102: 47-61.

Geider RJ, la Roche J (2002) Redfield revisited: variability of C:N:P in marine microalgae and its biochemical basis. Eur J Phycol 37: 1-17.

Ger KS, Faassen EJ, Pennino MG, Lurling M (2016) Effect of the toxin (microcystin) content of Microcystis on copepod grazing. Harmful Algae 52: 34-45.

Gleiber MR, Steinberg DK, Ducklow HW (2012) Time series of vertical flux of zooplankton fecal pellets on the continental shelf of the western Antarctic Peninsula. Mar Ecol Prog Ser 471: 23-36.

Goldthwait SA, Steinberg DK (2008) Elevated biomass of mesozooplankton and enhanced fecal pellet flux in cyclonic and mode-water eddies in the Sargasso Sea. Deep-Sea Res II 55: 1360-1377.

Green C H, Pershing AJ (2000) The response of Calanus finmarchicus populations to climate variability in the Northwest Atlantic: basin-scale forcing associated with the North Atlantic Oscillation. ICES J Mar Sci 57: 1536-1544.

Guidi L, Jackson GA, Stemmann L, Miquel JC, Picheral M, Gorsky G (2008) Relationships between particle size distribution and flux in the mesopelagic zone. Deep-Sea Res I 55: 1364-1374.

Hansen AN, Visser AW (2016) Carbon export by vertically migrating zooplankton: an optimal behavior model. Limnol Oceanogr 61: 701-710.

Harris V, Olhede SC, Edwards M (2015) Multidecadal spatial reorganization of plankton communities in the North East Atlantic. J Mar Sys 142: 16-24.

Hassett RP, Landry MR (1988) Short-term change sin feeding and digestion by the copepod Calanus pacificus. Mar Biol 99: 63-74.

Hirst AG (2012) Intraspecific scaling of mass to length in pelagic animals: Ontogenetic shape change and its implications. Limnol Oceanogr 57: 1579-1590.

Honjo S, Roman MR (1978) Marine copepod fecal pellets: Production, preservation and sedimentation. J Mar Res 36: 45-57.

Honjo S, Manganini SJ, Krishfield RA, Francois R (2008) Particulate organic carbon fluxes to the ocean interior and factors controlling the biological pump: A synthesis of global sediment trap programs since 1983. Prog Oceanogr 76: 217-285.

Huntley ME, Lopez MDG (1992) Temperature-dependent production of marine copepods: a global synthesis. Am Nat 140: 201-242.

Ide K, Takahashi K, Kuwata A, Nakamachi M, Saito H (2008) A rapid analysis of copepod feeding using FlowCAM. J Plankt Res 30: 275-281.

Iversen MH, Poulsen LK (2007) Coprohexy, coprophagy, and coprochaly in the copepods Calanus helgolandicus, Pseudocalanus elongates, and Oithona similis. Mar Ecol Prog Ser 350: 79-89.

Iversen MH, Ploug H (2013) Temperature effects on carbon-specific respiration rate and sinking velocity of diatom aggregates - potential implications for deep ocean export processes. Biogeosciences 10: 4073-4085.

Jonasdottir SH, Visser AW, Richardson K, Heath MR (2015) Seasonal copepod lipid pump promotes carbon sequestration in the deep North Atlantic. Proc Natl Acad Sci USA 112: 12122-12126.

Jones CG, Lawton JH, Shachak M (1994) Organisms as ecosystem engineers. Oikos 69: 373-386.

Jossi JW, John AWG, Sameoto D (2003) Continuous plankton recorder sampling off the east coast of North America: history and status. Prog Oceanogr 58: 313-325.

Kane J (2009) A comparison of two zooplankton time series data collected in the Gulf of Maine. J Plankton Res 31: 249-259.

Kiørboe T (2008) A mechanistic approach to plankton ecology. Princeton University Press, Princeton, NJ.

Klaas C, Verity PG, Schultes S (2008) Determination of copepod grazing on natural plankton communities: correcting for trophic cascade effects. Mar Ecol Prog Ser 357: 195-206.

Klausmeier CA, Litchman E, Daufresne, Levin SA (2008) Phytoplankton stoichiometry. Ecol Res 23: 479-485.

Köhl A, Stammer D (2008) Variability of the Meridional Overturning in the North Atlantic from the 50 years GECCO State Estimation. J Phys Oceanogr 38: 1913-1930.

Laurenceau-Cornec EC, Trull TW, Davies DM, Bray SG, Doran J, Planchon F, Carlotti F, Jouandet M-P, Cavagna A-J, Waite AM, Blain S (2015) The relative importance of phtyoplankton aggregates and zooplankton fecal pellets to carbon export: insights from free-drifting sediment trap deployments in naturally iron-fertilized waters near the Kerguelen Plateau. Biogeosci 12: 1007-1027.

Legendre L, Rassoulzadegan F (1996) Food-web mediated export of biogenic carbon in oceans: hydrodynamic control. Mar Ecol Prog Ser 145: 179-193.

Legendre L, Michaud J (1998) Flux of biogenic carbon in oceans: size-dependent regulation by pelagic food webs. Mar Ecol Prog Ser 164: 1-11.

Litchman E, Klausmeier CA (2008) Trait-based community ecology of phytoplankton. Annu Rev Ecol Syst 39: 615-639.

Litchman E, Ohman MD, Kiørboe T (2013) Trait-based approaches to zooplankton communities. J Plankton Res 35: 473-484.

Longhurst A (1995) Seasonal cycles of pelagic production and consumption. Prog Oceanogr 36: 77-167.

Lutz MJ, Caldeira K, Dunbar RB, Behrenfeld MJ (2007) Seasonal rhythms of net primary production and particulate organic carbon flux to depth describe the efficiency of biological pump in the global ocean. J Geophys Res 112: C10011.

Lynch DR, Gentleman WC, McGillicuddy DJ, Davis CS (1998) Biologicla/physical simulations of Calanus finmarchicus population dynamics in the Gulf of Maine. Mar Ecol Prog Ser 169: 189-210.

Marsay CM, Sanders RJ, Henson SA, Pabortsava K, Achterberg EP, Lampitt RS (2015) Attenuation of sinking particulate organic carbon flux through the mesopelagic ocean. Proc Natl Acad Sci 112: 1089-1094.

Martin JH, Knauer GA, Karl DM, Broenkow WW (1987) VERTEX: Carbon cycling in the northeast Pacific. Deep Sea Res I 34: 267-285.

Martin JH (1990) Glacial-interglacial CO2 change: the iron hypothesis. Paleoceanography 5: 1-13.

Mauchline J (1998) The biology of Calanoid copepods. Adv Mar Biol 33: 710 pp.

McDonnell AMP, Boyd PW, Buesseler KO (2015) Effects of sinking velocities and microbial respiration rates on the attenuation of particulate carbon fluxes through the mesopelgic zone. Global Biogeochem Cy 29: 175-193.

Melle W, Runge J, Head E, Plourde S, et al. (2014) The North Atlantic Ocean as habitat for Calanus finmarchicus: environmental factors and life history traits. Prog Oceanogr 129: 244-284.

Menden-Deuer S, Lessard EJ (2000) Carbon to volume relationships for dinoflagellates, diatoms, and other protist plankton. Limnol Oceanogr 45: 569-579.

MERCINA (2012) Recent Arctic climate change and its remote forcing of Northwest Atlantic Shelf ecosystems. Oceanography 25: 208–213.

Mills KE, Pershing AJ, Brown CJ, Chen Y, Chiang F-S, Holland DS, Lehuta S, Nye JA, Sun JC, Thomas AC, Wahle RA (2013) Fisheries management in a change climate: Lessons from the 2012 ocean heat wave in the Northwest Atlantic. Oceanography 26: 191-195.

Møller EF, Borg CMA, Jónasdóttir SH, Satapoomin S, Jaspers C, Nielsen TG (2011) Production and fate of copepod fecal pellets across the Southern Indian Ocean. Mar Biol 158: 677-688.

Morán XAG, López-Urrutia A, Calvo-Díaz A, Li WKW (2010) Increasing importance of small phytoplankton in a warmer ocean. Global Change Biol 16: 1137-1144.

Mullin MM, Sloan PR, Eppley RW (1966) Relationship between carbon content, cell volume, and area in phytoplankton. Limnol Oceanogr 11: 307-311.

Nejstgaard JC, Gismervik I, Solberg PT (1997) Feeding and reproduction by Calanus finmarchicus, and microzooplankton grazing during mesocosm blooms of diatoms and the coccolithophore Emiliania huxleyi. Mar Ecol Prog Ser 147: 197-217.

Ohman MD, Romagnan J-B (2015) Nonlinear effects of body size and optical attenuation on Diel Vertical Migration by zooplankton. Limnol Oceanogr 61: 765-770.

Paine RT (1966) Food web complexity and species diversity. Amer Natur 100: 65-75.

Parsons TR, LeBrasseur RJ, Fulton JD (1967) Some observations on the dependence of zooplankton grazing on the cell size and concentration of phytoplankton blooms. J Oceanogr Soc Japan 23: 10-17.

Passow U, Carlson CA (2012) The biological pump in a high CO2 world. Mar Ecol Prog Ser 470: 249-271.

Pasternak A, Arashkevich E, Wexels Riser C, Ratkova T, Wassmann P (2000) Seasonal variation in zooplankton and suspended faecal pellets in the subarctic Norwegian Baisfjorden in 1996. Sarsia 85: 439-452.

Pershing AJ, Greene CH, Jossi JW, O'Brien L, Brodziak JKT, Bailey BA (2005) Interdecadal variability in the Gulf of Maine zooplankton community, with potential impacts on fish recruitment. ICES J Mar Sci 62: 1511-1523.

Pilskaln CH, Anderson DM, McGillicuddy DJ, Keafer BA, Hayashi K, Norton K (2014) Spatial and temporal variability of Alexandirum cyst fluxes in the Gulf of Maine: Relationship to seasonal particle export and resuspension. Deep-Sea Res II 103: 40-54.

Poloczanska ES, Brown CJ, Sydeman WJ, Kiessling W, Schoeman DS, Moore PJ, Brander K, Bruno JF, Buckley LB, Burrows MT, et al. (2013) Global imprint of climate change on marine life. Nat Clim Change 3: 919-925.

Poulet SA (1973) Grazing of Pseudocalanus minutus on naturally occurring particulate matter. Limnol Oceanogr 18: 564-573.

Primeau F (2005) Characterizing transport between the surface mixed layer and the ocean interior with a forward and adjoint global ocean transport model. J Phys Oceanogr 35: 545-564.

Quigg A, Finkel ZV, Irwin AJ, Rosenthal Y, Ho T-Y, Reinfelder JR, Schofield O, Morel FMM, Falkowski PG (2003) The evolutionary inheritence of elemental stoichiometry in marine phytoplankton. Nature 425: 291-294.

Record NR, Pershing AJ (2012) First principles of copepod development help explain global marine diversity patterns. Oecologia 170: 289-295.

Record NR, Pershing AJ, Jossi JW (2010) Biodiversity as a dynamic variable in the Gulf of Maine continuous plankton recorder transect. J Plank Res 32: 1675-1684.

Reygondeau G, Beaugrand G (2011) Future climate-driven shifts in distribution of Calanus finmarchicus. Glob Change Biol 17: 756-766.

Reygondeau G, Molinero JC, Coombs S, MacKenzie BR, Bonnet D (2015) Progressive changes in the Western English Channel foster a reorganization in the plankton food web. Prog Oceanogr 137: 524-532.

Richardson AJ, Schoeman DS (2004) Climate impact on plankton ecosystems in the Northeast Atlantic. Science 305: 1609-1612.

Richardson AJ, Walne AW, John AWG, Jonas TD, Lindley JA, Sims DW, Stevens D, Witt M (2006) Using continuous plankton recorder data. Prog Oceanogr 68: 27-74.

Richman S, Heinle DR, Huff R (1977) Grazing by adult estuarine cloned copepods of the Chesapeake Bay. Mar Biol 42: 69-84.

de la Rocha CL, Passow U (2007) Factors influencing the sinking of POC and the efficiency of the biological carbon pump. Deep-Sea Res II 54: 639-658.

Runge JA (1980) Effects of hunger and season on the feeding behavior of Calanus pacificus. Limnol Oceanogr 25: 134-145.

Sabine CL, Feely RA, Gruber N, Key RM, Lee K, Bullister JL, Wanninkhof R, Wong CS, Wallace DWR, Tilbrook B, Millero FJ, Peng T-H, Kozyr A, Ono T, Rios AF (2004) The oceanic sink for anthropogenic CO2. Science 305: 367-371.

Sanders R, Henson SA, Koski M, de la Rocha CL, Painter SC, et al. (2014) The biological carbon pump in the North Atlantic. Prog Oceanogr 129: 200-218.

San Martin E, Harris RP, Irigoien X (2006) Latitudinal variation in plankton size spectra in the Atlantic Ocean. Deep-Sea Res II 53: 1560-1572.

Schnetzer A, Steinberg DK (2002) Active transport of particulate organic carbon and nitrogen by vertically migrating zooplankton in the Sargasso Sea. Mar Ecol Prog Ser 234: 71-84.

Shatova O, Koweek D, Conte MH, Weber JC (2012) Contribution of zooplankton fecal pellets to deep ocean particle flux in the Sargasso Sea assessed using quantitative image analysis. J Plank Res 34: 905-921.

Sheldon RW, Prakash A, Sutcliffe WH (1972) The size distribution of particles in the ocean. Limnol Oceanogr 17: 327-340

Sigman DM, Boyle EA (2000) Glacial/interglacial variations in atmospheric carbon dioxide. Nature 407: 859-869.

Sprules WG, Munawar M (1986) Plankton size spectra in relation to ecosystem productivity, size, and perturbation. Can J Fish Aquat Sci 43: 1789-1794.

Stamieszkin K, Pershing AJ, Record NR, Pilskaln CH, Dam HG, Feinberg LR (2015) Size as the master trait in modeled copepod fecal pellet carbon flux. Mar Ecol Prog Ser 60: 2090-2107.

Steinberg DK, Carlson CA, Bates NR, Goldthwait SA, Madin LP, Michaels AF (2000) Zooplankton vertical migration and the active transport of dissolved organic and inorganic carbon in the Sargasso Sea. Deep-Sea Res I 47: 1137-158.

Stukel MR, Ohman MD, Benitez-Nelson CR, Landry MR (2013) Contributions of mesozooplankton to vertical carbon export in a coastal upwelling system. Mar Ecol Prog Ser 491: 47-65.

Sutherland KR, Madin LP, Stocker R (2010) Filtration of submicrometer particles by pelagic tunicates. Proc Natl Acad Sci 107: 15129-15134.

Taniguchi DAA, Franks PJS, Poulin FJ (2014) Planktonic biomass size spectra: an emergent property of size-dependent physiological rates, good web dynamics, and nutrient regimes. Mar Ecol Prog Ser 514: 13-33.

Teegarden GJ (1999) Copepod grazing selection and particle discrimination on the basis of PSP toxin content. Mar Ecol Prog Ser 181: 163-176.

Teegarden GJ, Campbell RG, Durbin EG (2001) Zooplankton feeding behavior and particle selection in natural plankton assemblages containing toxic Alexandium spp. Mar Ecol Prog Ser 218: 213-226.

Thor P, Dam HG, Rogers DR (2003) Fate of organic carbon released from decomposing copepod fecal pellets in relation to bacterial production and extracellular enzymatic activity. Aquat Microb Ecol 33:279-288.

Tommasi D, Hunt BPV, Pakhomov EA, Mackas DL (2013) Mesozooplankton community seasonal succession and its drivers: Insights from a British Columbia, Canada, fjord. J Marine Syst 115: 10-32.

Turley CM, Lochte K, Lampitt RS (1995) Transformations of biogenic particles during sedimentation in the Northeastern Atlantic. Phil Ttrans R Soc B 348: 179-189.

Turner JT (2002) Zooplankton fecal pellets, marine snow and sinking phytoplankton blooms. Aquat Microb Ecol 27: 57-201.

Turner JT (2015) Zooplankton fecal pellets, marine snow, phytodetritus and the ocean's biological pump. Prog Oceanogr 130: 205-248

Urban-Rich J, Hansell DA, Roman MR (1998) Analysis of copepod fecal pellet carbon using a high temperature combustion method. Mar Ecol Prog Ser 171: 199-208.

Urban-Rich J (2001) Seston effects on faecal pellet carbon concentrations from a mixed community of copepods in Balsfjord, Norway, and the Antarctic Polar Front. ICES J Mar Sci 58: 700-710.

Uye S, Kaname K (1994) Relations between fecal pellet volume and body size for major zooplankters of the inland Sea of Japan. J Oceanogr 50: 43-49.

Uye S, Sano K (1998) Seasonal variations in biomass, growth rate and production rate of the small cyclopoid copepod Oithona davisae in a temperate eutrophic inlet. Mar Ecol Prog Ser 163: 37-44.

Van Valen, LM (1973) A new evolutionary law. Evol Theory 1: 1–30.

Verity PG, Paffenhöfer G-A (1996) On assessment of prey ingestion by copepods. J Plankton Res 18: 1767-1779.

Villarino E, Chust G, Lincandro P, Butenschon M, Ibaibarriaga L, Larranaga A, Irigoien X (2015) Modelling the future biogeography of North Atlantic zooplankton communities in response to climate change. Mar Ecol Prog Ser 531: 121-142.

Wanamaker AD, Kurtz KJ, Schöne BR, Maasch KA, Pershing AJ, Borns HW, Introne DS, Feindel S (2009) A late Holocene paleo-productivity record in the western Gulf of Maine, USA, inferred from growth histories of the long-lived ocean quahog. Int J Earth Sci 98: 19-29.

Ward BA, Dutkiewicz S, Follows MJ (2014) Modelling spatial and temporal patterns in size-structured marine plankton communities: top-down and bottom-up controls. J Plankton Res 36: 31-47.

Wexels Riser C, Wassmann P, Olli K, Arashkevich E (2001) Production retention and export of zooplankton faecal pellets on and off the Iberian shelf, north-west Spain. Prog Oceanogr 51: 423-441.

Wexels Riser C, Wassmann P, Olli K, Pasternak A, Arashkevich E (2002) Seasonal variation in production, retention and export of zooplankton faecal pellets in the marginal ice zone and central Barents Sea. J Marine Syst (38): 1175-188.

Wexels Riser C, Reigstad M, Wassmann P (2010) Zooplankton-mediated carbon export: A seasonal study in a northern Norwegian fjord. Mar Biol Res 6: 461-471.

Wiedmann I, Reigstad M, Sundfjord A, Basedown S (2014) Potential drivers of sinking particle's size spectra and vertical flux of particulate organic carbon (POC): Turbulence, phtoplankton, and zooplankton. J Geophys Res 119: 6900-6917.

Wirtz KW (2012) Who is eating whom? Morphology and feeding type determine the size relation between planktonic predators and their ideal prey. Mar Ecol Prog Ser 445: 1-12.

Wohlers J, Engel A, Zöllner E, Breithaupt P, Jürgens, Hoppe H-G, Sommer U, Riebesell U (2009) Changes in biogenic carbon flux in response to sea surface warming. Proc Natl Acad Sci 106: 7067-7072.

Wu C-J, Chiang K-P, Liu H (2010) Diel feeding pattern and prey selection of mesozooplankton on microplankton community. J Exp Mar Biol Ecol 390: 134-142.

Zhou M (2006) What determines the slope of a plankton biomass spectrum? J Plank Res 28: 437-448.

Zhou M, Carlotti F, Zhu YW (2010) A size-spectrum zooplankton closure model for ecosystem modelling. J Plank Res 32: 1147-1165.

APPENDICES

Appendix A. Full citations of literature used for prosome length-temperature relationships (§), fecal pellet volume-copepod length relationships (+), and fecal pellet production modeling (*)

Abou Debs C (1984) Carbon and nitrogen budget of the calanoid copepod *Temora stylifera*: effect of concentration and composition of food. Mar Ecol Prog Ser 15: 213-223. +*

Ashjian CJ, Wishner KF (1993) Temporal and spatial changes in body size and reproductive state of *Nannocalanus minor* (Copepoda) females across and along the Gulf Stream. J Plankton Res 15: 67-98. §

Ayukai T, Hattori H (1992) Production and downward flux of zooplankton fecal pellets in the anticyclonic gyre off Shikoku, Japan. Oceanol Acta 15: 163-172.+*

Batchelder HP, Williams R (1995) Individual-based modeling of the population dynamics of *Metridia lucens* in the North Atlantic. ICES J Mar Sci 52: 469-482. §

Bathmann UV, Noji TT, Voss M, Peinert R (1987) Copepod fecal pellets: abundance, sedimentation and content at a permanent station in the Norwegian Sea in May/ June 1986. Mar Ecol Prog Ser 38: 45-51. +

Besiktepe S, Dam HG (2002) Coupling of ingestion and defecation as a function of diet in the calanoid copepod *Acartia tonsa*. Mar Ecol Prog Ser 229: 151-164. +*

Butler M, Dam HG (1994) Production rates and characteristics of fecal pellets of the copepod *Acartia tonsa* under simulated phytoplankton bloom conditions: implications for vertical fluxes. Mar Ecol Prog Ser 114: 81-91. +*

Calbet A, IrigoienX (1997) Egg and faecal pellet production rates of the marine copepod *Metridia gerlachei* northwest of the Antarctic Peninsula. Polar Biol 18: 273-279. *

Campbell RG, Wagner MM, Teegarden GJ, Boudreau CA, Durbin EG (2001) Growth and development rates of the copepod *Calanus finmarchicus* reared in the laboratory. Mar Ecol Prog Ser 221: 161-183. §

Carlotti F, Rey C, Javanshir A, Nival S (1997) Laboratory studies on egg and faecal pellet production of *Centropages typicus*: effect of age, effect of temperature, individual variability. J Plankton Res 19: 1143-1165. *

Dagg MJ, Walser WE (1986) The effect of food concentration on fecal pellet size in marine copepods. Limnol Oceanogr 31: 1066-1071. +

Daly KL (1997) Flux of particulate matter through copepods in the Northeast Water Polynya. J Marine Syst 10: 319-342. +*

Deevey GB (1960) Relative effects of temperature and food on seasonal variations in length of marine copepods in some eastern American and western European waters. Bulletin of the Bingham Oceanographic Collection 17: 54-86.§

Durbin AG, Durbin EG (1978) Length and weight relationships of *Acartia clausi* from Narragansett Bay, R.I. Limnol Oceanogr 23: 958-969. §

Feinberg LR, Dam HG (1998) Effects of diet on dimensions, density and sinking rates of fecal pellets of the copepod *Acartia tonsa.* Mar Ecol Prog Ser 175: 87-96. +

Griffin SL (2000) Influence of food type on the production and settling rate of faecal pellets produced by an estuarine copepod. Mar Freshwater Res 51: 371-378. +

Hays GC, Webb PI, Frears SL (1998) Diel changes in the carbon and nitrogen content of the copepod *Metridia lucens*. J Plankton Res 20: 727-737. §

Henriksen MV, Jung-Madsen S, Nielsen TG, Møller EF, Henriksen KV, Markager S, Hansen BW (2012) Effects of temperature and food availability on feeding and egg production of *Calanus hyperboreus* from Disko Bay, western Greenland. Mar Ecol Prog Ser 447: 109-126. +*

Hirst AG, Sheader M, Williams JA (1999) Annual pattern of Calanoid copepod abundance, prosome length and minor role in pelagic carbon flux in the Solent, UK. Mar Ecol Prog Ser 177: 133-146. §

Honjo S, Roman MR (1978) Marine copepod fecal pellets: production, preservation and sedimentation. J Mar Res 36: 45-57. +*

Ji R, Davis CS, Chen C, Beardsley RC (2009) Life history traits and spatiotemporal distributional patterns of copepod populations in the Gulf of Maine-Georges Bank region. Mar Ecol Prog Ser 384: 187-205. §

Koski M, Wexels Riser C (2006) Post-bloom feeding of *Calanus Finmarchicus* copepodites: Selection for autotrophic versus heterotrophic prey. Mar Biol Res 2: 109-119. +*

Lane PVZ, Smith SL, Urban JL, Biscayes PE (1994) Carbon flux and recycling associated with zooplanktonic fecal pellets on the shelf of the Middle Atlantic Bight. Deep-Sea Res II 41: 437-457. +*

Liang D, Uye S-I, Onbé T (1996) Population dynamics and production of the planktonic copepods in a eutrophic inlet of the Inland Sea of Japan. I. *Centropages abdominalis*. Mar Biol 124: 527-536. §

Martynova DM (2003) Copepod fecal pellets in the White Sea: Experimental and *in situ* studies. Mar Biol 43: S123-S133.+

Martynova DM, Kazus NA, Bathmann UV, Graeve M, Sukhotin AA (2011) Seasonal abundance and feeding patterns of copepods *Temora longicornis*, *Centropages hamatus* and *Acartia* spp. Polar Biol 34: 1175-1195. *

McLaren IA (1978) Generation lengths of some temperate marine copepods: estimation, prediction, and implications. J Fish Res Board Can 35: 1330-1342.§

McLaren IA, Tremblay MJ, Corkett CJ, Roff JC (1989) Copepod production on the Scotian Shelf based on life-history analyses and laboratory rearings. Can J Fish Aquat Sci 46: 560-583.§

Peruyeva YG (1983) Copepodite stage IV of *Calanus glacilais* Jaschnov of the White Sea and its feeding on the colonial alga *Chaetoceros crinitus* Schütt. Oceanology 23: 134-138.+*

Ploug H, Iversen MH, Koski M, Buitenhuis ET (2008) Production, oxygen respiration rates, and sinking velocity of copepod fecal pellets: Direct measurements of ballasting by opal and calcite. Limnol Oceanogr 53: 469-476. +*

Rey C, Carlotti F, Tande K, Hygum BH (1999) Egg and faecal pellet production of *Calanus finmarchicus* females from controlled mesocosms and in situ populations: influence of age and feeding history. Mar Ecol Prog Ser 188: 133-148. *

Richardson AJ, Verheye HM, Herbert V, Rogers C, Arendse LM (2001) Egg production, somatic growth and productivity of copepods in the Benguela Current system and Angola-Benguela Front. S Afr J Sci 97: 251-257.§

Seuthe L, Darnis G, Wexels Riser C, Wassmann P, Fortier L (2007) Winter-spring feeding and metabolism of Arctic copepods: insights from faecal pellet production and respiration measurements in the southeastern Beaufort Sea. Polar Biol 30: 427-436. *

Sun X, Sun S, Li C, Wang M (2012) Seasonal change in body length of important small copepods and relationship with environmental factors in Jiaozhou Bay, China. Chin J Oceanol and Limn 30: 404-409.§

Tönnesson K, Nielsen TG, Tiselius P (2006) Feeding and production of the carnivorous copepod *Paraeuchaeta norvegica* in the Skagerrak. Mar Ecol Prog Ser 314: 213-225. §

Tsuda A, Nemoto T (1990) The effect of food concentration on the faecal pellet size of the marine copepod *Pseudocalanus newmani* Frost. Bulletin of Plankton Society of Japan 37: 83-90.+

Uye S-I (1991) Temperature-dependent development and growth of the planktonic copepod *Paracalanus* sp. in the laboratory. Bulletin of Plankton Society of Japan, Special Volume, 627-636.§

Uye S-I, Sano K (1998) Seasonal variations in biomass, growth rate and production rate of the small cyclopoid copepod *Oithona davinsae* in a temperate eutrophic inlet. Mar Ecol Prog Ser 163: 37-44. §

Wexels Riser C, Reigstad M, Wassmann P, Arashkevich E, Falk-Petersen S (2007) Export or retention? Copepod abundance, faecal pellet production and vertical flux in the marginal ice zone through snap shorts from the northern Barents Sea. Polar Biol 30: 719-730. +*

Appendix B. Derivation of fecal pellet carbon flux and fecal pellet decay rate

Let n be the density of copepods (individuals m^{-3}) near the surface of the ocean (approximately 7 m, where the Continuous Plankton Recorder tows). The copepods are producing sinking fecal pellets at a rate of FPP (fecal pellets $time^{-1}$); and the pellets contain a constant amount of carbon, κ for volume, FPV. These pellets decay at a rate r ($time^{-1}$), and sink at a rate SR (m $time^{-1}$). Near the surface, the concentration of fecal pellet carbon FPC_{sfc} (gC m^{-3}) changes according to:

$$\frac{dFPC}{dt} = FPP\ \kappa\ FPV\ n$$

In one unit of time, the fecal pellet carbon concentration near the surface where it is produced, FPC_{sfc} (gC m^{-3}) is:

$$FPC_{sfc} = FPP\ \kappa\ FPV\ n \text{ dt, where dt is 1}$$

Now consider the fate of copepod fecal pellets as they sink through the water column. The rate of change in the concentration at a depth z is a partial differential equation:

$$\frac{\partial FPC}{\partial t} = \text{-SR}\ \frac{\partial FPC}{\partial z} - rFPC$$

At equilibrium (= 0) we get an ordinary differential equation:

$$\frac{dFPC}{dz} = -\frac{r}{SR} FPC$$

which has the solution:

$$FPC(z) = FPC_{sfc}\ e^{-r/SR\ z}$$

Where FPC_{sfc} is the concentration where the fecal pellets are produced. If FPC_{sfc} is the equilibrium concentration at the source depth, the concentration at z meters below that depth (FPC_d) is:

$$FPC_d = (FPP \; \kappa \; FPV \; n) \; e^{-r/s \; z}$$

The fecal pellet carbon flux (gC m^{-2} $time^{-1}$) at a particular depth (z) is the concentration times the pellets' sinking rates (*SR*):

$$FPCflux_d = SR \; (FPP \; \kappa \; FPV \; n) \; e^{-r/s \; z}$$

We determined the fecal pellet decay rate, *r* ($time^{-1}$) by setting the proportion of fecal pellet carbon produced near the surface that reaches a given depth ($FPC_d : FPC_{sfc}$) to a range of reasonable retention values (ret), based upon the literature.

$$(1\text{-ret}) = FPC_d / FPC_{sfc}$$

We then solved for either one decay rate for the entire dataset, or one decay rate per sample, to give the estimated fecal pellet carbon retention:

$$(1\text{-ret}) = (FPP \; \kappa \; FPV \; n) \; e^{-r/s \; z} \; / \; (FPP \; \kappa \; FPV \; n)$$

$$r = \ln(1\text{-ret}) \frac{SR}{\Delta z}$$

BIOGRAPHY OF THE AUTHOR

Karen Stamieszkin, the author, was born in a hospital in Portland, Maine and grew up in Cape Elizabeth, Maine. As a kindergartner she showed promise as either a scientist or an artist when she produced a detailed and scientifically accurate drawing of a dragonfly. She graduated from Cape Elizabeth High School, and then attended Yale University where she intended to major in art or literature, or maybe medieval studies, or perhaps *Russian* literature. Half-way through her undergraduate program she decided to switch to an environmental studies major. After being told that she did not have enough time to complete the major's requirements and was delinquent in making this decision, she graduated in 2006 with a B.A. in environmental studies. Her senior research project was about the social and ecological carrying capacity of the Damariscotta River, Maine, for oyster farming. She then graduated from the Yale School of Forestry and Environmental Studies with a Master of Environmental Science degree in 2007. Her thesis was about the social and ecological challenges facing a marine reserve in the Gulf of California, off of Loreto, Baja California Sur, Mexico. It is entitled, "Management of a marine protected area for sustainability and conflict resolution." Following this anthropological and economic research project, Karen decided neither of these fields was for her.

Her first job after graduating mainly consisted of chasing bats around the woods and swamps of (really far) upstate New York. Narrowly escaping with her life several times there, she decided to head west and became a research field technician for the State of Utah, working to save desert fish: a futile mission considering that these were the type

of fish that live in water, a resource which is prioritized for golf courses and retirement community lawns in that arid part of the country. Karen had always harbored a love of the ocean, cultivated by uncountable hours boogie boarding at Scarboro Beach near her childhood home, and sought to get her foot in the door of marine science. Her lucky break came when a person named Stormy Mayo hired her as a research assistant for a right whale habitat studies program in Provincetown, MA. Provincetown is at the end of the world (tip of Cape Cod), and rests on a spit of land shaped like a vortex: a vortex famous for sucking people up and never letting them go. While there she lived on a sailboat, followed whales around, stared at thousands of copepods under a microscope, learned how to perform gynecological exams on diamondback terrapins, perfected the art of eating snacks for every meal of the day, and published a paper entitled, "Dangerous dining: surface foraging of right whales increase risk for vessel collisions." After three and-a-half years of spiraling into the magnificent vortex that is the beauty of the outer Cape, surrounded by whales of all kinds, sea birds, fish, crustaceans and crazy people, Karen broke free to seek her Ph.D. back in her dear home state of Maine.

While in the UMaine School of Marine Sciences program, Karen managed to involve most of the state's marine research institutions in her work. She traveled between the Darling Marine Center, Bigelow Laboratory for Ocean Sciences, the Gulf of Maine Research Institute (GMRI) and UMaine Orono, wrangling as many collaborators as possible. She even went to Antarctica in search of fellow plankton enthusiasts. All of the wrangling paid off in a few publications: "Evaluating trophic cascades as drivers of regime shifts in different ocean ecosystems," which was a group effort by the Ecosystem

Modeling Lab at GMRI, “Size as a master trait in modeled copepod fecal pellet carbon flux,” which is a paper about the importance of tiny poop, and “Student-led retreats for graduate student cohesion and career success,” which is about a club that she formed with other graduate students in her department. In addition to her new-found love of computer modeling, Karen is also an orchid enthusiast, an entirely addicted horse woman, and is smitten with farm life and one farmer in particular. She is a candidate for the Doctor of Philosophy degree in Oceanography from the University of Maine in August 2016.